

**Analysis of c-MYC-induced chromosomal instability
and
generation of a conditional microRNA expression system**

Dissertation zur Erlangung des Doktorwürde des Dr. rer. nat.
an der Fakultät für Biologie
der Ludwig-Maximilians-Universität München
vorgelegt von
Alexey Epanchintsev
September 2007

angefertigt am Max-Planck-Institut für Biochemie
in der Selbständigen Nachwuchsgruppe Molekulare Onkologie
(Leiter: PD Heiko Hermeking)

Erklärung

Hiermit erkläre ich, dass ich die vorliegende Dissertation selbständig und ohne unerlaubte Hilfe angefertigt habe. Sämtliche Experimente sind von mir selbst durchgeführt, außer wenn explizit auf dritte verwiesen wird. Ich habe weder anderweitig versucht, eine Dissertation oder Teile einer Dissertation einzureichen bzw. einer Prüfungskommission vorzulegen, noch eine Doktorprüfung durchzuführen.

München, den 1. September 2007

Alexey Epanchintsev

Tag der mündlichen Prüfung: 31.03.2008

Erstgutachter: PD. Dr. Heiko Hermeking

Zweitgutachter: Prof. Dr. Michael Ackmann

Betreuer: PD Dr. Heiko Hermeking

Table of content

Publication list

1	Introduction	1
1.1	The <i>c-MYC</i> oncogene	1
1.2	Genomic instability: MIN and CIN	2
1.3	Mechanisms of <i>c-MYC</i> activation in cancer	4
1.4	Potential mechanisms of <i>c-MYC</i> -induced genomic instability	5
1.4.1	Transition into S phase	5
1.4.2	<i>c-MYC</i> overcomes DNA damage-induced G ₁ /S arrest	7
1.4.3	<i>c-MYC</i> abrogates G ₂ /M arrest	9
1.4.4	<i>c-MYC</i> modulates DNA replication, DNA damage response and DNA repair pathways	9
1.4.5	<i>c-MYC</i> increases reactive oxygen species	10
1.4.6	<i>c-MYC</i> induces telomere remodeling	11
1.5	The spindle assembly checkpoint	11
1.6	RNA interference	15
2	Aims of the study	18
3	Materials	19
3.1	Chemicals	19
3.2	Reagents	21
3.3	Antibodies	21
3.3.1	Primary antibodies	21
3.3.2	Secondary antibodies	21
3.4	DNA constructs	21
3.5	Bacterial strains	22
3.6	Disposable kits	22
3.7	Laboratory equipment	23
4	Methods	24
4.1	Bacterial cell culture	24
4.1.1	Propagation of bacteria strains	24
4.1.2	Mating-assisted genetically integrated cloning (MAGIC)	24
4.2	Generation of plasmids	25
4.2.1	pSHUMI/pEMI vector construction	25
4.2.2	Restriction-mediated microRNA transfer	25
4.2.3	Subcloning of shRNA constructs into pRetroSuper	26
4.3	Cell culture and treatments	26
4.4	Generation of cell lines	27
4.5	Western blot analysis	27

4.6	DNA content analysis by FACS	28
4.7	Indirect immunofluorescence	28
4.8	Micronucleus assessment	28
4.9	Quantitative real-time PCR	29
4.10	Chromatin immunoprecipitation	30
4.11	Time-lapse microscopy	30
4.12	Tissue samples and immunohistochemistry	31
4.13	Statistical analysis	32
5	Results	33
5.1	c-MYC induces expression of <i>MAD2</i> and <i>BubR1</i>	33
5.2	c-MYC binds to human <i>MAD2</i> and <i>BubR1</i> promoters <i>in vivo</i>	37
5.3	c-MYC induces a mitotic delay	39
5.4	Synchronous apoptosis in cells with delayed mitosis	51
5.5	c-MYC induces CIN in MIN cell lines	53
5.6	Analysis of putative mediators of c-MYC-induced CIN	56
5.7	Construction of episomal vectors for RNAi	57
5.8	Functional evaluation of pEMI vectors	59
6	Discussion	65
6.1	c-MYC-induced genomic instability	65
6.2	c-MYC-induced mitotic delay	68
6.3	BubR1/MAD2-dependent mitotic delay does not influence c-MYC-induced genomic instability	69
6.4	c-MYC-induced apoptosis	71
6.5	All-in-one conditional microRNA expressing system	73
7	Summary	75
8	Abbreviations	76
9	References	78
10	Acknowledgements	94
11	Curriculum Vitae	95

Publication list

During the preparation of this dissertation the following co-authored papers have been published:

Tarasov, V., Jung, P., Verdoodt, B., Lodygin, D., Epanchintsev, A., Menssen, A., Meister, G., and Hermeking, H. (2007). Differential regulation of microRNAs by p53 revealed by massively parallel sequencing: miR-34a is a p53 target that induces apoptosis and G1-arrest. *Cell Cycle* 6, 1586-1593.

Menssen*, A., Epanchintsev*, A., Lodygin, D., Rezaei, N., Jung, P., Verdoodt, B., Diebold, J., and Hermeking, H. (2007). c-MYC Delays Prometaphase by Direct Transactivation of MAD2 and BubR1: Identification of Mechanisms Underlying c-MYC-Induced DNA Damage and Chromosomal Instability. *Cell Cycle* 6, 339-352.

***equally contributing authors**

Korner*, H., Epanchintsev*, A., Berking, C., Schuler-Thurner, B., Speicher, M. R., Menssen, A., and Hermeking, H. (2007). Digital karyotyping reveals frequent inactivation of the dystrophin/DMD gene in malignant melanoma. *Cell Cycle* 6, 189-198.

***equally contributing authors**

Epanchintsev*, A., Jung*, P., Menssen, A., and Hermeking, H. (2006). Inducible microRNA expression by an all-in-one episomal vector system. *Nucleic Acids Res* 34, e119.

***equally contributing authors**

Lodygin, D., Epanchintsev, A., Menssen, A., Diebold, J., and Hermeking, H. (2005). Functional epigenomics identifies genes frequently silenced in prostate cancer. *Cancer Res* 65, 4218-4227.

1. Introduction

1.1 *c-MYC* oncogene

c-MYC proto-oncogene was identified as the cellular homolog of the viral oncogene *v-MYC* encoded by the avian myelocytomatosis virus (Vennstrom et al., 1982). *c-MYC* is a transcription factor which specifically binds to so-called E-boxes (CACGTG) and regulates expression of multiple genes involved in control of cell growth, proliferation, differentiation, apoptosis, angiogenesis, cellular adhesion, DNA metabolism and repair (Dang, 1999; Eisenman, 2001; Oster et al., 2002; Pelengaris et al., 2002a).

Deregulation of *c-MYC* expression is observed in many human cancers and has been implicated in a number of cellular processes associated with tumorigenesis such as reduction of growth-factor requirements, immortalization, resistance to anti-mitogenic signalling, increase of angiogenesis, changes in adhesion and genomic instability (Baudino et al., 2002; Lutz et al., 2002; Pelengaris et al., 2002b). The ability of *c-MYC* to induce unrestrained and autonomous cell growth and proliferation seems to be particularly important for tumorigenesis.

c-MYC acts at different stages of cell cycle. *c-MYC* enforces transition through G_1/S and prolongs the G_2/M phase (Felsher and Bishop, 1999; Karn et al., 1989) and is able to overcome cell cycle arrest induced by DNA damage (Chernova et al., 1998; Sheen and Dickson, 2002). The effects of *c-MYC* on the cell cycle are mediated by transcriptional activation or repression of genes encoding cell cycle regulators (Daksis et al., 1994; Hermeking et al., 2000; Hoang et al., 1995; Yang et al., 2001; Yin et al., 2001).

One of the factors limiting *c-MYC*-dependent transformation and tumorigenesis is programmed cell death (apoptosis) (Meyer et al., 2006; Nilsson and Cleveland, 2003; Prendergast, 1999), which seems to be a cellular response to unscheduled proliferation and is mediated by p53 activation (Hermeking and Eick, 1994). The tumor suppressor p14^{arf} mediates activation of p53 by *c-MYC* (Zindy et al., 1998). Furthermore, activation of *c-MYC* was shown to promote the release of cytochrom *c* from mitochondria, where it functions through activation of BAX (Mitchell et al., 2000; Soucie et al., 2001), induction of BIM (Egle et al., 2004) or repression of the anti-apoptotic BCL-X_L and Bcl2 proteins (Eischen et al., 2001). More recently, activation of *c-MYC* was shown to induce

apoptosis via generation of DNA damage (Herold et al., 2002; Seoane et al., 2002; Sheen and Dickson, 2002).

Genomic damage induced by c-MYC may involve a variety of different mechanisms including inappropriate cell cycle transition, perturbation of DNA replication, bypass of cellular check-points, suppression of DNA repair, induction of ROS production, chromosome and telomere remodeling (Chernova et al., 1998; Felsher and Bishop, 1999; Felsher et al., 2000; Karlsson et al., 2003; Li and Dang, 1999; Mai et al., 1996b; Yin et al., 2001). c-MYC-induced genomic instability can be classified into two categories: abnormal chromosomal numbers (aneuploidy) and defects in chromosomal integrity including chromosomal breaks, fusions and translocations. However, the exact mechanisms and pathways, which mediate genomic instability after c-MYC activation have remained elusive.

1.2 Genomic instability: MIN and CIN

It was shown that genetic instability is a common characteristic of most human cancers (Loeb, 2001; Rajagopalan et al., 2003). Genomic instability can be subdivided into two classes. A small fraction of cancers displays defects in mismatch repair (MMR) system, which result in an elevated mutation rate at the nucleotide level. These mutations comprise base substitutions, deletions or insertions of few nucleotides. Often they occur in stretches of simple mono-, di- and trinucleotide repeats (e.g. (CA)_n) as a consequence of DNA polymerase slippage errors during DNA replication. As a consequence widespread expansions and contractions of short, repetitive DNA sequences (called microsatellites) occur. Therefore, this type of instability has been named microsatellite instability (MIN). The majority of other cancers display abnormal chromosome number (aneuploidy) or/and structure, which is referred to as chromosomal instability (CIN).

Defects in *mutS* and *mutL* genes were first found to cause MMR deficiency in bacteria and *Saccharomyces cerevisiae*. Germline mutations in the human homologs of these genes, *MSH2* and *MLH1*, have been implicated in the hereditary nonpolyposis colon cancer (HNPCC) syndrome, and predispose to a variety of cancers. In mouse models homozygous deletion of the mismatch repair genes *Msh2*, *Msh6*, *Mlh1*, *Pms2* or double mutant *Msh3/Msh6* show a high incidence of tumor formation. *Msh3* knockout mice display a low predisposition for tumor formation, furthermore *Msh4*^{-/-}, *Msh5*^{-/-} and *Pms1*^{-/-} mice do not show elevated tumor formation

(Wei et al., 2002). Genetic screens in *Saccharomyces cerevisiae* for mutations which cause CIN identified several candidate genes. So called "CIN genes" are involved in chromosome condensation, sister-chromatid cohesion, kinetochore structure and function, and microtubule formation as well as in cell cycle check-points. However, only a small number of human CIN genes has been identified until now (Rajagopalan et al., 2003). Germline mutations in several of them were shown to cause aneuploidy (*hBub1*, *BubR1*, *Mad2*, *APC*, *BRCA1* and *BRCA2*).

At the beginning of the last century chromosomal instability was already proposed as a potential cause of cancer by the German zoologist Theodor Boveri (Boveri, 1914; Hansemann, 1890). He observed that sea urchin embryos undergoing mitosis in the presence of multipolar spindles generated aneuploid progeny. Furthermore, he described that tumor cells frequently display aberrant chromosome numbers (aneuploidy). He proposed that aneuploidy itself may be the cause of cancer. This proposal is still a matter of debate. Opponents argue that CIN is irrelevant to tumor initiation (Hahn et al., 1999), but rather contributes to tumor progression (Zimonjic et al., 2001). Moreover, some authors proposed that aneuploidy is a side-effect of transformation (Marx, 2002). The detailed molecular mechanism and determinants of aberrant chromosome segregation, which commonly occurs in cancer cells, are not clearly understood. However, it is obvious that the proper function of the spindle checkpoint is necessary for correct segregation of chromosomes and prevents aneuploidy. Any deregulation of the spindle checkpoint may therefore lead to CIN and as a consequence promote tumorigenesis.

It was reported that tumor-associated viruses cause genomic instability in birds and rodents (Rous sarcoma virus (RSV))(Nichols et al., 1965). Also human papillomavirus *E6* and *E7* (HPV) (Duensing and Munger, 2002; Munger and Howley, 2002; White et al., 1994; zur Hausen, 1991) and the viral protein *v-src* and its cellular homologs *c-src* cause CIN (Nanus et al., 1991). Additionally, the activation of endogenous proto-oncogenes like *c-MYC* (Alitalo and Schwab, 1986; Tsichlis, 1987), *Ras* (Denko et al., 1994; Kim et al., 2003) and *Mos* (Fukasawa and Vande Woude, 1997) by diverse mechanisms results in structural and numerical chromosomal changes.

1.3 Mechanisms of c-MYC activation in cancer

Over-expression of *c-MYC* has been found in up to 50% of all human cancers (Alitalo and Schwab, 1986; Pompetti et al., 1996). Elevated *c-MYC* expression correlates with clinically aggressive tumors, which have a worse prognosis than tumors without *MYC* over-expression (Gamberi et al., 1998). The activation of *c-MYC* occurs mainly through genomic and transcriptional alterations. One of the common genomic changes in hematopoietic malignancies as Burkitt's lymphoma are translocations of the *c-MYC* gene, which is located on chromosome 8, to the immunoglobulin μ heavy chain or the λ and κ light chain enhancers located on chromosome 2, 14 or 22, respectively (Boxer and Dang, 2001; Dalla-Favera et al., 1982; Popescu and Zimonjic, 2002). Rearrangements of *c-MYC* gene were also found in diffuse large cell lymphoma (DLCL), acute lymphocytic leukemia (AML), multiple myeloma (MM), and primary plasma cell leukemia (PCL) (Avet-Loiseau et al., 2001; Burmeister et al., 2005; Frost et al., 2004; Miranda Peralta et al., 1991; Nesbit et al., 1999). Rare cases of T-cell leukemia, in which the *c-MYC* gene is translocated to T-cell receptor, have also been reported (Harrison, 2000).

The transcription of *c-MYC* is frequently activated by mutations in pathways upstream of *c-MYC*. E.g. mutations in the APC/ β -catenin pathway lead to activation of *c-MYC* in colorectal cancer (He et al., 1998). *c-MYC* expression in malignant melanoma might also be deregulated via APC/ β -catenin pathway, as *β -catenin* mutations were described in some cell lines (Rubinfeld et al., 1997).

Another mechanism of *c-MYC* activation in solid tumors is gene amplification (Vita and Henriksson, 2006). In case of malignant melanoma, extra *c-MYC* copies were found in 61% of nodular melanomas, in 28% of superficially spreading melanomas, and in 30% of metastatic tumors (Treszl et al., 2004). Amplification of *c-Myc* was detected in 40% of tumors with over-expression of *c-MYC* protein in ovarian cancer (Baker et al., 1990). In cervical cancer, the *c-Myc* gene is amplified in 29% of abnormal epithelia compared to 8% in control tissues (Abba et al., 2004). Up to 23% of lung carcinoma samples displayed amplifications (Gugger et al., 2002), which were also found in 10% of esophageal squamous cell carcinoma (SCC) patients treated by surgery and in 30% of patients subjected to multimodal treatment (Bitzer et al., 2003). All three transforming members of the *Myc* family have been shown to be amplified in small cell lung carcinoma (SCLC), with a frequency of 10% (*MycN*), 13% (*L-Myc*), and 20% (*c-Myc*) (Gugger et al., 2002; Lui et al., 2001; Nesbit et al., 1999), whereas 30%

of all neuroblastoma (NBL) show specific amplification of *MycN* (Brodeur, 1994, 1995). In breast cancer *c-MYC* is amplified in 17.1%, whereas the *HER2/neu* was amplified in 18.7% of analyzed cases (Berns et al., 1992). In prostate cancer, *c-MYC* amplification was detected at a frequency of 29% (Nupponen et al., 1998). Mutational inactivation of the Myc-antagonist Mxi-1 may be another mechanism of c-Myc activation in prostate carcinoma (Eagle et al., 1995; Prochownik et al., 1998).

1.4 Potential mechanisms of c-Myc-induced genomic instability

In solid tumors abnormal *c-MYC* expression correlates with genomic instability. *In vivo* and *in vitro* models of *c-MYC* overexpression revealed induction of karyotypic changes, including alterations in copy number and chromosomal rearrangements (Felsher and Bishop, 1999; Louis et al., 2005; Vafa et al., 2002) or locus specific instability involving amplification of certain genes (Kuschak et al., 1999; Mai, 1994; Mai et al., 1996b) (*cyclin D2*, *ribonucleotide reductase R2*, *PALA*, *CAD*, *DHFR*). After inactivation of MYC in conditional mice models most tumors undergo proliferative arrest, differentiation and apoptosis (Arvanitis and Felsher, 2006). However, some of tumors can become independent of MYC overexpression by acquiring additional genetic events such as chromosomal translocations (Felsher and Bishop, 1999; Karlsson et al., 2003; Louis et al., 2005; Vafa et al., 2002). These observations suggest that c-MYC functions as dominant mutator gene by promoting CIN. Identical translocations were present in multiple relapsed tumors arguing that these genomic events may contribute to the independence from c-MYC (Arvanitis and Felsher, 2006).

1.4.1 Transition into S phase

c-MYC activation is sufficient and necessary for induction of G₁/S-transition (Eilers et al., 1989; Trumpp et al., 2001) In *Drosophila* ectopic expression of *dMYC* increases both cell mass and cell number (Johnston et al., 1999). Targeted disruption of the *c-MYC* gene in rat fibroblast resulted in a significant lengthening of the G₁ and G₂ phases, whereas the duration of S phase was not affected (Iritani and Eisenman, 1999; Johnston et al., 1999; Mateyak et al., 1997; Trumpp et al., 2001). *c-MYC* induces transcription of several target genes involved in G₁/S transition such as *ODC*, *Cul1*, *CDK4*, *Cdc25A* and *Id2* (Bello-Fernandez et al., 1993; Berns et al., 1997; Galaktionov et al., 1996; Hermeking et al., 2000; Lasorella et al., 2000; Leone et al., 1997; Muller et al., 1997; O'Hagan et al., 2000; Wagner et al., 1993). Furthermore, c-

MYC activation leads to down-regulation of inhibitors of cyclin/CDK complexes. As a result, *c-MYC* leads to activation of cyclin/CDK complexes, phosphorylation of pRB and release of active E2F/DP transcription factors (Blagosklonny and Pardee, 2002).

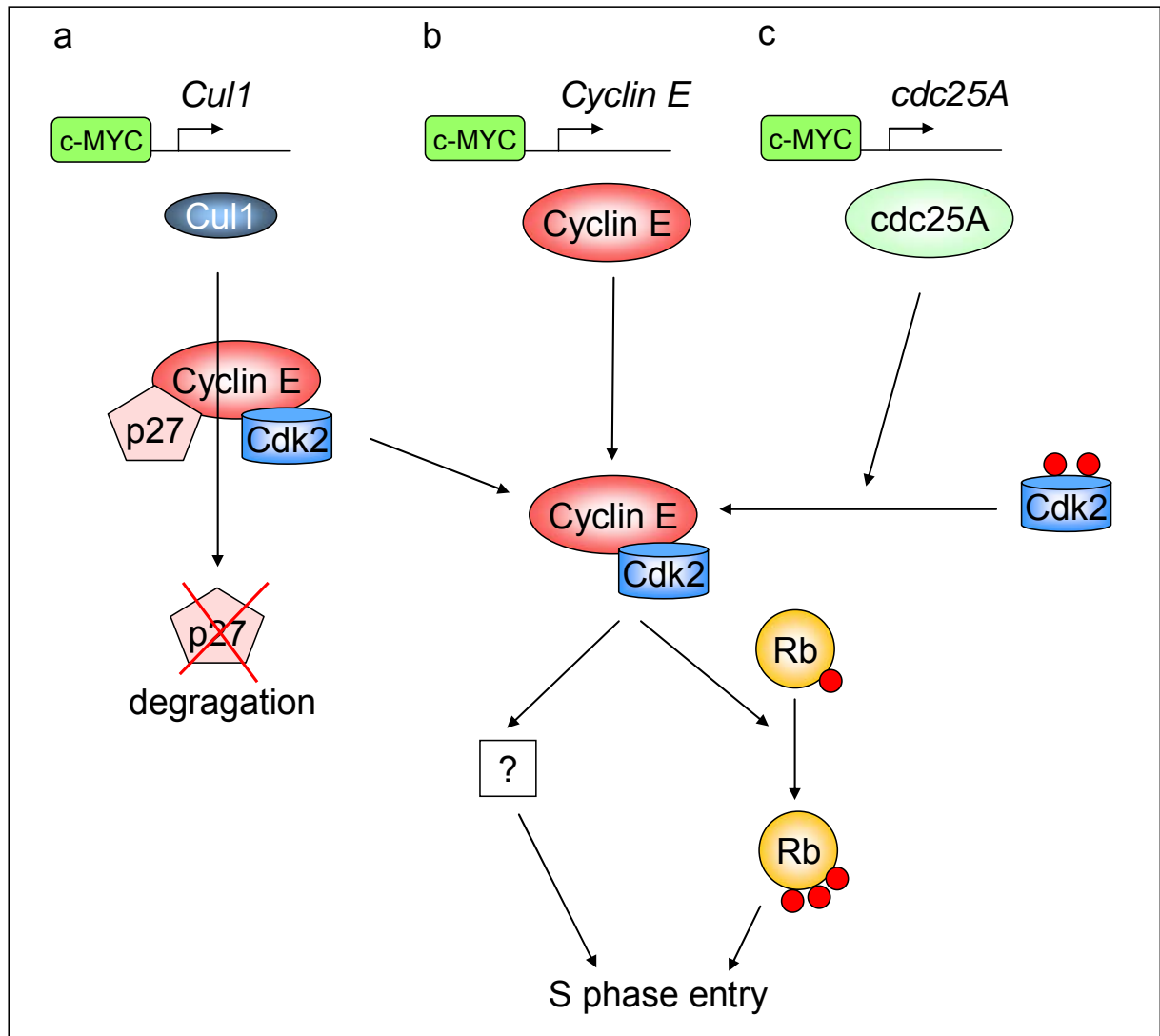


Figure 1 *c-MYC* overcomes restriction point (adapted from (Wade and Wahl, 2006)).

c-MYC transactivates expression of genes involved in regulation of CyclinE/Cdk2 complex activity, which modulate Rb function, release E2Fs and facilitate progression through S-phase. **(a)** Up-regulation of *Cul1*, a transcriptional target of *c-MYC*, leads to degradation of the Cyclin/Cdk2 inhibitor, p27. **(b)** *c-MYC* directly activates transcription of *Cyclin E*. **(c)** *c-MYC* dependent inducer of *cdc25A* phosphatase activates *cdk2*.

Under such conditions inappropriate expression of cyclin E can lead to genomic instability (Spruck et al., 1999). Also, excessive CDK activity influences the fidelity of chromosome transmission, including the licensing of replication origins, which has been linked to instability (Hua et al., 1997; Walter et al., 1998) (Figure 1). In addition, studies in yeast suggested that precocious CDK activation may cause genomic

instability via delayed firing of replication origins, leading to breaks during mitosis of incompletely replicated chromosomes (Lengronne and Schwob, 2002).

1.4.2 c-MYC overcomes DNA damage-induced G₁/S arrest

When genetic material is damaged, the activated checkpoints delay replication, allowing the DNA repair machinery to remove brakes. If the damage is too severe apoptosis is initiated to permanently remove damaged cells. After DNA damage activation of ATM and ATR are the initial steps (Bartek and Lukas, 2001b; Kastan and Bartek, 2004). For the DNA damage response at G₁/S transition a two-wave checkpoint response has been suggested (Bartek and Lukas, 2001a; Falck et al., 2001). The initial, transient response is an inhibition of Cdk2 within 20-30 minutes, which is restricted to several hours (Mailand et al., 2000; Rotman and Shiloh, 1999). This prompt cell cycle delay is independent of p53 and transcription, and is mediated via dephosphorylation of CDC2 by the phosphatase Cdc25A. This early response temporarily slows down cell cycle progression to provide more time for DNA repair. The second, delayed and significantly extended response is mediated by the transcription factor p53, which is activated by phosphorylation of ATM/ATR (on serine 15) and the checkpoint kinases Chk2 and Chk1 (on serine 20). These modifications activate p53 either by decreasing p53 binding to its negative regulator, mdm2, or by increasing association with transcriptional co-activator p300/CBP (Lambert et al., 1998; Unger et al., 1999). Activated p53 regulates transcription of a large number of genes leading to cell cycle arrest, apoptosis or increased DNA repair (Wahl and Carr, 2001). Among them is the p21^{Waf1/Cip1}, which encodes an inhibitor of cyclin dependent kinases (CDKs), which are essential for entry into S phase (Sherr and Roberts, 1999; Vogelstein et al., 2000). The process of p53 modification, accumulation, activation and finally transcriptional induction of the effectors requires several hours and may last for several days (Carr, 2000).

G₁ arrest caused by ionizing radiation-induced DNA damage is compromised by ectopic c-MYC overexpression (Sheen and Dickson, 2002). As a result cells perform DNA replication in the presence of DNA strand breaks which may ultimately lead to the generation of dicentric chromosomes and chromosomal instability. Abrogation of a p53-dependent arrest by constitutive c-MYC expression may result in apoptosis (Hermeking and Eick, 1994), which provides a safeguard mechanism to prevent the persistence genomic instability caused by oncogene activation.

Presumably, modulation of p21 protein levels by c-MYC can determine this apoptotic response. For example, DNA damage-induced accumulation of p21 protein can be specifically blocked by c-MYC/MIZ1 (Seoane et al., 2002). This reduction of p21 levels may redirect the response to DNA damage from arrest to apoptosis. However, in cells with defects in the apoptotic signalling pathway oncogenic, constitutive c-MYC expression allows cells to evade from DNA damage-induced arrest and apoptosis.

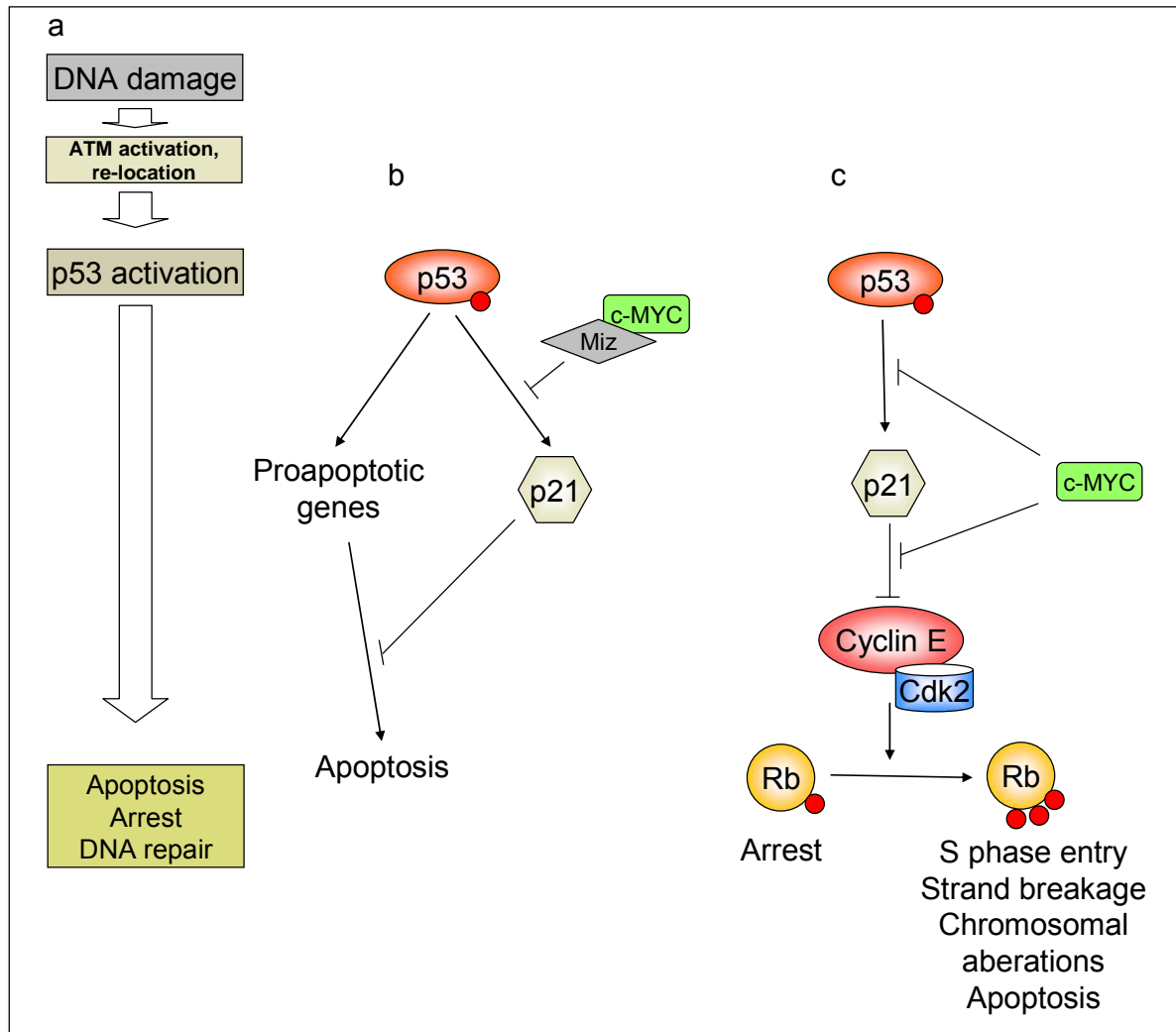


Figure 2. c-MYC activation abrogates the DNA damage response (adapted from (Wade and Wahl, 2006)).

(a) The scheme describes the signaling downstream of DNA damage through ATM-dependent activation of p53 resulting in cell-type specific apoptosis or cell-cycle arrest with following DNA repair. (b) Heterodimerisation of c-MYC with Miz protein can specifically block p21 induction from its promoter and result in apoptosis in some cell types. (c) Miz independent c-MYC-mediated p21 inhibition through sequestration of it to the other cyclin-cdk complexes leads to cell-cycle entry.

1.4.3 c-MYC abrogates G₂/M arrest

The error-free transmission of genomic information to the next generation of cells requires complete, damage-free DNA replication and faithful mitotic segregation of chromosomes into two daughter cells. Checkpoint mechanisms in G₂- and M-phase ensure the proper segregation of the duplicated chromosomes. Dysfunction of both G₂ and/or mitotic checkpoints may result in karyotypic abnormalities and/or endoreduplication (Bates et al., 1998; Niculescu et al., 1998; Stewart et al., 1999).

Ectopic expression of c-MYC compromises a stable G₂-arrest and causes aneuploidy and endoreduplication (Andreassen and Margolis, 1994; Khan and Wahl, 1998; Kung et al., 1990; Lanni and Jacks, 1998; Li and Dang, 1999). c-MYC can compromise a G₁-like arrest of cells undergoing mitotic slippage caused by drug-induced microtubule perturbation (Li and Dang, 1999; Yin et al., 2001) or sequestration of E2F transcription factors (Li and Dang, 1999; Santoni-Rugiu et al., 2000) and leads to reduplication. p27 suppresses c-MYC-induced endoreduplication at low, but not at high levels of c-MYC expression (Deb-Basu et al., 2006). In the latter case no influence on c-MYC dependent chromosomal breaks or fusion formation was detected. A possible explanation for this observation is that p27 suppresses mitotic division and endoreduplication or the ability of c-MYC to cause accelerated entry into the S phase.

The DNA damage generated by c-MYC over-expression is sufficient to activate the G₂/M checkpoint (Felsher 2000) and arrest cells with a 4N DNA content (Felsher et al., 2000). Nevertheless, c-MYC activation is able to enforce G₂ to S transition probably through the re-initiation of DNA synthesis or potential leakiness of the G₂/M checkpoint. This bypass contributes to an increase in ploidy. An explanation for such mechanism could be the premature activation of cyclin/CDK complexes or other factors involved in replication origin licensing and initiation of S-phase by c-MYC.

1.4.4 c-MYC modulates replication, DNA damage response and repair pathway

c-MYC expression was also shown to influence processes which maintain the integrity of the genome such as DNA repair and the response to DNA damage. Perturbation or attenuation of these processes may contribute to genomic instability.

Several gene expression studies revealed that c-MYC can upregulate genes involved in DNA replication including: *MCM4*, *MCM6*, *MCM7*, *Cdt1*, *CDC6* and *TOP1* (Fernandez et al., 2003; O'Hagan et al., 2000; Schuhmacher et al., 1999; Watson et al., 2002). In a proteomic approach c-MYC was recently shown to directly interact with

MCM7, *RFC* and others components of DNA replication machinery (Koch et al., 2007). Therefore, c-MYC activation presumably interferes with or modulates DNA replication, which in the case of constitutively active, oncogenic c-MYC expression may lead to induction of DNA damage and genomic instability (Labib and Diffley, 2001; Pourquier and Pommier, 2001).

c-MYC overexpression also interferes with the repair of double strand breaks (DSBs) and results in an increase in chromosomal breaks and translocations (Karlsson et al., 2003). In this context it would be interesting to know whether c-MYC is able to inhibit repair directly via modulation of DNA damage response or repair genes or its function is more indirect.

c-MYC dependent induction of DNA repair genes (Chiang et al., 2003; Grandori et al., 2003; Menssen and Hermeking, 2002) might have a dual effect on c-MYC-driven tumorigenesis. On one hand activation of repair genes might increase fidelity of DNA replication and facilitate resolution of breaks arising during replication and thus ensures replication fork progression. On the other hand, aberrant activation of repair enzymes may cause unscheduled repair of replication intermediates and increase the probability of chromosomal aberrations (Schar, 2001).

1.4.5 c-MYC increases reactive oxygen species

c-MYC couples mitogenic signalling to transcriptional induction of genes which promote growth and proliferation. Furthermore, c-MYC induces a numerous target genes involved in glycolytic, respiratory and biosynthetic pathways (Gomez-Roman et al., 2003; O'Connell et al., 2003; Shim et al., 1997). Rapid elevation of metabolism associated with transition from quiescence to S-phase could potentially lead to permanent accumulation of reactive oxygen species (ROS), which may cause modifications and breaks of genomic DNA. Several studies suggest that c-MYC induces ROS which generate DNA damage (Tanaka et al., 2002; Vafa et al., 2002). However, other authors suggest that c-MYC induces genomic instability through inappropriate cell cycle entry and progression (Felsher and Bishop, 1999). Interestingly, c-MYC also induces oxidative stress and DNA lesions in resting cells (Felsher and Bishop, 1999)(Mai et al., 1996a)(Vafa et al., 2002).

1.4.6 c-MYC induces telomere remodeling

Telomere organisation and behaviour appear to be cell cycle-dependent (Chuang et al., 2004). During the G₀/G₁- and S-phases of normal cells telomeres are widely distributed throughout the nucleus, however in G₂, they change positions and organize in telomeric discs and align in the center of the interphase nucleus (Mai and Garini, 2005). Tumor cells have distorted telomeric structures and display telomeric aggregate formation (Chuang et al., 2004). Interestingly, c-MYC activation induces telomeric aggregates in immortalized cells, which are accompanied by breakage-bridge-fusion cycles and result in unbalanced chromosomal translocations (Louis et al., 2005).

1.5 The spindle assembly checkpoint

The mitotic checkpoint, also known as spindle assembly checkpoint (SAC) prevents chromosomal missegregation by inhibiting the irreversible transition through anaphase. Only when each chromatid has made proper attachments to microtubules connected to opposite spindle poles anaphase is initiated. This mechanism ensures even and accurate chromosome separation onto two daughter cells and can therefore be envisioned as a tumour suppressive mechanism, which prevents the acquisition of oncogenic chromosomal missegregations. The connection between chromosomes and spindle microtubules occurs on so called kinetochores, attachment sites, which assemble from proteins and centromeric DNA during every mitosis. The outer surface of unattached kinetochores acts as a catalytic site which recruits mitotic checkpoint proteins (Bub1, BubR1, Bub3, Mad1, Mad2, MPS1 and CENP) and converts them to partially diffusible complexes that comprise a “wait anaphase” signal, which inhibits the anaphase promoting complex/cyclosome (APC/C), preventing premature chromosome segregation until each kinetochore properly attaches to the mitotic spindle. The function of the APC/C E3 ubiquitin ligase, on which the mitotic checkpoint signaling converges, is ubiquitination of mitotic substrates whose subsequent proteasome-mediated destruction is necessary for the onset of anaphase (securin) and mitotic exit (cyclin B). Activated complexes of the inhibitors Bub3, BubR1 and Mad2 directly bind to CDC20, a specificity factor required for recognition of mitotic substrates by the APC/C. As soon as both kinetochores of a sister chromatid are attached to microtubule of the opposite spindle poles through microtubule motors

(CENP-E), tension is generated by this motor, which leads to silencing of checkpoint inhibitor at those kinetochores (Figure 3).

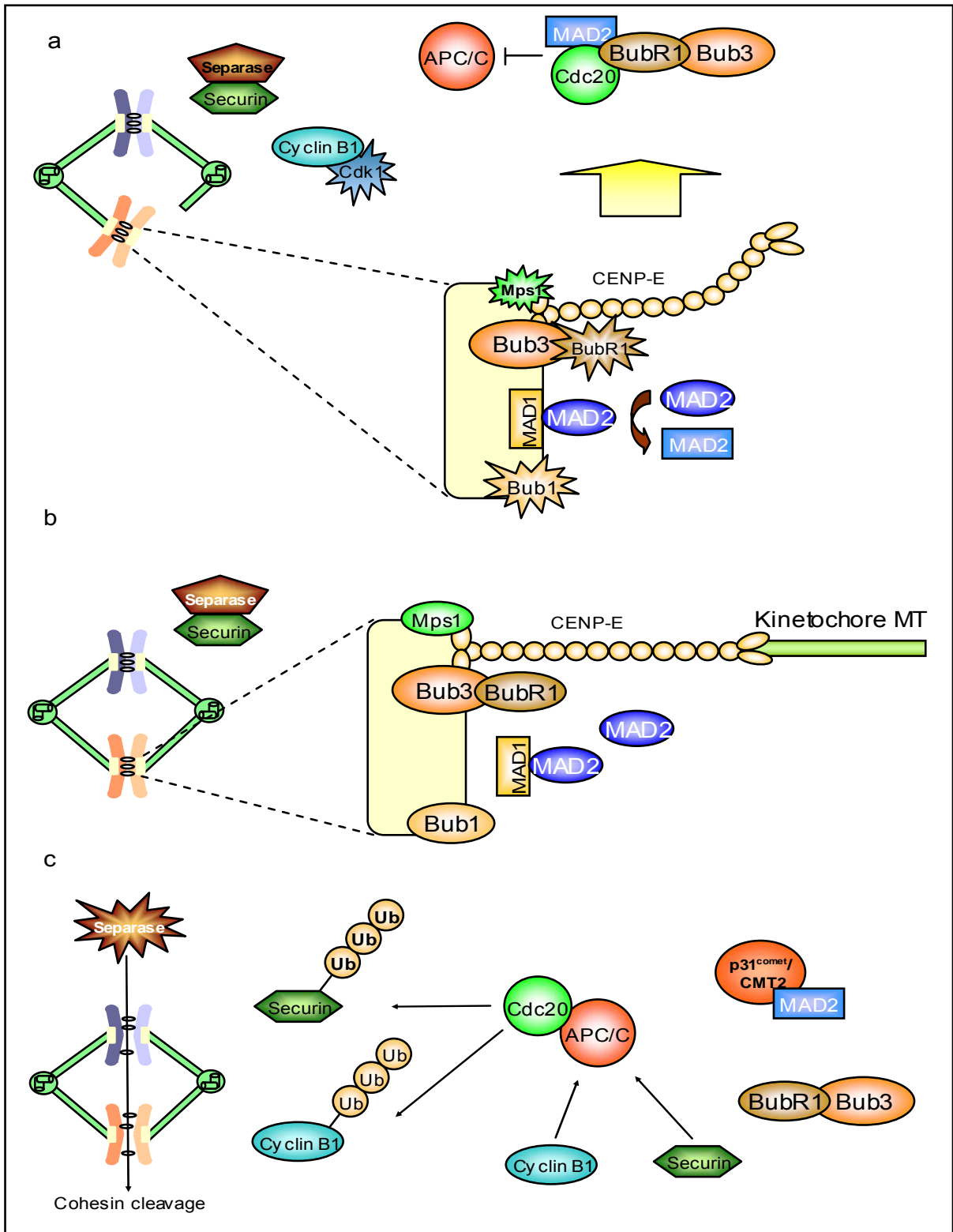


Figure 3. The mammalian mitotic checkpoint signaling. (adapted from (Kops et al., 2005))

(a) Prophase-early prometaphase. After nuclear envelope breakdown pools of spindle checkpoint proteins occupy kinetochores of unattached chromosomes. CENP-E protein bound to the kinetochore and not attached to the spindle microtubules activates BubR1 kinase activity which further facilitates recruitment of MAD1-MAD2 heterodimers to kinetochores for transmitting a "wait anaphase signal". Presence of other essential checkpoint components leads to recruitment and conformational activation of MAD2 through the MAD1-MAD2 heterodimer. These events, which occur on free kinetochores, generate a pool of activated MAD2 and BubR1 molecules which in combination with BUB3 deplete CDC20 preventing activation by APC/C. Thereby, cyclin B1 and securin degradation is inhibited **(b)** As soon as all kinetochores attach to the microtubule spindles from opposite poles the microtubule motor proteins stretch the sister chromatids via microtubules, which terminates the "wait anaphase signal". **(c)** As the "wait anaphase signal" ceases the APC/C-mediated ubiquitination of cyclin B1 and securin triggers transition into anaphase.

Interestingly, mitotic checkpoint proteins are present through interphase and participate in additional cellular processes besides chromosomal segregation. For instance, MAD1 and MAD2 bind to the nuclear envelope and pores (Campbell et al., 2001; Louk et al., 2002), MAD2 participates in the DNA replication checkpoint (Sugimoto et al., 2004). Bub3 is involved in transcriptional repression via interaction with histone deacetylases (Yoon et al., 2004). The BubR1 protein is implicated in variety of processes like premature aging (Baker et al., 2004), fertility (Baker et al., 2004), megakaryopoiesis (Wang et al., 2004a), response to DNA damage (Fang et al., 2006) and apoptosis (Baek et al., 2005; Kim et al., 2005; Shin et al., 2003). Mitotic checkpoint proteins are also involved in promoting of gross chromosomal rearrangements in yeast (Myung et al., 2004).

Dysfunction of the spindle checkpoint machinery leads to improper propagation of chromosomes through mitosis and causes aneuploidy and susceptibility to tumorigenesis. Several mouse models were described which characterized the function of a particular checkpoint genes, such as mitotic arrest deficient (MAD) *MAD1* (Iwanaga et al., 2007; Kienitz et al., 2005) and *MAD2* (Dobles et al., 2000; Hernando et al., 2004; Michel et al., 2001; Sotillo et al., 2007), budding uninhibited by benzimidazoles (BUB) proteins *Bub3* (Babu et al., 2003; Baker et al., 2006; Kalitsis et al., 2005) and *BubR1* (Baker et al., 2006; Dai et al., 2004), and kinesin-like motor CENtromere-associated Protein-E *CENP-E* (Weaver et al., 2007). Complete loss of spindle checkpoint proteins is lethal for cells (Babu et al., 2003; Dobles et al., 2000; Wang et al., 2004a) and leads to massive chromosome missegregation and catastrophic cell death (Kops et al., 2004; Michel et al., 2004). *MAD1* haploinsufficiency or down-regulation both in human and mouse cells results in

elevated levels of aneuploidy. In mouse models *MAD1*^{+/-} littermates show a 2-fold higher incidence of constitutive tumors in comparison to wild-type mice and develop neoplasia upon vincristine treatment (Iwanaga et al., 2007). In *MAD2* haploinsufficient models cells display elevated rates of chromosome missegregation and mice develop spontaneous lung tumors after long latencies (Michel et al., 2001). Interestingly, overexpression of *MAD2* in transgenic mice leads to much higher incidences of aneuploidy characterized as appearance of broken chromosomes, anaphase bridges and whole-chromosome gains and losses, and wide spectrum of tumors with relatively short latencies, high incidence and aggressiveness in comparison to haploinsufficient *MAD2* mice (Sotillo et al., 2007; van Deursen, 2007). *MAD2* overexpression was shown to cause aneuploidy in human cells (Hernando et al., 2004). High level of *MAD2* was detected in a set of tumors such as lymphomas and neuroblastomas where c-MYC and MYCN are involved in tumorigenesis, respectively (Hernando et al., 2004; Sotillo et al., 2007). This suggests that *MAD2* activation is an oncogenic event in these models. Haplo-insufficiency of *Bub3* leads to chromosome missegregation, but mice do not show any spontaneous tumorigenesis. They however, exhibit susceptibility to chemical induced lung tumors (Babu et al., 2003; Baker et al., 2006; Kalitsis et al., 2005). *BubR1*^{+/-} mice display elevated levels of aneuploidy and rapidly developed tumors upon carcinogen treatment (Baker et al., 2006; Dai et al., 2004). *BubR1*^{+/-}-*Apc*^{Min}/⁺ mutant mice develop colonic tumors 10 times more efficient than *Apc*^{Min}/⁺ mice (Rao et al., 2005). This observation supports the idea that c-MYC activation, caused due to *Apc* inactivation, leads to increased tumorigenesis due to the compromised spindle checkpoint caused by *BubR1* haploinsufficiency. Therefore, the spindle checkpoint may have a tumor suppressive function. The most recently reported mouse model showed that down-regulation of the centromere-associated motor protein CENP-E leads to an increased rate of chromosomal instability and elevated levels of spontaneous tumors in aged animals (Weaver et al., 2007). Unexpectedly, chromosomal instability caused by CENP-E reduction was shown to rather inhibit chemically or genetically induced tumorigenesis.

Meanwhile, it has been shown that genetic instability caused by CIN or MIN is an inherent feature of most cancer cells which promotes carcinogenesis by increasing the rate of mutations in critical genes and thereby allows unrestrained growth and metastasis (Lengauer, 2005; Rajagopalan and Lengauer, 2004). As mutations in genes encoding components of the SAC occur at a low frequency (Cahill et al., 1999;

Hernando et al., 2001; Wang et al., 2004b), other cancer-specific alterations are suspected to contribute to CIN.

1.6 RNA interference

RNA interference was discovered almost a decade ago and became a very elegant and effective method for probing gene function, and thereby also revolutionized the genetic analysis in mammalian cellular systems (Hannon, 2002; Meister and Tuschl, 2004; Paddison and Hannon, 2002; Paddison et al., 2004; Silva et al., 2004) (Figure 4). RNAi allows the modulation of gene expression at more physiological conditions in comparison to ecopic gene expression systems, and has advantages when applied to functional genetics analyses: it allows to modulate gene expression with high efficiency, specifically turn off gene isoforms or allelic variants, or repress endogenous RNA in the presence of a mutant transcript of the same gene. Furthermore, various loss-of-function screens were made possible by RNA interference. In the last years RNAi was also applied to gene therapeutic approaches, where it has great potential but faces problems as efficient delivery and tissue specificity (Aagaard and Rossi, 2007; Kim and Rossi, 2007; Li et al., 2006; Martin and Caplen, 2007). In cellular systems there are several ways to achieve RNAi: (1) direct delivery of dsRNA (double stranded RNA) or (2) transfection of siRNA (short interfering RNA) duplexes and (3) stable expression of shRNA/miRNAs (short hairpin/microRNAs) from plasmids. These approaches function through different pathways to cause down-regulation of protein expression (Figure 4). For a number of applications expression vector based systems were advantageous and have been modified in several directions to reach effective gene silencing, simple and effective delivery into the cells and stable integration. The application of conditional regulation (doxycycline- or ecdysone-controlled units and Cre- or Flp-dependent recombination) allows the analysis of “off” and “on” states of gene expression and the functional analysis of essential genes (Wiznerowicz et al., 2006). The major problem of conditional systems is leakiness. Even a slight basal shRNA expression might cause a pronounced phenotype due to the catalytic nature of RNAi. Two types of promoters driving transcription by Pol-III or Pol-II systems are currently available (Bernards et al., 2006; Dickins et al., 2005; Root et al., 2006; Wadhwa et al., 2004). The U6 and H1 based Polymerase III promoters have the advantage of generating small-sized shRNA

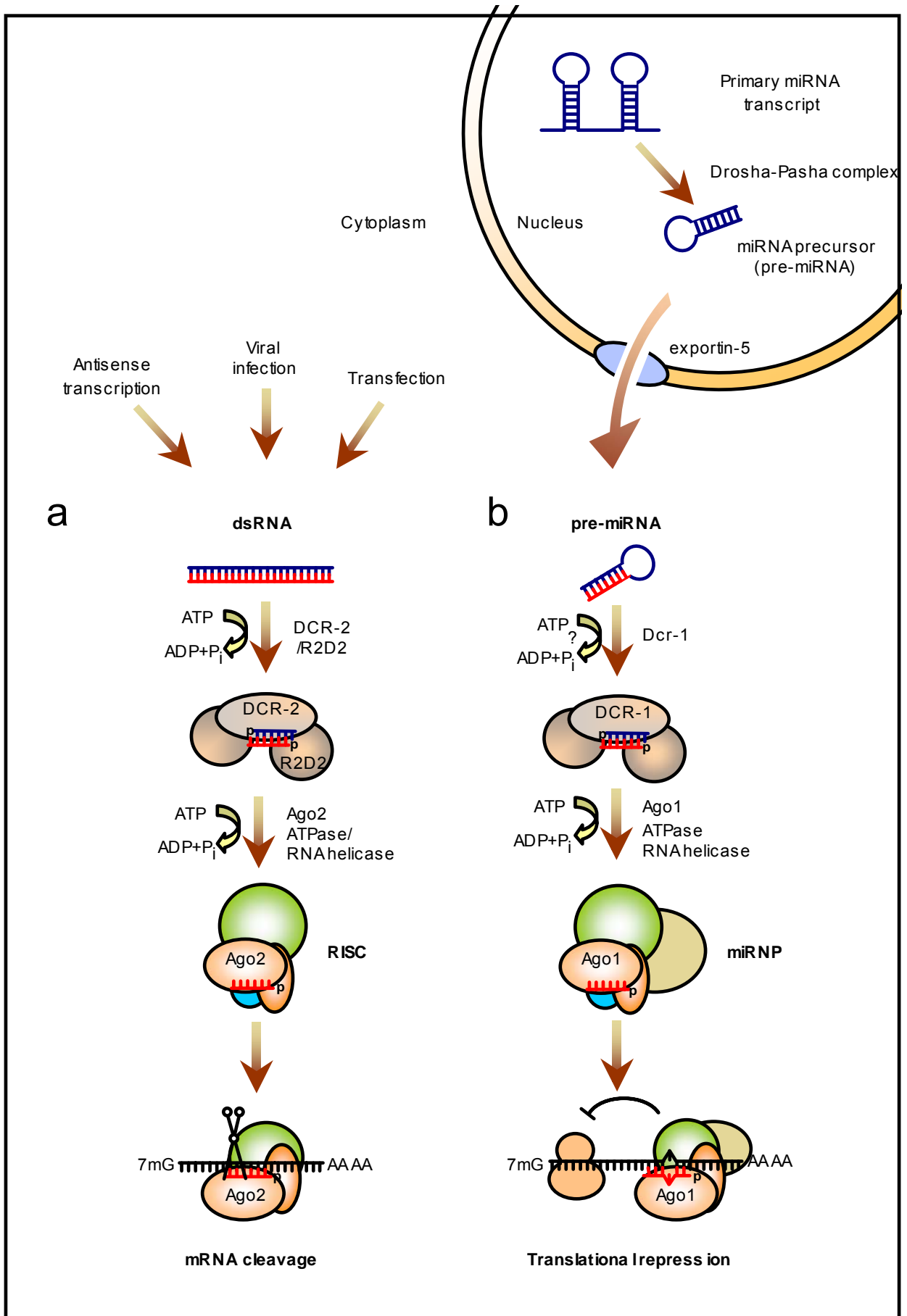


Figure 4. A model of post-transcriptional gene silencing by RNAi. (adapted from (Filipowicz et al., 2005; Meister and Tuschl, 2004)).

dsRNA can be delivered into the cells by different ways. **(a)** Processing of dsRNA by Dicer produces 21-23 nucleotide dsRNA intermediates. RNA helicase Armitage and R2D2 unwind them and incorporate single-stranded RNA into the RISC complex, which mediates sequence-specific mRNA cleavage. Primary miRNA transcripts are processed by the Drosha enzyme in the nucleus and exported into the cytoplasm. **(b)** The miRNA hairpin is further processed by Dicer, unwound and incorporated into the miRNP/RISC complex. Such single-stranded RNAs bound to Ago proteins mediate translational repression of target mRNAs. The initiation of cleavage or translation repression mechanism is determined by the complementarity of the miRNA with the target sequence.

transcripts, high activity in most cell types and robust level of knockdown. Pol-II promoters were also used to express either shRNA or miRNA cassettes and achieve higher levels of transcript expression compared to Pol-III systems. These promoters were integrated into retro- or lenti-viral vectors, which allow stable integration into the genome. Furthermore, expression vectors can contain a number of useful features: antibiotic selection markers, tracking fluorescent or receptor proteins, tet repressors and/or activators, cDNAs of interest and bar codes for rapid identification using micro-arrays. The currently available bar code systems are based on expression of shRNA and shRNAmir cassettes (Fewell and Schmitt, 2006). shRNAmir transcripts processed by both Drosha and Dicer have higher target specificity and produce more RNAs for incorporation into RISC complexes for subsequent mRNA degradation than standard shRNAs. Recently developed libraries of both shRNA and shRNAmir expressing vectors allow to perform genome-wide screens for gene functions.

2. Aim of the study

The present study had the following aims:

1. To investigate whether c-MYC activation affects the progression through mitosis.
2. To identify direct c-MYC target genes which may affect mitotic progression.
3. To determine whether potential effects of c-MYC on mitosis result in chromosomal instability
4. To develop an episomal vector system for conditional expression of microRNAs.

3. Materials

3.1 Chemicals

Reagent	Supplier
Antifade solution	<i>Vector Laboratories, Ltd., Peterborough</i>
3-Amino-1,2,4-triazole	<i>Sigma-Aldrich GmbH, Deisenhofen</i>
Agarose	<i>PEQLAB Biotechnologie GmbH, Erlangen</i>
Ampicillin	<i>Roche Diagnostics GmbH, Mannheim</i>
Ammonium peroxodisulfate (APS)	<i>Bio-Rad Laboratories GmbH, Munich</i>
Acrylamide	<i>SERVA Electrophoresis GmbH, Heidelberg</i>
Bradford protein assay	<i>Bio-Rad Laboratories GmbH, Munich</i>
Bacto® agar	<i>Becton Dickinson GmbH, Heidelberg</i>
Bacto® tryptone	<i>Becton Dickinson GmbH, Heidelberg</i>
Bacto® yeast extract	<i>Becton Dickinson GmbH, Heidelberg</i>
β-Mercaptoethanol	<i>Merck KGaA, Darmstadt</i>
Bisacrylamide	<i>Carl Roth GmbH & Co, Karlsruhe</i>
Bovine serum albumin (BSA)	<i>New England Biolabs GmbH, Frankfurt</i>
Bromphenol blue	<i>Sigma-Aldrich GmbH, Deisenhofen</i>
Caffein	<i>Sigma-Aldrich GmbH, Deisenhofen</i>
Complete mini protease inhibitor cocktail	<i>Roche Diagnostics GmbH, Mannheim</i>
Coomassie G250	<i>SERVA Electrophoresis GmbH, Heidelberg</i>
Chloramphenicol	<i>Sigma-Aldrich GmbH, Deisenhofen</i>
Chloroquine diphosphate	<i>Sigma-Aldrich GmbH, Deisenhofen</i>
Carbenecillin	<i>Sigma-Aldrich GmbH, Deisenhofen</i>
Deoxynucleotides triphosphate (dNTPs)	<i>ABgene Deutschland, Hamburg</i>
DABCO (1,4-Diazabicyclo[2,2,2]octane)	<i>Sigma-Aldrich GmbH, Deisenhofen</i>
DAPI (2-(4-Amidinophenyl)-6-indolecarb	<i>Sigma-Aldrich GmbH, Deisenhofen</i>
Dithiothreitol (DTT)	<i>Sigma-Aldrich GmbH, Deisenhofen</i>
DMSO	<i>Sigma-Aldrich GmbH, Deisenhofen</i>
Doxycycline hydrochloride	<i>Sigma-Aldrich GmbH, Deisenhofen</i>
DL-p-chlorophenylalanine	<i>Sigma-Aldrich GmbH, Deisenhofen</i>
DMEM (Dulbecco's modified eagle medium)	<i>Invitrogen GmbH, Karlsruhe</i>
Demicolcine solution	<i>Sigma-Aldrich GmbH, Deisenhofen</i>
DNA/RNA oligonucleotides	<i>Metabion GmbH, Martinsried</i>
	<i>MWG Biotech AG, Ebersberg</i>
Ethidium bromide	<i>Carl Roth GmbH & Co, Karlsruhe</i>
Ethanolamine	<i>Sigma-Aldrich GmbH, Deisenhofen</i>
Ethanol	<i>Carl Roth GmbH & Co, Karlsruhe</i>
FuGENE®6 transfection reagent	<i>Roche Diagnostics GmbH, Mannheim</i>
Ficoll® 400	<i>Sigma-Aldrich GmbH, Deisenhofen</i>
Foetal bovine serum (FBS)	<i>Perbio Science Deutschland GmbH, Bonn</i>

Glycogen from mussels	<i>Roche Diagnostics GmbH, Mannheim</i>
Geneticin® (G418)	<i>Invitrogen GmbH, Karlsruhe</i>
Glucose	<i>Sigma-Aldrich GmbH, Deisenhofen</i>
4 hydroxytamoxifen (4-OHT)	<i>Sigma-Aldrich GmbH, Deisenhofen</i>
Hanks' balanced salt solution (HBSS)	<i>Invitrogen GmbH, Karlsruhe</i>
Hygromycin B (HygB)	<i>Invitrogen GmbH, Karlsruhe</i>
Herring sperm carrier DNA	<i>Promega GmbH, Mannheim</i>
HighPerefect	<i>QIAGEN GmbH, Hilden</i>
Isopropanol	<i>Sigma-Aldrich GmbH, Deisenhofen</i>
Kanamycin	<i>Sigma-Aldrich GmbH, Deisenhofen</i>
Lipofectamine™ 2000	<i>Invitrogen GmbH, Karlsruhe</i>
L-Glutamine (200 mM)	<i>Invitrogen GmbH, Karlsruhe</i>
L-arabinose	<i>Sigma-Aldrich GmbH, Deisenhofen</i>
L-rhamnose	<i>Sigma-Aldrich GmbH, Deisenhofen</i>
McCoy's 5A medium	<i>Invitrogen GmbH, Karlsruhe</i>
Methanol	<i>Carl Roth GmbH & Co, Karlsruhe</i>
Nocodazol	<i>Sigma-Aldrich GmbH, Deisenhofen</i>
Nonidet-P40 (NP40)	<i>Sigma-Aldrich GmbH, Deisenhofen</i>
OptiMEM® reduced-serum medium	<i>Invitrogen GmbH, Karlsruhe</i>
Paraformaldehyde	<i>Merck KGaA, Darmstadt</i>
Phenol/chloroform/isoamylalcohol (25/24/1)	<i>Carl Roth GmbH & Co, Karlsruhe</i>
Phosphatase inhibitor cocktail 1	<i>Sigma-Aldrich GmbH, Deisenhofen</i>
Protein A-sepharose®	<i>Sigma-Aldrich GmbH, Deisenhofen</i>
Puromycin dihydrochloride	<i>Sigma-Aldrich GmbH, Deisenhofen</i>
Penicillin-streptomycin	<i>Invitrogen GmbH, Karlsruhe</i>
PageRuler™ prestained protein ladder	<i>Fermentas GmbH, St. Leon-Rot</i>
Propidium Iodid	<i>ICN Biomedicals, CA</i>
Sodium dodecyl sulfate (SDS)	<i>Carl Roth GmbH & Co, Karlsruhe</i>
Sodium orthovanadate	<i>Sigma-Aldrich GmbH, Deisenhofen</i>
Skim milk powder	<i>Fluka Chemie AG, Buchs (CH)</i>
Spectinomycin	<i>Sigma-Aldrich GmbH, Deisenhofen</i>
Triton X-100	<i>Carl Roth GmbH & Co, Karlsruhe</i>
Tetracycline	<i>Sigma-Aldrich GmbH, Deisenhofen</i>
Tween® 20	<i>Sigma-Aldrich GmbH, Deisenhofen</i>
YPD-agar / YPD-broth	<i>Sigma-Aldrich GmbH, Deisenhofen</i>
Yeast nitrogen base without amino acids	<i>Fisher Scientific GmbH, Schwerte</i>

3.2 Reagents

Reagent	Supplier
Alkaline phosphatase, shrimp (1 U/ μ l)	<i>Roche Diagnostics GmbH, Mannheim</i>
DNase I, RNase-free (10 U/ μ l)	<i>Roche Diagnostics GmbH, Mannheim</i>
FIREPol® DNA polymerase (5 U/ μ l)	<i>Solis BioDyne, Tartu (EE)</i>
Platinum® Taq DNA polymerase (5 U/ μ l)	<i>Invitrogen GmbH, Karlsruhe</i>
Restriction endonucleases (3-50 U/ μ l)	<i>Fermentas GmbH, St. Leon-Rot</i>
	<i>New England Biolabs GmbH, Frankfurt</i>
	<i>Promega GmbH, Mannheim</i>
RNase A	<i>Sigma-Aldrich GmbH, Deisenhofen</i>
T4 DNA ligase (400 U/ μ l)	<i>New England Biolabs GmbH, Frankfurt</i>
Trypsin-EDTA	<i>Invitrogen GmbH, Karlsruhe</i>
Proteinase K	<i>Sigma-Aldrich GmbH, Deisenhofen</i>

3.3 Antibodies

3.3.1 Primary antibodies

Antibody	Supplier
Rabbit polyclonal anti- β -actin	<i>Sigma-Aldrich GmbH, Deisenhofen</i>
Mouse monoclonal anti- α -tubulin	<i>Sigma-Aldrich GmbH, Deisenhofen</i>
Mouse monoclonal anti- γ -tubulin	<i>Sigma-Aldrich GmbH, Deisenhofen</i>
Mouse monoclonal anti-Mad2	<i>BD Biosciences Pharmingen</i>
Mouse monoclonal anti- γ -H2AX (Ser139) clone JBW301	<i>Upstate cell signaling solutions, CA</i>
Mouse monoclonal [8G1] anti-BubR1 (ab4637)	<i>BIOZOL Diagnostica Vertrieb GmbH, Eching</i>
Rabbit polyclonal anti-c-Myc (sc-764)	<i>Santa Cruz Biotechnology, California</i>
Rabbit anti mouse IgG (M-7023)	<i>Sigma-Aldrich GmbH, Deisenhofen</i>

3.3.2 Secondary antibodies

Antibody	Supplier
Goat anti-mouse IgG HRP-conjugate	<i>Promega GmbH, Mannheim</i>
Goat anti-rabbit IgGHRP-conjugate	<i>Sigma-Aldrich GmbH, Deisenhofen</i>
Goat anti-mouse IgG Cy3-conjugate	<i>Jackson ImmunoResearch Laboratories, Inc. Newmarket</i>

3.4 DNA constructs

Plasmid	Refernce/Supplier
pRTS-1	<i>Bornkamm et al., 2005</i>
pEMI	<i>Epanchintsev et al., 2006</i>
pShumi	<i>Epanchintsev et al., 2006</i>
TOPO-TA vector (pCR®4-TOPO)	<i>Invitrogen GmbH, Karlsruhe</i>

LMP	<i>Dickins et al., 2005</i>
TMP	<i>Dickins et al., 2005</i>
pPRIME	<i>Stegmeier et al., 2005</i>
pSMc2	<i>Open Biosystems</i>
pUC19	<i>University of California</i>
pSuper	<i>Brummelkamp et al., 2002b</i>
pRetroSuper	<i>Brummelkamp et al., 2002a</i>
pMYC-eYFP-N1	<i>Koch et al., 2007</i>
pLPCX - H2B-GFP	<i>Gift from Stephen Taylor</i>
pcDNA3.1-H2B-YFP	<i>Gift from Dmitri Lodygin</i>
pMK10tTA	<i>Gift from Bert Vogelstein</i>

3.5 Bacteria strains

Bacteria strain	Genotype	Reference/Supplier
DH10 β F'FOT sbcC	mcrA Δ (mrr-hsdRMS-mcrBC) ϕ 80lacZ Δ M15 Δ lacX74 deoR recA1 end A1 ara Δ 139 Δ (ara,leu)7697 galU galK λ^- rpsL nupG tonA umuC::pir116-frt F'(lac ⁺ pro ⁺ Δ oriT::Tc) sbcC::Frt	<i>Li et al. 2005</i>
BW287051/pML300	Laclq rrnB3 Δ lacZ4787 hsdR514 Δ (araBAD)567 Δ (rhaBAD)568 galU95 Δ endA9::FRT Δ recA635::FRT umuC::ParaBAD-I-SceI-FRT + pML300(PrhaB- γ β exo Ts(ori) Spectinomycin resistant)	<i>Li et al. 2005</i>
E. coli XL1-Blue	endA1 gyrA96 hsdR17 lac- recA1 relA1 supE44 thi-1 [F' laclq Z Δ M15, proAB, Tn 10, TetR]	<i>Stratagene GmbH, Heidelberg</i>

3.6 Disposable kits

Product	Supplier
TOPO-TA cloning kit for sequencing	<i>Invitrogen GmbH, Karlsruhe</i>
BigDye® terminator v3.1 sequencing mix	<i>Applied Biosystems GmbH, Darmstadt</i>
FastStart-DNA Master SYBR Green 1 kit	<i>Roche Diagnostics GmbH, Mannheim</i>
RNAagent RNA isolation kit	<i>Promega GmbH, Mannheim</i>
Ribomax T7 in vitro transcription kit	<i>Promega GmbH, Mannheim</i>
SuperScript™ III first strand cDNA synthesis kit	<i>Invitrogen GmbH, Karlsruhe</i>
QIAGEN Plasmid Maxi Kit	<i>QIAGEN GmbH, Hilden</i>
QIAprep Spin Miniprep Kit	<i>QIAGEN GmbH, Hilden</i>
QIAquick Gel Extraction Kit	<i>QIAGEN GmbH, Hilden</i>
QIAquick PCR Purification Kit	<i>QIAGEN GmbH, Hilden</i>
Nucleotide removal kit	<i>QIAGEN GmbH, Hilden</i>
3MM Whatman® filter paper	<i>Whatman GmbH, Dassel</i>
Immobilon-P PVDF Transfer Membrane	<i>Millipore GmbH, Schwalbach</i>

Pierce ECL Western blotting substrate	<i>Pierce Biotechnology Inc., Rockford</i>
Western Lightning® Western Blot Chemiluminescence Reagent Plus	<i>PerkinElmer GmbH, Cologne</i>
0.45 µm Millex-HV filter units	<i>Millipore GmbH, Schwalbach</i>
CELLocate gridded cover slips	<i>Eppendorf, Hamburg</i>
Costar® Spin-X tubes	<i>Corning GmbH, Kaiserslautern</i>
Lab-Tek® II Chamber Slide™ System	<i>Nunc GmbH & Co. KG, Wiesbaden</i>
Tissue culture plastic ware	<i>Corning GmbH, Kaiserslautern</i>
	<i>Greiner bio-one, Frickenhausen</i>
	<i>Nunc GmbH & Co. KG, Wiesbaden</i>
Dual-Luciferase® Reporter Assay System	<i>Promega GmbH, Mannheim</i>

3.7 Laboratory equipment

Reagent	Supplier
Axiovert 25 microscope	<i>Carl Zeiss GmbH, Oberkochen</i>
Axiovert 200M fluorescence microscope	<i>Carl Zeiss GmbH, Oberkochen</i>
Microscope Temperature Control System	<i>Life Imaging Services, Reihnach</i>
Ludin chamber	<i>Life Imaging Services, Reihnach</i>
CoolSNAP™-HQ CCD camera	<i>Photometrics, Tucson (USA)</i>
DXC-390P 3CCD camera	<i>Sony Electronics Inc., Tokyo (JP)</i>
HyperHAD CCD camera	<i>Sony Electronics Inc., Tokyo (JP)</i>
KODAK Image Station 440CF	<i>Eastman Kodak Company, Rochester (USA)</i>
KODAK Molecular Imaging Software	<i>Eastman Kodak Company, Rochester (USA)</i>
MetaMorph® software	<i>Universal Imaging, Downingtown (USA)</i>
GeneAmp® PCR System 9700	<i>Applied Biosystems, Foster City (USA)</i>
LightCycler™ real-time PCR system	<i>Roche Diagnostics GmbH, Mannheim</i>
Mini-PROTEAN® electrophoresis system	<i>Bio-Rad Laboratories GmbH, Munich</i>
Mini Trans-Blot® cell system	<i>Bio-Rad Laboratories GmbH, Munich</i>
BioPhotometer	<i>Eppendorf, Hamburg</i>
Neubauer counting chamber	<i>Carl Roth GmbH & Co, Karlsruhe</i>
Z1™ series Coulter counter®	<i>Coulter electronics, Beds (UK)</i>
Phosphoimager BAS-2500	<i>Fuji, Tokyo</i>
FACScan unit	<i>BD Biosciences, Mountain View (USA)</i>
Tissue culture Lamin Air®	<i>Heraeus Sepatech GmbH, Osterode</i>
Incubator for cell culture	<i>Heraeus Sepatech GmbH, Osterode</i>
Sonicator Bandelin Sonopuls HD 70 w. MS73 Sonotrode (3 mm))	<i>Bandelin Electronic GmbH & Co. KG, Berlin</i>

4. Methods

4.1 Bacterial cell culture

4.1.1 Propagation of bacteria strains

E. coli XL1-Blue bacteria strain was used for all conventional cloning procedures and grown at 37°C. DH10 β F'FOT sbcC and BW287051/pML300 were used as a donor and recipient strains for mating experiments and grown at 37 and 30°C. Luria-Bertani broth was used as complex medium for cloning and for growth of donor and recipient plasmids. To maintain plasmids, were added antibiotics as follows: ampicillin (100 μ g/ml), kanamycin (50 μ g/ml), chloramphenicol (30 μ g/ml), tetracycline (25 μ g/ml) and spectinomycin (50 μ g/ml). To reduce the background on plates after recombination carbeneicillin (100 μ g/ml) as a stronger antibiotic was used instead of ampicillin. IPTG (0.4 mM), L-arabinose (0.2% w/v) and L-rhamnose (0.2% w/v) were used to induce the P_{lac}, P_{araBAD} and P_{rheB} promoters, respectively. For conventional cloning transformed *E. coli* XL1-Blue was plated on LB-agar plates. Chloramphenicol agar plates (0.5% w/v yeast extract, 1% w/v NaCl, 0.4% w/v glycerol, 2% w/v agar, 10 mM DL-p-CI-Phe and 0.2% w/v arabinose) and the appropriate amounts of antibiotics for the counterselective marker *PheS* Gly294 were used in the final selection step.

Competent bacteria of all used strains were generated by resuspension of lag-proliferating bacteria in TSS-buffer and further freezing in nitrogen.

4.1.2 Mating-assisted genetically integrated cloning (MAGIC)

Ligation-free gene transfer using the MAGIC system was done essentially as described (Li and Elledge, 2005). In brief, the donor bacterial strain (DH10 β F'DOT sbcC, PIR1 positive) was transformed with a p53-specific pSM2c vector and grown on kanamycin containing LB plates at 37°C. The recipient strain (BW287051/pML300) was transformed with pEMI-recipient and grown in the presence of ampicillin, spectinomycin and glucose on LB plates at 30°C. Donor and recipient colonies were used to inoculate overnight liquid cultures. The recipient strain was washed twice with LB. Both donor and recipient bacteria were diluted 1:50 with LB/0.2% (w/v) L-rhamnose and grown at 30°C until an OD₆₀₀ of 0.15-0.25. The bacteria were mixed for conjugation in the presence of 0.2% (w/v) L-arabinose and incubated at 37°C for 2 h without and for

2 h with agitation. Recombinant bacteria were plated on a chloramphenicol agar plates and incubated at 42°C overnight. Recombination events were detected by colony PCR using the primers (CmR-fw: 5'-CCGTTTGTGATGGCTTCCATGTC-3' (corresponding to the chloramphenicol resistance) and pEMI-rev 5'-AATCAAGGGTCCCCAAACTC-3' (matching to pEMI).

4.2 Generation of plasmids

4.2.1 pSHUMI/pEMI vector construction

For generation of the shuttle vector pSHUMI the oligos pUC19linker-fw 5'-AATTGGGCCTCACTGGCCACCGGAGATCTGTGACGGACGCGTACCGGTG-3' and pUC19linker-rv 5'-TCGACACCGGTACGCGTCCGTGACAGATCTCCGGTGGCCAGTGAGGCC-3' were annealed and inserted into the *EcoR* I/*Xho* I sites of pUC19 resulting in pUC19m. A *Bgl* II/*Age* I fragment containing miR30 sequences from the LMP plasmid (Dickins et al., 2005) was inserted into the *Bgl* II/*Age* I sites of pUC19m. The resulting pSHUMI plasmid can be used to sub-clone short hairpin sequences using the *Xho* I and *EcoR* I restriction sites.

For generation of the pEMI vector, regions containing 5'miR30 and homology region 2 (HR2) were amplified from pSM2c (Silva et al., 2005) using the primers 5'miR30-fw 5'-CGAGATCTTGTGTTGAATGAGGCTTCAGTAC-3' and 5'miR30-rev 5'-GCACCGGTGCGGCCGCCTCGAGCCTTCTGTTGGGTTAACC-3' and HR2-fw 5'-CGCTCGAGATCCATGGCATATGGGATCCAAGGCAGTTATTGGTGCCCTTAAAC-3' HR2-rev 5'-GCACCGGTTTCAGATCCTCTTCGGAGATCAG -3' and inserted into the pTOPO vector (Invitrogen). The 5'miR30 part was subcloned into pSHUMI using *Bgl* II/*Age* I restriction sites and the HR2 region was introduced using *Xho* I/*Age* I restriction sites. The PheS expressing cassette was released from pBSPheS (Li and Elledge, 2005) using *Nco* I/*Bgl* II and ligated between the 5'miR30 and HR2 sequences into the *Nco* I/*Bam*H I sites. From the resulting vector a fragment containing the 5'miR30/PheS/HR2 region was released by *Sfi* I and inserted into the *Sfi* I sites of pRTS-1 resulting in pEMI (plasmid for episomal microRNAs).

4.2.2 Restriction mediated microRNA transfer

A p53-specific hairpin was released from pSM2c (Oligo ID: v2HS_93615, current accession: NM_000546) (Silva et al., 2005) using *Xho* I / *EcoR* I and inserted into

pSHUMI. MAD2-specific microRNA were generated in 2-step PCR: the primers fw 5'-tgctgttgacagtgagcgCTGGGAAGAGTCGGGACCACAGtagtgaagccacagatg-3' and rv 5'-tccgagcagtaggcaATGGGAAGAGTCGGGACCACAGtacatctgtggcttcac-3' were annealed, extended by PCR and amplified using universal miR30XhoI/EcoRI primers (miR30Xho I Fw: 5'-CAGAAGGCTCGAGAAGGTATATTGCTGTTGACAGTGAGCG-3', miR30EcoR I Rv: 5'-CTAAAGTAGCCCCTTGAATTCGAGGCAGTAGGCA-3'). The resulting fragment was cut with *Xho* I and *Eco*R I and inserted into pSHUMI. The *Sfi* I fragments from pSHUMI containing the microRNA cassettes were inserted into pRTS-1 (Bornkamm et al., 2005).

4.2.3 Subcloning shRNA constructs into pRetroSuper

Synthetic sense and antisense oligonucleotides specifically targeting the DP1 (target sequence: ATGGCAAAGATGCCGGTC), *MAD2* (n1-CTGGGAAGAGTCGGGACCA, n2- TACGGACTCACCTTGCTTG) or *BubR1* (n1-AGATCCTGGCTAACTGTTC, n2- AAGGGTTCAGAGCCATCAG) mRNA and a non-silencing control (CTCGCTTGGGCGAGAGTAA) oligonucleotides were annealed, subjected to one PCR cycle, restricted and ligated into the pSUPER vector backbone. The hairpin-containing cassette was excised with *Eco*R I and *Xho* I, and subcloned into pRetro-SUPER (Brummelkamp et al., 2002). The insert was confirmed by sequencing.

4.3 Cell culture and treatment

The human colorectal cancer cell lines HCT116 and DLD-1 were maintained in McCoy's 5A supplemented with 10% fetal bovine serum, U2Os and MCF-7/PJMMR1 in DMEM with 10% FBS, LS174-T in RPMI with 5% FBS and the 293T-derived packaging cell line Phoenix-A in DMEM supplemented with 5% FBS. RAT1A fibroblasts (TGR-1 and HO15.19) and P493-6 B-cells were maintained as described previously (Hermeking et al., 2000). All cell lines were cultivated in presence of 100 units/ml penicillin and 0.1 mg/ml streptomycin. Etoposide was resolved in DMSO (40 mg/ml) and used at a final concentration of 20 µg/ml. Poly I:C (Sigma) was resolved in water (10 mg/ml) and used at a final concentration of 10 µg/ml.

4.4 Generation of cell lines

DLD-1 cells stably expressing a tetracycline regulated transactivator (DLD-1-tTA) were a kind gift from Bert Vogelstein (Yu et al., 1999). DLD-1-tTA cells were transfected with pBI-c-MYC-HA and pTK-Hyg and selected in hygromycin B (250 µg/ml) and G418 (500 µg/ml). After limiting dilution the clone DLD-1-tTA-MYC was characterized by Western blot analysis and indirect immunofluorescence (supplemental Figure 4). DLD-1-tTA-MYC cells were transfected with pcDNA3.1-H2B-YFP and cultured in the presence of G418 (1 mg/ml) for two weeks, FACS-sorted for YFP expression and subjected to limiting dilution to generate single cell clones positive for H2B-YFP expression in the presence of 500 ng/ml DOX. The generation of MCF-7 cell lines conditionally expressing c-MYC (PJMMR1) under control of a tet-on system will be described elsewhere (Jung and Hermeking, *in preparation*). For virus production Phoenix-A packaging cells were transfected either with pRetro-SUPER-shcontrol, pRetro-SUPER-shMAD2 (n1 or n2) or pRetro-SUPER-shBubR1 (n1 or n2) using calcium phosphate precipitation. Twenty-four hours after transfection, retrovirus containing supernatants were harvested, passed through 0.45 µm filters and used to infect DLD-1-H2B-YFP or PJMMR1 cells in the presence of polybrene (8 µg/ml) four times in four hour intervals. Twenty-four hours after infection the cells were split 1:10 and selected for 10 days in the presence of 1-2 µg/ml puromycin. To visualize chromatin the resulting pools of resistant PJMMR1 cells were infected with a pLPCX retroviral vector expressing a H2B-GFP fusion protein.

U2OS osteosarcoma cells were transfected by lipofection with pEMI-plasmids using FuGene reagents according to the manufacturer. After 48 hours cells were selected in media containing 150 µg/ml hygromycin for 7 days. Homogeneity of the selected cell pools was tested by addition of 100 ng/ml doxycycline for 24 hours and mRFP-fluorescence detection.

4.5 Western blot analysis

Cells were lysed for 15 minutes in RIPA buffer (50 mM Tris-HCl pH 7.4, 150 mM NaCl, 1 mM EDTA, 1% NP-40, 0.1% SDS, 0.25% Na-deoxycholate, 1 mM PMSF, 1 mM Na₃VO₄, protease inhibitor mixture (Complete Mini, Roche)). After sonication lysates were centrifuged for 20 minutes and 30-80 µg of protein were separated by gel electrophoresis using 9% or 12% TRIS-glycine gels. The proteins were transferred

onto PVDF membranes. After drying and brief incubation in methanol, the membranes were blocked with 10% skim milk/TBS-T (0.1% Tween-20) for 1-2 hours. The primary antibody was incubated in TBS-T. The membranes were washed and after using the respective HRP-conjugated secondary antibodies and washing with TBS, signals were obtained with enhanced chemiluminescence reagent, and recorded with a 440CF Kodak imaging system. Primary antibodies specific for c-MYC, MAD2, BubR1, p-53, p21, α -tubulin and β -actin were used.

4.6 DNA content analysis by FACS

5×10^4 U2OS or MCF7 cells were plated into T25 cell culture flasks. Floating cells and trypsinized cells were collected by centrifugation at 1.700 rpm for 7 minutes, cells were fixed with ice cold 70% ethanol and stored over night on ice. After washing with PBS, 1 ml FACS solution (PBS, 0.1% Triton X100, 60 μ g/ml propidium iodide (PI), 0.5 mg/ml DNase free RNase) was added per sample and incubated at room temperature for 30 min. DNA content was determined by propidium iodide staining.

4.7 Indirect immunofluorescence

Cells were fixed in 4% paraformaldehyde/PBS for 8 min, permeabilized in 0.2% Triton X-100 and blocked in 100% FBS. For detection of epitopes the following primary antibodies were used: anti-HA and α - or γ -tubulin. Images were acquired using 100x and 63x oil-immersion objectives and the MetaMorph software package.

4.8 Micronucleus assessment

Cells were washed with PBS and fixed in 4% formaldehyde/PBS at room temperature for 10 minutes. After washing with PBS, cells were incubated for 1 h at 37°C in PBS with 1 μ g/ml 4',6-diamidino-2-phenylindole (DAPI) and then embedded in antifade solution supplemented with 5 μ g/ml DAPI. Micronuclei were microscopically determined as rounded chromatin fragments located adjacent to nuclei, with a diameter not exceeding one third of the diameter of the neighbouring nucleus. Microscopic analysis was performed with a 630x magnification.

4.9 Quantitative real-time PCR

qPCR was performed using the LightCycler instrument and the FastStart DNA Master SYBR Green 1 kit (Roche Applied Science) as described previously (Menssen and Hermeking, 2002). Primer pairs were in use:

Primer name	qPCR primer
DKC frw	CGGCTGGTTATGAAAGAC
DKC rev	TGGTCGCAGGTAGAGATG
MAD2 frw	CCTGGAAAGATGGCAGTTTG
MAD2 rev	GTAATGAACGAAGGCGGACT
BubR1 fwr	CTCTGGCTTCTCTGGTTCTTCT
BubR1 rw	CAACTTAGGCATTGGTCTGTCTT
PHB frw	CAGGTGGCTCAGCAGGAAGC
PHB rev	TGAAGTGATTTTACCTTTATTTCC
β -actin frw	TGACATTAAGGAGAAGCTGTGCTAC
β -actin rev	GAGTTGAAGGTAGTTTCGTGGATG
DP-1 fwr	ATGGCAAAGATGCCGGTC
DP-1 rev	GTCGTCCTCGTCATTCTCGTT
IFIT1-frw	GCCATTTTCTTTGCTTCCCCTA
IFIT1-rev	TGCCCTTTTGTAGCCTCCTTG
Mad2-specific-microRNA-frw	GATGTACTGTGGTCCCGACTCT
Mad2-specific-microRNA-rev	TCAAAGAGATAGCAAGGTATTCAGT
Primer name	ChIP qPCR primer
16q22/6000+frw	CTACTCACTTATCCATCCAGGCTAC
16q22/6000+ rev	ATTTACACACTCAGACATCACAG
CAD PCR-I frw	CCGCAGTCTCTGCTGCTG
CAD PCR-I rev	ATACGGAAAACGGGAAGGAC
CAD PCR-A frw (control)	TGGGTTTGGTAGGGGACATA
CAD PCR-A rev (control)	CTGGGCTCTGCTGGCTTA
MAD2 ebC1 frw	GACATCCTCTAGCCTCATAATCTG
MAD2 ebA rev	CAGCTATAAATGACTGAACACAC
MAD2 I4 frw	GCTGGCATCACTATTCTTGTG
MAD2 I4 rev	AGGTCATTTGGCTTGGTCTC
BubR1 fwr	GACACGGCCTGGTAGGTAAT
BubR1 rev	GCAGCCTTCTTCGCTTTG

4.10 Chromatin immunoprecipitation

Chromatin immunoprecipitations (ChIP) were performed as described previously (Frank et al., 2001). PJMMR1 cells at <70% confluence were fixed in 1% formaldehyde. Chromatin was sheared to an average size of 500 bp by sonication (4x 20sec on ice with 90sec intervals) at continuous maximum power setting. After pre-clearing with pre-blocked protein A beads for 1 hour, lysates were rotated at 4°C for 18 hours with a polyclonal antibody specific for c-MYC or rabbit anti mouse IgG. Washing and reversal of cross-linking was performed as described previously (Frank et al., 2001). Purified DNA was first analyzed by amplification of a genomic fragment from chromosome 16q22 that did not display any E-boxes up to 3 kb up- and downstream. This amplification product was used to control for equal DNA input into the PCR reactions. For the analysis of c-MYC binding to the MAD2 locus equal amounts of DNA were analyzed by PCR with a primer pair flanking the two E-boxes in the first intron of the human *MAD2* gene. A second primer pair spanning the exon 4 intron 4 boundaries was used to control for specificity of localized E-box binding. For analysis of *BubR1* a primer pair flanking an E-box in the first intron of the *BubR1* genomic region was used. All PCR reactions were analyzed in the exponential phase. Enrichment of DNA-fragments bound by c-MYC was documented by gel-electrophoresis and ethidium bromide staining. For oligonucleotide sequences see qPCR ChIP primer list in qPCR section.

4.11 Time-lapse microscopy

H2B-YFP/GFP pools were seeded in a 6 well plate and cultured for 36 hours before time lapse imaging. DOX concentrations were 100 ng/ml and 1 μ g/ml for DLD-1 tTA Myc and PJMMR1 cells, respectively. Six hours before recording the cells were placed on inverted Axiovert 200M microscope surrounded by a chamber which provided a constant temperature of 37°C and a humidified atmosphere of 5% CO₂. Images were recorded with a CCD camera and processed with the software MetaMorph. Digital pictures of phase contrast (100 ms) and YFP/GFP fluorescence (20-100 ms) were taken from four different positions of two separate wells for each state (with or without DOX) every 5 minutes over a period of 18 hours. Between the exposures cells were not exposed to halogen or UV light as it was blocked by a non-transparent position in a motorized condenser. Allocation of individual frames to a particular stage of mitosis was done according to following criteria. In prophase, the

cell shape begins to change to rounded morphology and the chromatin condenses to the level of grain-like structure throughout nucleus and the nucleus itself slightly changes its shape before nuclear envelope breakdown. The following breakage of nuclear envelope determines beginning of pro-metaphase. After nuclear envelope completely dissolves, further condensation of chromatin is continued until distinct chromosomes are formed and organized in a plate. The metaphase was defined as a short stage, during which chromosomes clearly align in metaphase plate without any appearance of lagging chromosomes. The anaphase was defined as a stage when separation of sister chromatids to the opposite poles takes place. The duration of telophase was determined as time period between complete separation of chromatids and complete decondensation of chromatin in one of the daughter cells. Since sequential frames were taken in 5 minutes interval, minor changes in duration of specific stages were not detected.

4.12 Tissue samples and immunohistochemistry

15 consecutive cases of sporadic colorectal carcinomas were retrieved from the archives of the Institute of Pathology. All carcinomas were WHO grade 2 or 3. None of the patients had undergone cancer therapy before surgical resection of the lesions. For immunohistochemistry we used biopsies from diagnostic colonoscopies to ensure that the tumor tissue had been immediately fixed in neutral 4% buffered formalin. The primary antibodies applied were a c-MYC-specific (N-term) rabbit monoclonal (Epitomics) and a MAD2-specific mouse monoclonal (BD Transduction). Sections were deparaffinized and pretreated by microwave (750 W, 2 × 15 min) in TUF target unmasking fluid (Dako) for c-MYC and target retrieval solution (Dako) for MAD2. Sections were covered with hydrogen peroxide at a final concentration of 7.5% for 10 minutes and then blocked with serum (Vector, Vectastain ABC Kit Elite Universal). Primary antibody (c-MYC) was used at a dilution 1:20, MAD2 1:50 for 60 min. For detection a biotinylated secondary antibody was used (Vector, Vectastain ABC Kit Elite Universal). Sections were treated with chromogen (AEC Zymed) for 10 min and counterstained with hematoxylin Gill's Formula (Vector).

4.13 Statistical analysis

The Chi square test was used to determine statistical significance in comparisons of micronucleus frequencies. In the figures, if not indicated explicitly columns and bars show the mean and standard deviation, respectively.

5. Results

5.1 c-MYC directly transactivates *MAD2* and *BubR1* genes

MAD2 mRNA induction was identified in a micro-array analysis of genes expression altered upon adenoviral expression of c-MYC in primary human endothelial cells (Menssen et al., data not shown). These data were independently confirmed by quantitative, real-time PCR (qPCR) in two additional cell types: *MAD2* mRNA was induced after activation of a tetracycline regulated c-MYC allele in the B-cell line P493-6 (Menssen et al., data not shown) and in the breast cancer cell line MCF-7/PJMMR1 (Figure 5 a).

The induction of *MAD2* by c-MYC motivated us to analyze whether other important components of the SAC are also induced by c-MYC. *CDC20*, *BubR1*, *Bub1*, *Bub3*, *MPS1*, *MAD1*, *Cenp-E* and *Cenp-J* were inspected for the presence of E-boxes in close proximity to transcriptional start site (+/- 2 kbp) and for a significant induction of mRNA in the micro-array data sets of genes induced by c-MYC. Furthermore, a micro-array screen in PJMMR1 cells harboring an inducible c-MYC allele, revealed that *BubR1* mRNA was up-regulated upon c-MYC activation (Jung et al., unpublished results). The induction of *BubR1* mRNA was confirmed by qPCR analysis (Figure 5b).

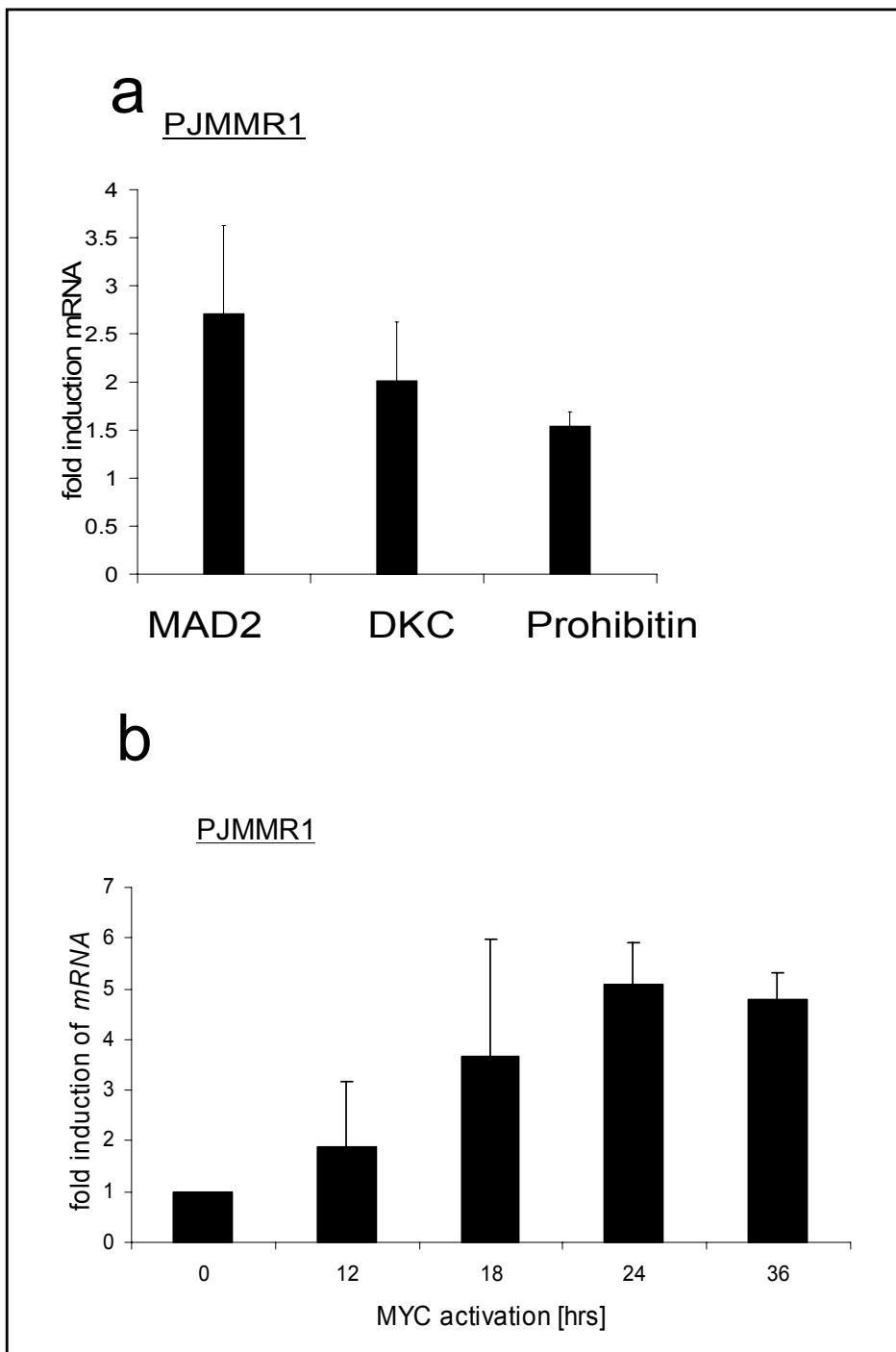


Figure 5 Quantitative real-time PCR (qPCR) analysis of *MAD2* and *BubR1* mRNA expression in PJMMR1 cell lines

(a) qPCR determination of mRNA expression after activation of a conditional *c-MYC* allele in MCF-7 cells. PJMMR1 cells were treated with 1 $\mu\text{g/ml}$ of the anti-estrogen ICI 182,780 for 72 hours. For induction of ectopic *c-MYC*, 1 $\mu\text{g/ml}$ doxycycline was added for 12 h. Fold induction of the indicated mRNAs was determined by qPCR relative to β -actin in biological triplicates. The induction of the known *c-MYC* target *Prohibitin* served as positive controls. (the analysis was performed by Dr. Antje Menssen, MPI of Biochemistry). **(b)** qPCR determination of *BubR1* mRNA expression after *c-MYC* activation in MCF7 cells. PJMMR1 cells were treated as described in **(a)** and then stimulated with 1 $\mu\text{g/ml}$ of DOX for the indicated periods. Relative induction of *BubR1* mRNA in comparison to β -actin mRNA was determined by qPCR in three independent experiments.

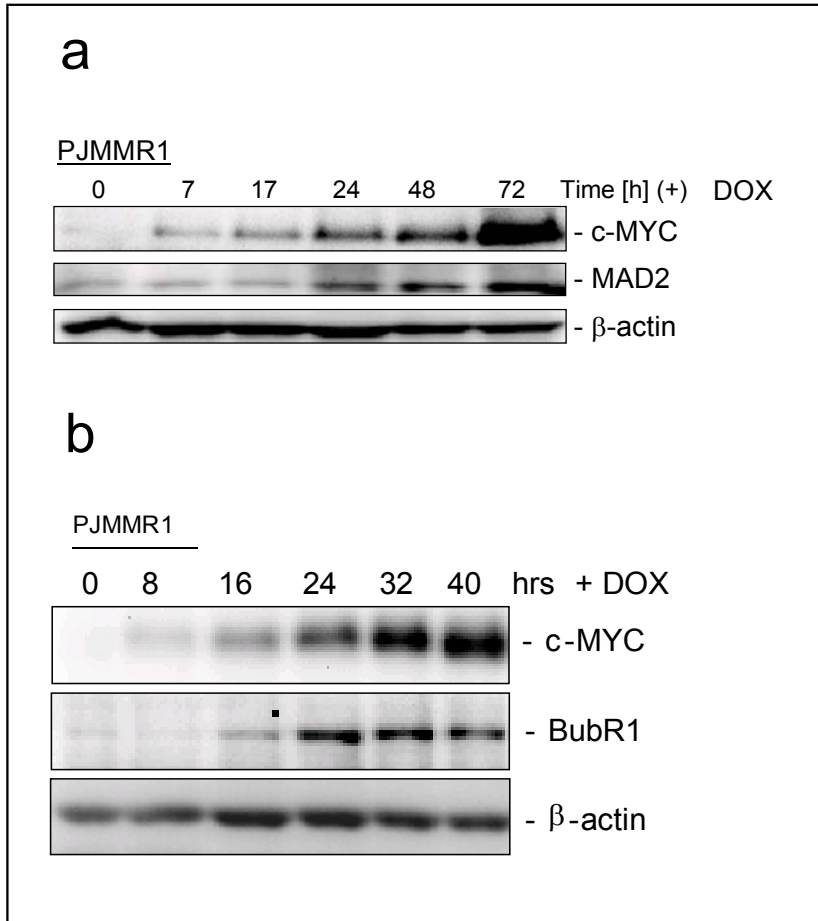


Figure 6 Increase of *MAD2* and *BubR1* proteins level upon activation of c-MYC expression

(a) Cells were treated as described in Figure 1 b. Lysates obtained at the indicated time points were subjected to Western blot analysis to detect the indicated epitopes. β -actin served as loading control. (the analysis was performed by Dr. Antje Menssen, MPI of Biochemistry). (b) Western blot analysis of BubR1 protein expression after c-MYC activation in PJMMR1 cells. Cells were treated as in (Figure 5 b) and lysates were subjected to Western blot analysis. The membrane was probed for c-MYC and BubR1 epitopes, β -actin served as loading control.

The increase in *MAD2* and *BubR1* mRNAs was accompanied by an increase in *MAD2* and *BubR1* protein in PJMMR1 after activation of c-MYC (Figure 6, a and b). The induction of these genes was also found in the colorectal cancer cell line DLD-1 harboring a conditional c-MYC allele (Figure 11, a and b). Taken together these results suggested that c-MYC may directly regulate *MAD2* and *BubR1* expression.

To prove that c-MYC can directly activate *MAD2* expression, and exclude indirect transcriptional activation through the E2F transcription machinery (Hernando et al., 2004; Sears et al., 1997), c-MYC dependent *MAD2* induction was studied in the

presence of inhibition of DP-1, which heterodimerizes with E2F and is necessary for DNA binding. The down-regulation of DP-1 was achieved by retroviral infection of shRNA expressing construct directed against *DP1* and confirmed on mRNA level by qPCR (Figure 7a).

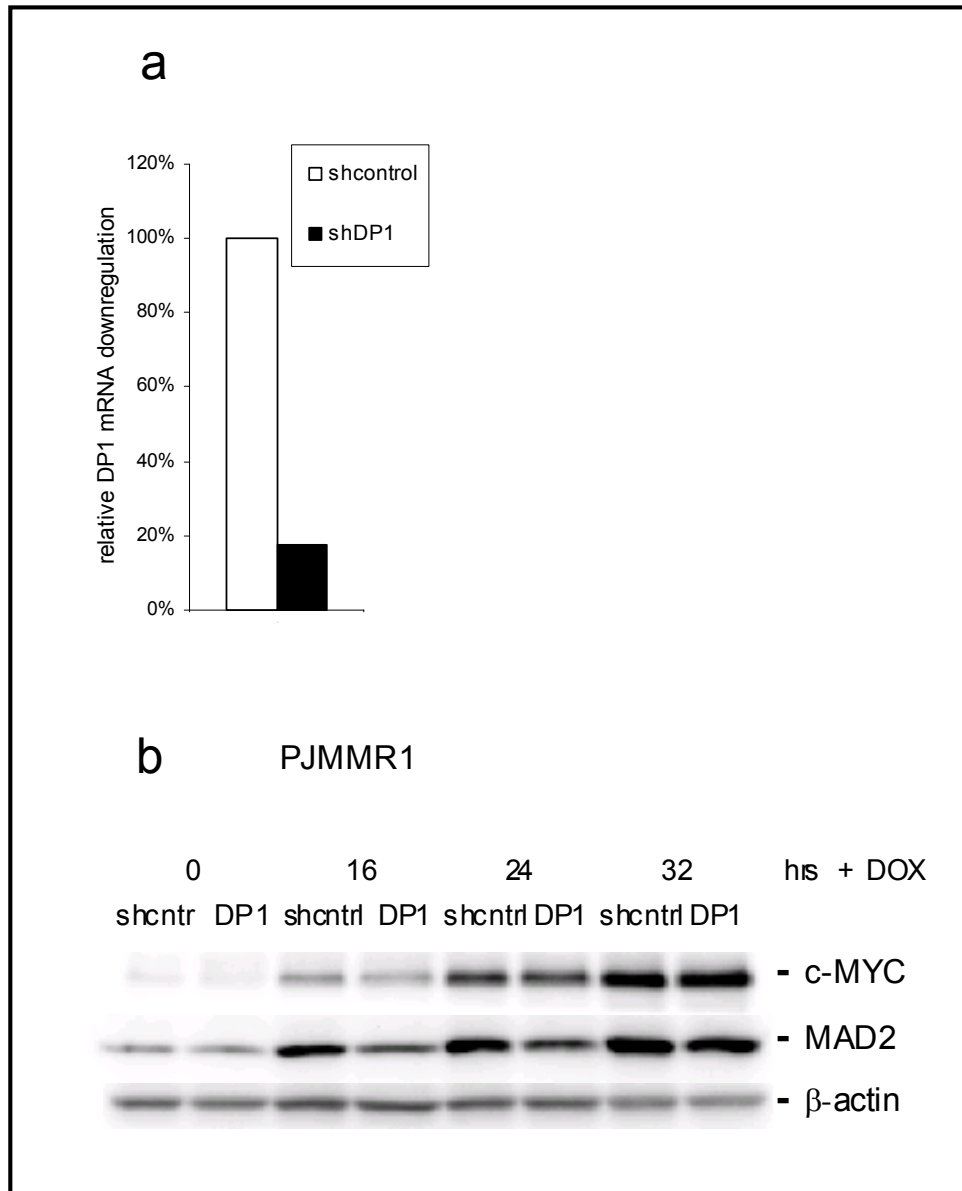


Figure 7 c-MYC induces *MAD2* protein expression in the presence of DP1 knockdown

(a) Analysis of *DP1* mRNA expression in PJMMR1 cell lines. Relative fold of mRNA reduction was measured by qPCR analysis in PJMMR1 cells infected either with non-silenced retroviral construct or expressing a shRNA directed against the *DP1* coding region. (b) Western blot analysis of *MAD2* protein induction upon activation of a conditional c-MYC allele in PJMMR1 cells. Cells were treated as describe in Figure 6b. Protein lysates were harvested at the indicated time points. The membrane was probed against the indicated epitopes, with β -actin serving as a loading control.

The efficiency of the E2F pathway inactivation was confirmed by RT-PCR analysis for the genes controlled either by E2F1, c-MYC or not involved in transcriptional

regulation by them (data not shown). In the presence of a DP1 knockdown c-MYC activation was attenuated, but still resulted in a pronounced induction of *MAD2* protein (Figure 7b).

5.2 c-MYC binds to human *MAD2* and *BubR1* promoters *in vivo*

Examination of the human *MAD2* (*MAD2L1*) promoter revealed the presence of two canonical E-box sequences, which represent putative c-MYC binding sites, separated by 90 base pairs in the first intron (Figure 8a). Chromatin-immunoprecipitation (ChIP) analysis confirmed *in vivo* binding of c-MYC to the E-boxes in the first intron of the human *MAD2* gene, whereas a region located ~6 kbp downstream in the 4th intron was not bound by c-MYC (Figure 9a). Enrichment of the fragment amplified from the first intron of *MAD2* was detected after activation of a conditional c-MYC allele. As a positive control, promoter occupation by c-MYC was also detected for the known c-MYC target gene *CAD*.

The promoter element of the *BubR1* gene was also investigated for the presence of E-boxes, where one E-box was found in the first intron in close proximity to its transcriptional start site (Figure 8b). Using the same conditions as for *MAD2* ChIP analysis, it was confirmed that c-MYC occupies this site *in vivo* (Figure 9a), whereas a region located ~10 kbp upstream of the promoter was not bound by c-MYC (data not shown). Therefore, c-MYC directly regulates *MAD2* and *BubR1* expression.

Both *MAD2* and *BubR1* promoter regions in mouse and rat also contain several E-boxes. However, positions of these E-boxes were not conserved between species (Figure 8, a and b). A similar divergence in the positioning of E-boxes has been described for *bona fide* c-MYC target genes (Haggerty et al., 2003).

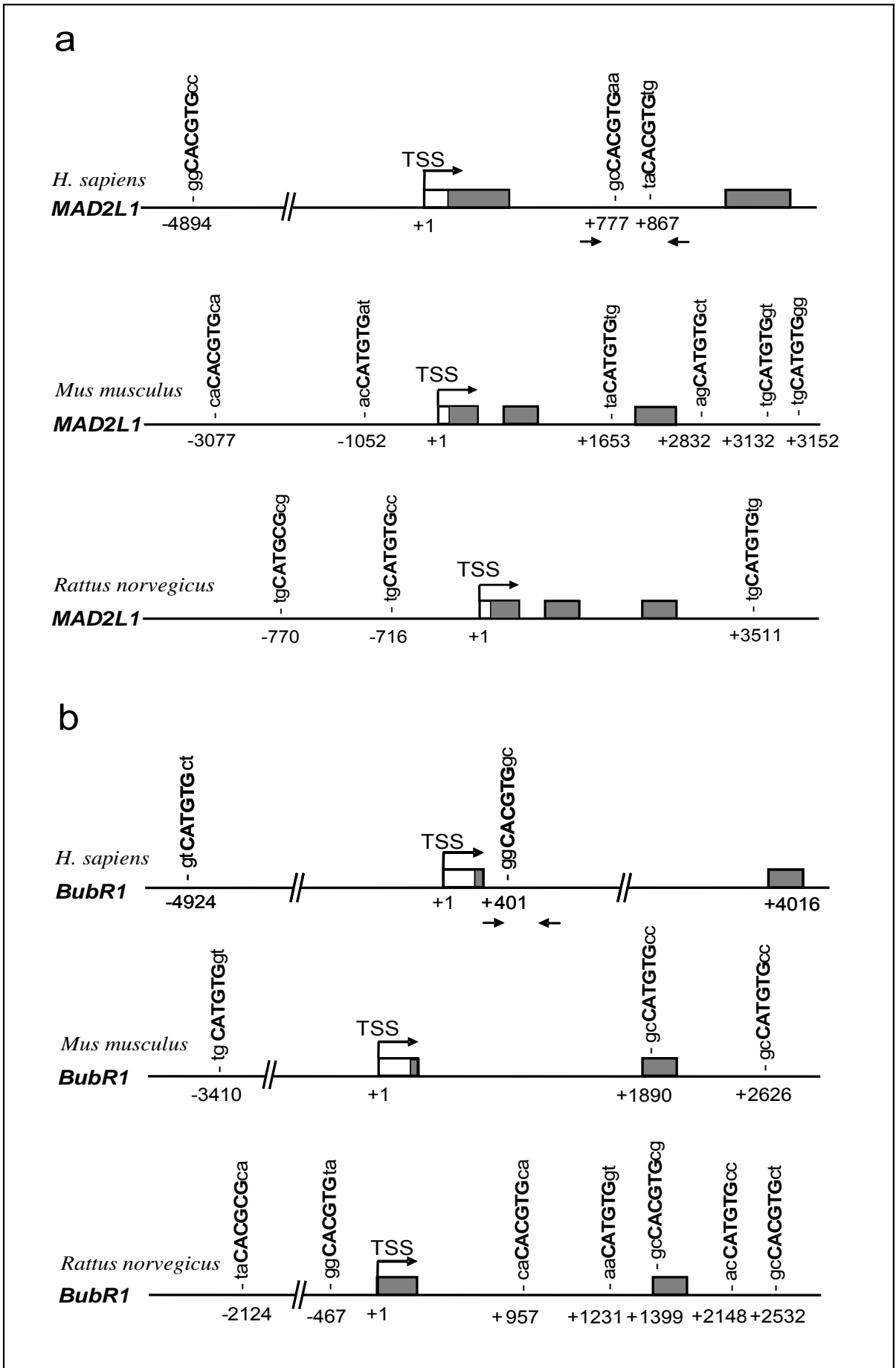


Figure 8 The positions of E-boxes in the human, rat and mouse *MAD2* and *BubR1* genes

(a) *MAD2* (=MADL1) and (b) *BubR1* E-box elements are indicated relative to the transcriptional start site (TSS; arrow). Exons are represented by rectangles. Protein coding sequences are shaded in grey. Arrow heads represent the position of oligonucleotides used for ChIP analysis.

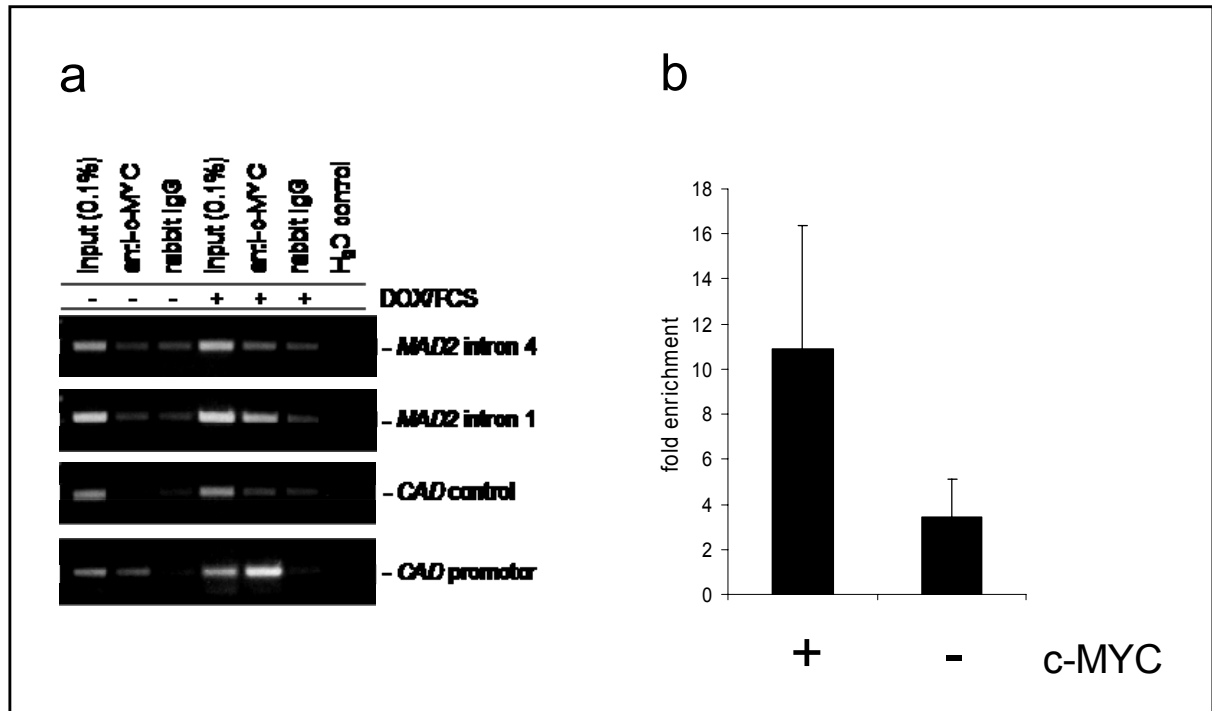


Figure 9 Detection of c-MYC occupancy at the human *MAD2* and *BubR1* promoters

(a) Chromatin-immunoprecipitation (ChIP) of *MAD2* promoter element was performed on PJMMR1 cells. PJMMR1 cells were starved for 72 hours (0.05% FCS) and then restimulated with 15% FCS and doxycycline (1 μ g/ml) for 16 hours. Cells were subjected to chromatin immunoprecipitation (ChIP) analysis. For details see **Methods**. Enrichment of DNA fragments bound by c-MYC was determined by qPCR of a region encompassing the two E-boxes in the first intron of *MAD2*. E-box containing fragments in the *CAD* promoter served as a positive control, *MAD2 intron 4* as negative controls. (the analysis was performed by Dr. Berlinda Verdoot, MPI of Biochemistry). (b) Chromatin-immunoprecipitation (ChIP) of *BubR1* promoter element was performed using PJMMR1 cells. Relative enrichment of the E-box amplicon derived from the first *BubR1* exon was determined by qPCR. As reference an amplicon on 16q22 devoid of E-boxes was used. Depicted is the average of two experiments with error bars indicating the standard error.

5.3 c-MYC induces a mitotic delay

The *MAD2* and *BubR1* proteins transmit a “wait signal” from kinetochores not properly attached to the spindle apparatus which inhibits the APC/cyclosome and prevents the premature onset of anaphase (Musacchio and Hardwick, 2002). To monitor the effects of c-MYC activation on the progression through mitosis or chromatin behavior two c-MYC inducible cell lines were generated (DLD-1-tTA-MYC).

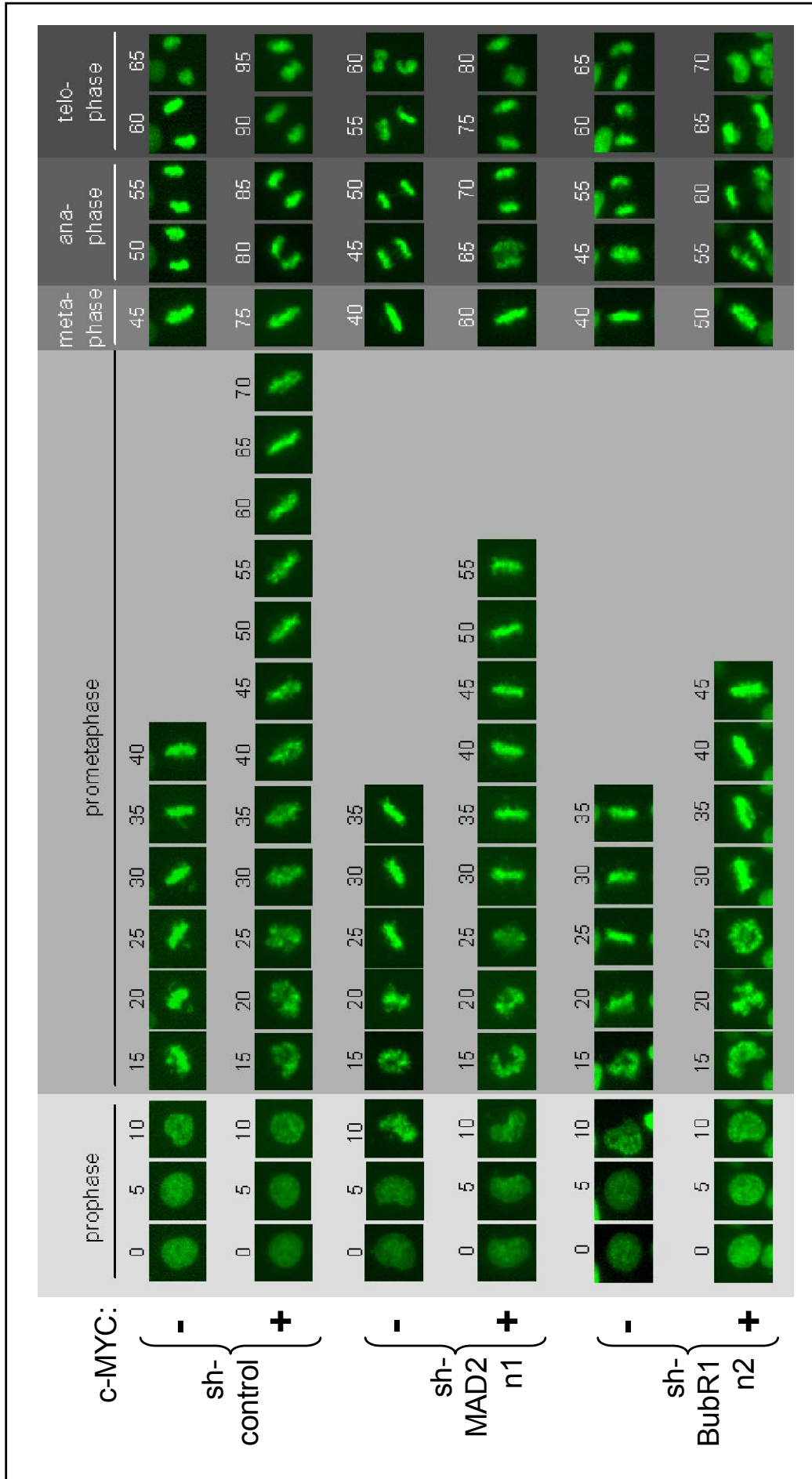


Figure 10 Effects of c-MYC induction on mitotic phases in the presence of MAD2 or BubR1 knockdown

Representative examples of cells progressing through mitosis in the presence or absence of c-MYC activation. DLD-1 cells harboring a conditional c-MYC allele and expressing H2B-YFP were monitored by time-lapse microscopy 36 hours after activation of c-MYC. Time points are indicated above the frames in minutes. Cell pools stably expressing shRNAs directed against *MAD2*, *BubR1* or non-silencing shRNAs (sh-control) were compared. DLD-1-tTA-MYC cells were cultured in the presence of 100 ng/ml of DOX. For activation of c-MYC DOX was removed.

(Figure 10) and PJMMR1 (data not shown) stably expressing yellow and green fluorescent protein (YFP/GFP)-tagged histone H2B protein, respectively. To determine the length of mitosis after c-MYC activation these cells were subjected to time-lapse microscopy (Figure 12 and 13). A large fraction of mitotic events in DLD-1-tTA-MYC cells displayed a significant extension after activation of c-MYC, in comparison to PJMMR1. A similar extension of mitosis length by c-MYC was found in DLD-1, PJMMR1 or hDF-MYCER cells not expressing H2B fusion proteins (data not shown) and in hDF constitutively expressing c-MYC (Figure 16c). In order to determine whether the c-MYC-induced increase in *MAD2* or *BubR1* expression mediates the c-MYC-induced mitotic delay the levels of the *MAD2* and *BubR1* proteins were limited by stable expression of retroviral constructs mediating *MAD2*- or *BubR1*-specific RNA interference (Figure 7). These analyses were performed with two different short-hairpin RNA (shRNA) encoding constructs targeting the same mRNA to exclude off-target effects (n1 and n2). As a control cells expressing a non-silencing shRNA were generated (sh-control).

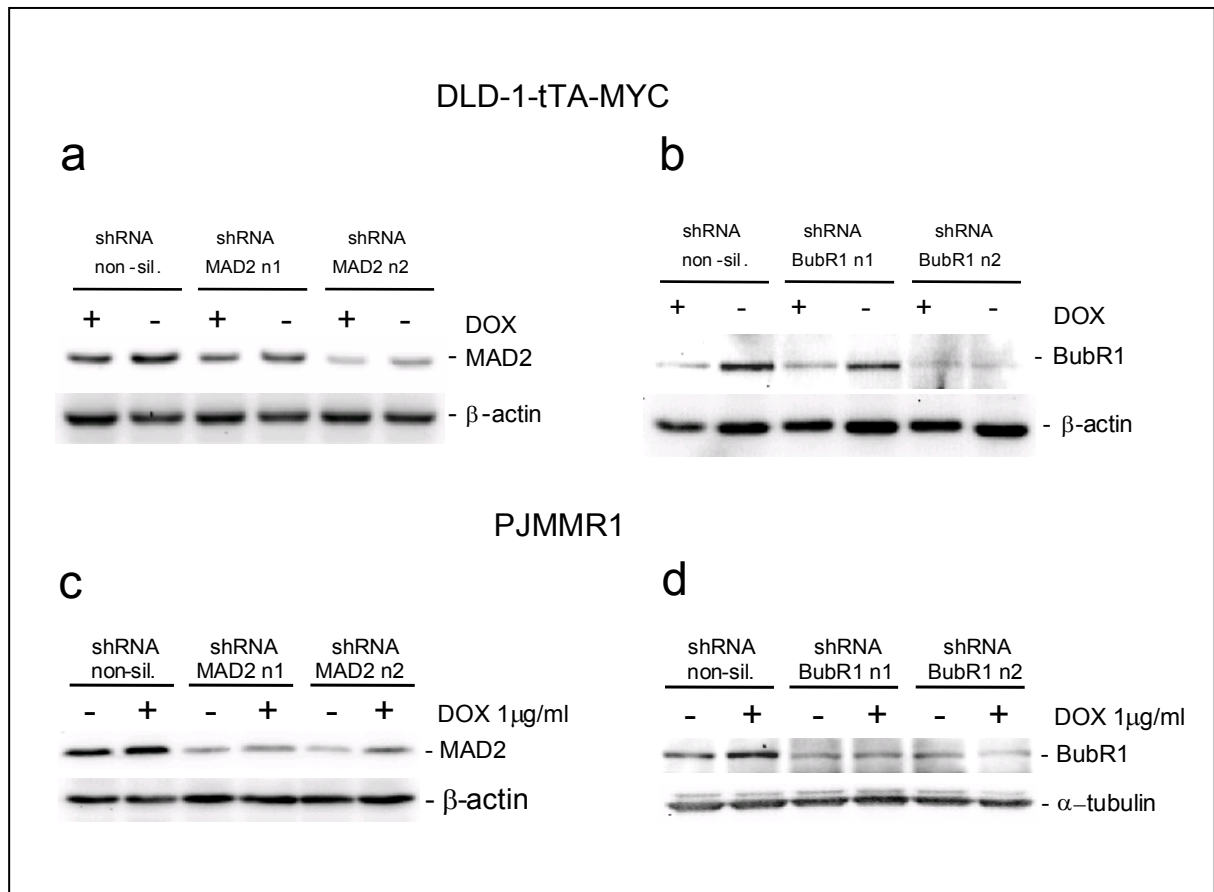


Figure 11 Western blot analysis of MAD2 and BubR1 protein downregulation in DLD-1-tTA-MYC and PJMMR1 cell lines.

(a) Downregulation of MAD2 protein by stable expression of a *MAD2*-specific short-hairpin RNA (shMAD2) in DLD-1-tTA-MYC cells was confirmed by Western blot analysis. *c-MYC* was induced for 48 hours. (b) Downregulation of BubR1 protein level in DLD-tTA-MYC stably expressing *BubR1*-specific short-hairpin RNA (shBubR1) cells was confirmed by Western blot analysis. *c-MYC* was induced for 48 hours. PJMMR1 cells stably expressing a short RNA hairpin directed against (c) *MAD2* or (d) *BubR1* were subjected to Western blot analysis. *c-MYC* was induced for 48 hours.

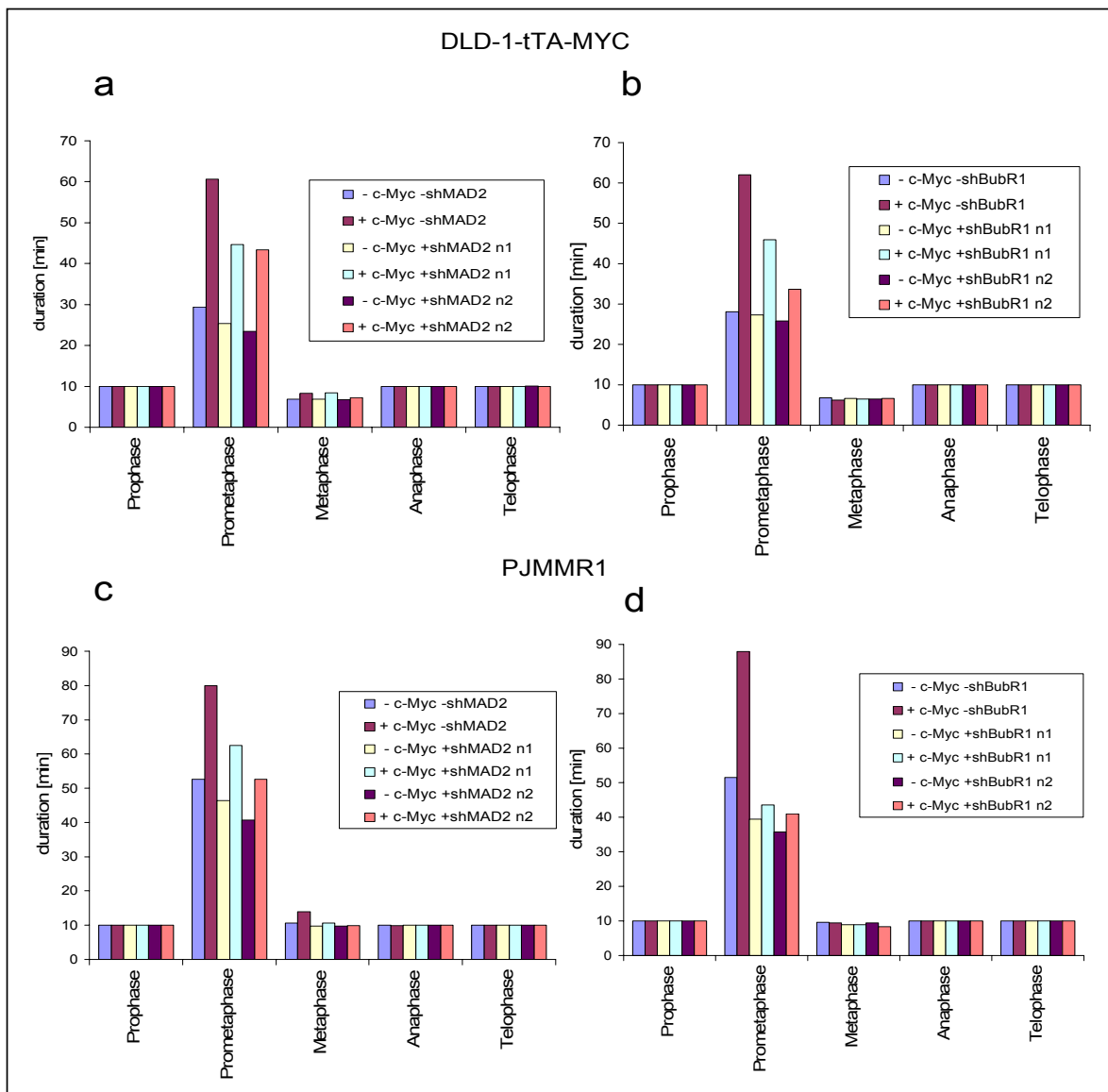


Figure 12 Determination of the length of different mitotic phases after activation of ectopic c-MYC in DLD-tTA-MYC and PJMMR1 cells

After activation of c-MYC for 36 hours DLD-tTA-MYC and PJMMR1 cells were subjected to time-laps recording for 18 hours. Each bar represents 100 mitotic events.

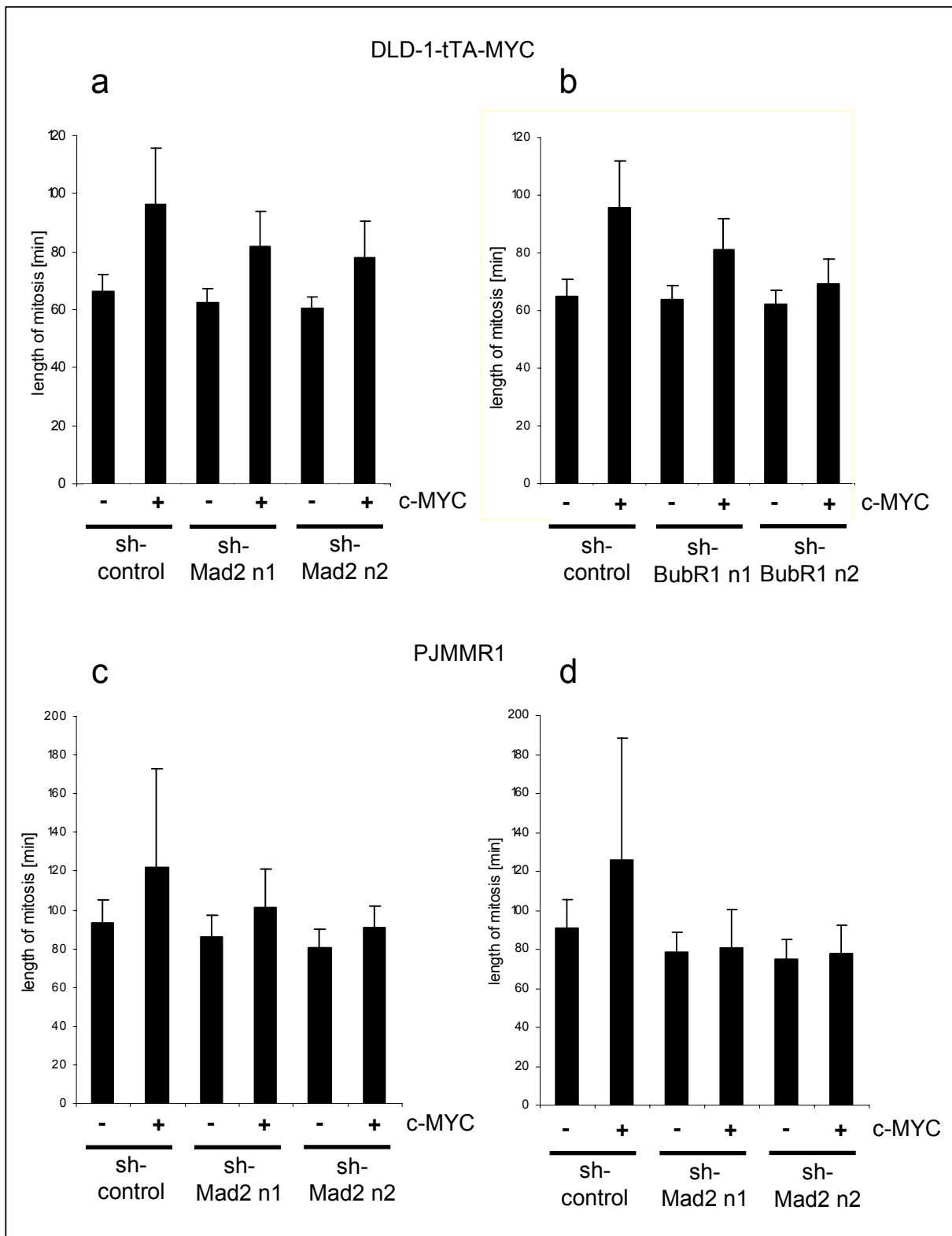


Figure 13 Determination of mitotic length after activation of ectopic *c-MYC* in DLD-tTA-MYC and PJMMR1 cell lines

The evaluation of the mitotic length after *c-MYC* activation in DLD-tTA-MYC and PJMMR1 cells. Counting is based on results obtained for Figure 12. Each bar represents 100 mitotic events.

For each genotype and state 100 mitotic events recorded by time-lapse microscopy were analyzed in detail. Representative examples are shown in Figure 6. DLD-1 cells required on average ~65 minutes from the first signs of nuclear envelope breakdown until completion of cytokinesis. However, after activation of ectopic c-MYC ~95 minutes were required for passage through mitosis. After down-regulation of *MAD2* by constitutive shRNA expression the c-MYC-induced extension of mitosis was significantly reduced (Figure 12a and 13a). Therefore, the c-MYC-induced mitotic delay is mediated, at least in part, by the c-MYC-mediated induction of *MAD2* expression. Also the down-regulation of BubR1 diminished the c-MYC-induced mitotic delay by shortening the prolonged mitosis (Figure 13). We observed a higher efficiency in the down-regulation of BubR1 protein expression by the BubR1-specific shRNA n2 versus the n1 shRNA (Figure 11b). This presumably caused a more pronounced reversion of the c-MYC-induced delay by the n2-shRNA, indicating a dependence of the mitotic delay on the concentration of BubR1. The effects of c-MYC activation and inhibition of *MAD2* and BubR1 were restricted to prometaphase (Figure 12, a and b).

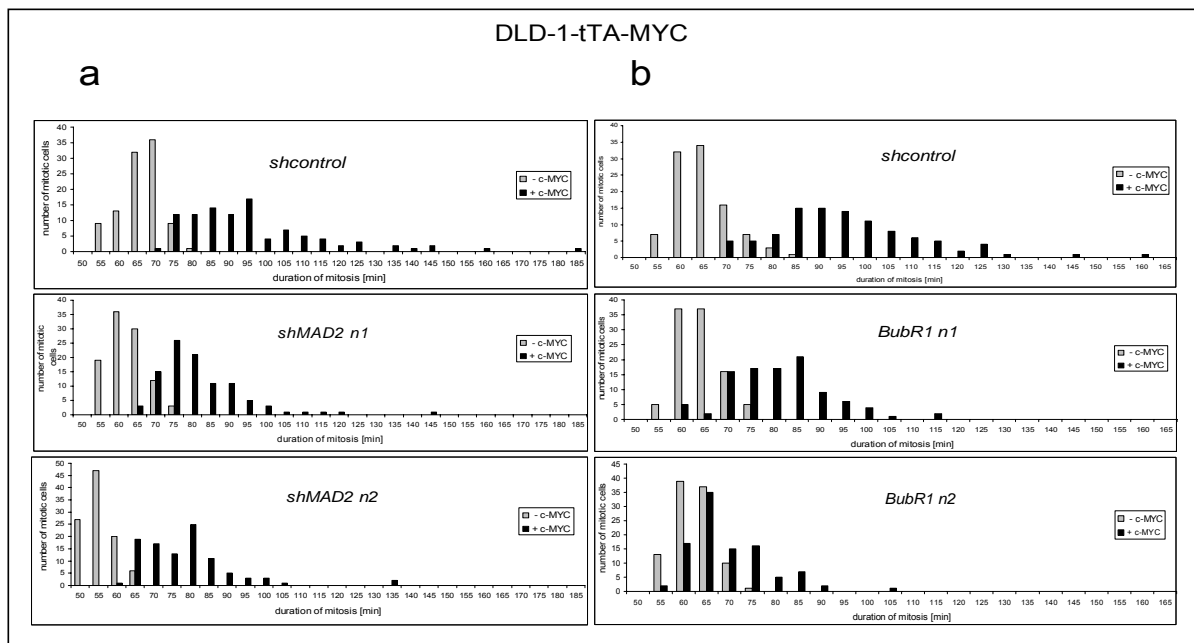


Figure 14 Distribution of mitotic durations after c-MYC activation

Distribution of mitotic length after c-MYC activation in DLD-1-tTA-MYC cells exhibiting down-regulation of (a) *MAD2* or (b) *BubR1* by RNA interference. One graph represents 100 mitotic events.

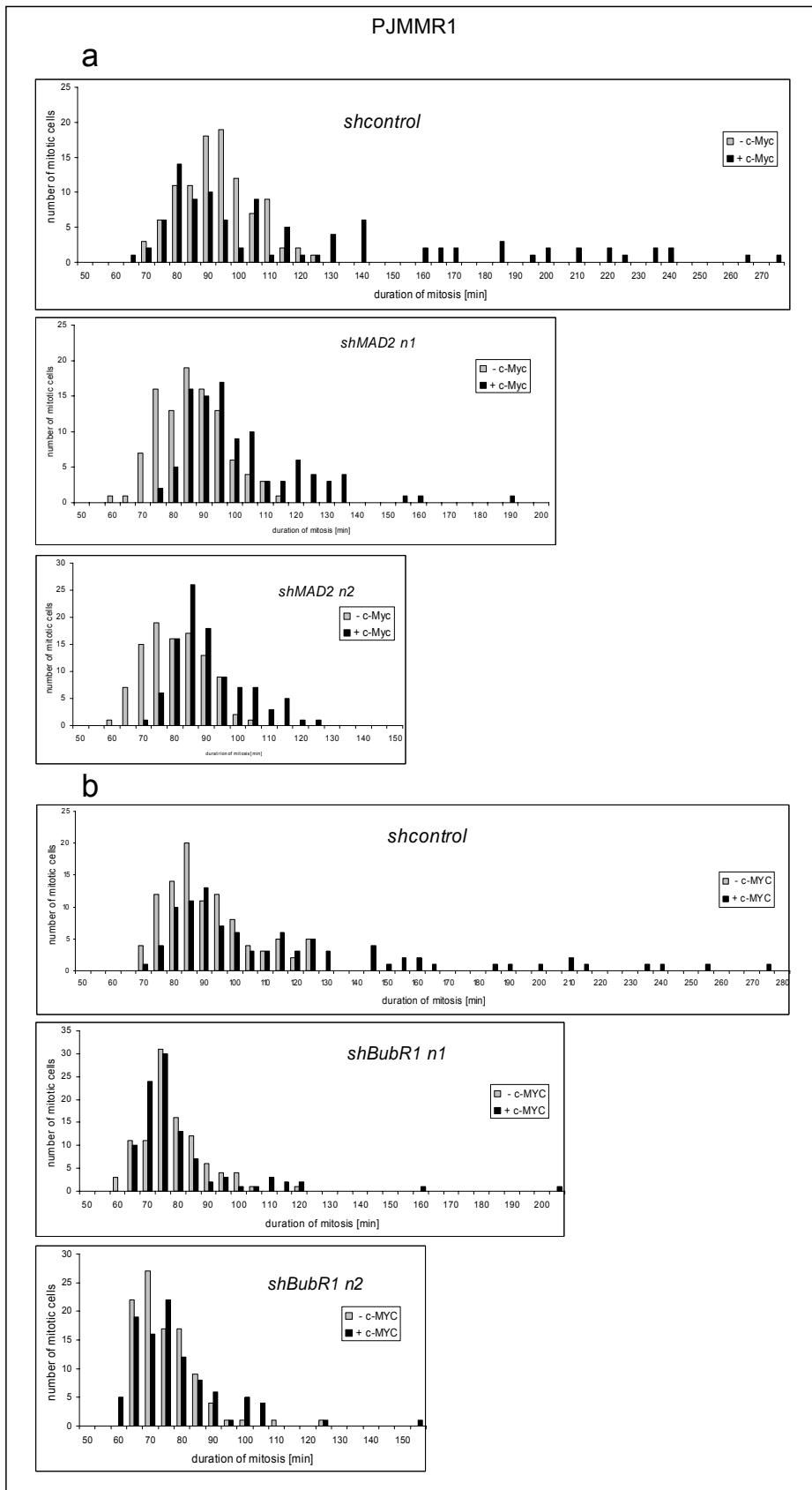


Figure 15 Distribution of mitotic durations after c-MYC activation

Distribution of mitotic length after c-MYC activation in PJMMR1 cells exhibiting down-regulation of **(a)** MAD2 or **(b)** BubR1 by RNA interference. One graph represents 100 mitotic events.

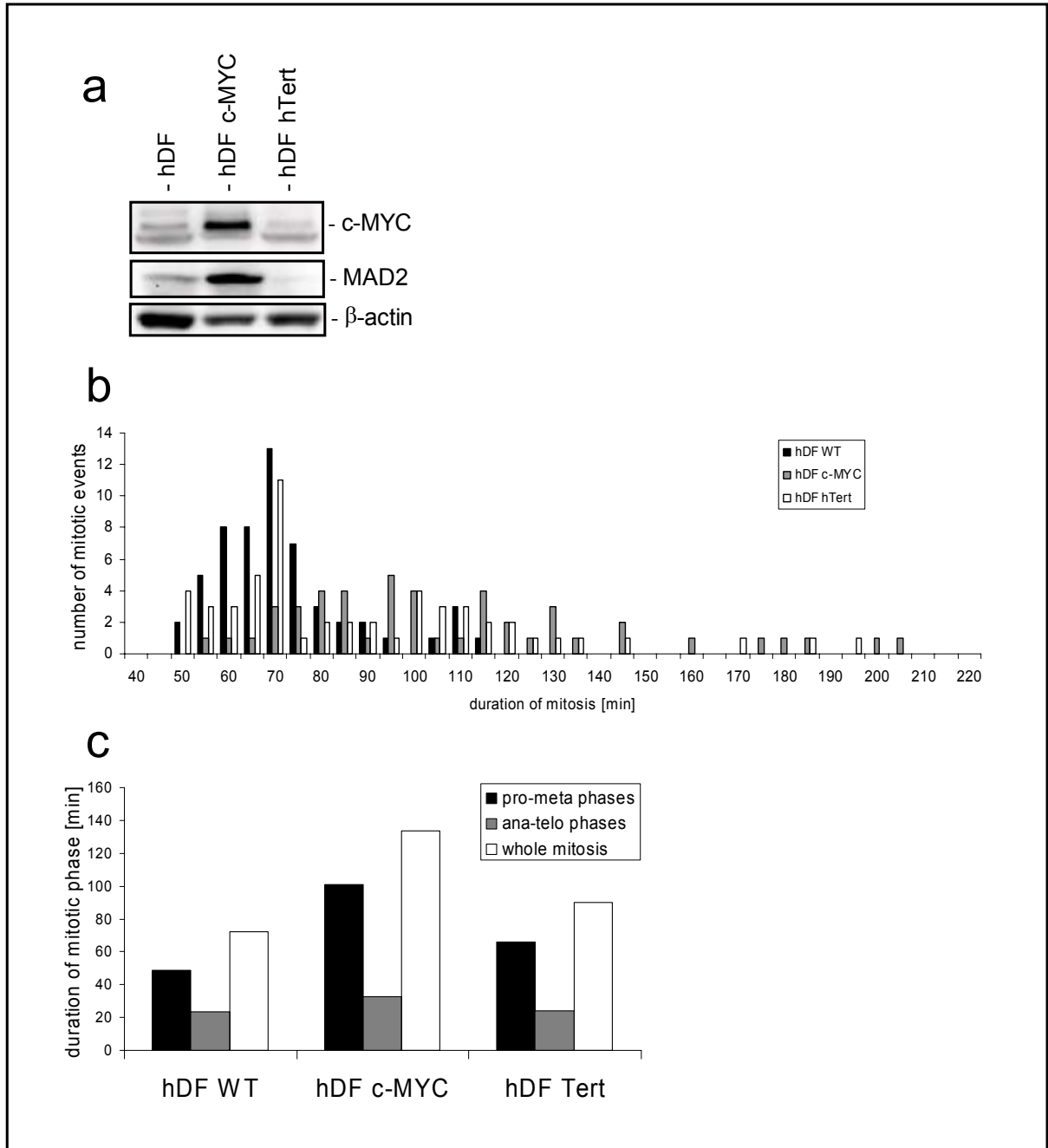


Figure 16 c-MYC induces *MAD2* and *BubR1* and mitotic delay in primary human diploid fibroblasts

(a) Western blot analysis of c-MYC and MAD2 protein expression in primary hDFs and hDFs immortalized by c-MYC or hTert expression. **(b)** Distribution of mitotic durations in the population of hDFs immortalized by c-MYC or Tert in comparison to non immortal hDFs with a passage 20. For each cell type 25 mitotic events recorded by time-lapse video-microscopy were evaluated. **(c)** Evaluation of distribution of mitotic phases in hDF constitutively expressing the indicated genes. pro-meta: sum of the length of prophase, prometaphase and metaphase, ana-telo: sum of anaphase and telophase, sum: length of whole mitosis.

The number of cells displaying extremely delayed mitosis (more than 100 minutes) was relatively low (Figure 14). When MAD2 or BubR1 was down-regulated by RNA interference the increased variation in the length of mitotic events observed after c-MYC activation was reversed towards the smaller range observed in DLD-1 cells without c-MYC activation (Figure 14).

Similar analyses were performed in the aneuploid breast cancer cell line MCF7. The MCF7-derived PJMMR1 cells showed a c-MYC-induced mitotic delay and reversion after knock-down of MAD2 and BubR1 (Figure 13, c and d, 14, c and d). However, in these cells the variations in the mitotic length as well as the reversal of the delay by knock-down of MAD2 or BubR1 expression were more pronounced than in DLD-1 cells (Figure 14, c and d, 15).

In the population of DLD-1-tTA-MYC and PJMMR1 (data not shown) cells were observed a number of mitotic and chromatin abnormalities (Figure 17) which correlated with the duration of c-MYC activation (Figure 18, a). Initially, c-MYC overexpression increased abnormal meta-anaphase transition and led to distortion of metaphase plate formation (Figure 17, b and c). Presumably, these alterations, together with additional effects, like lagging chromosomes, chromatin bridges or micronuclei formation (Figure 17, d, e, f, g and h) resulted in the extension of mitotic length (Figure 18, b). Furthermore, extended mitotic events were frequently followed by synchronous post-mitotic apoptosis of two daughter cells (Figure 17, k, and 18, c).

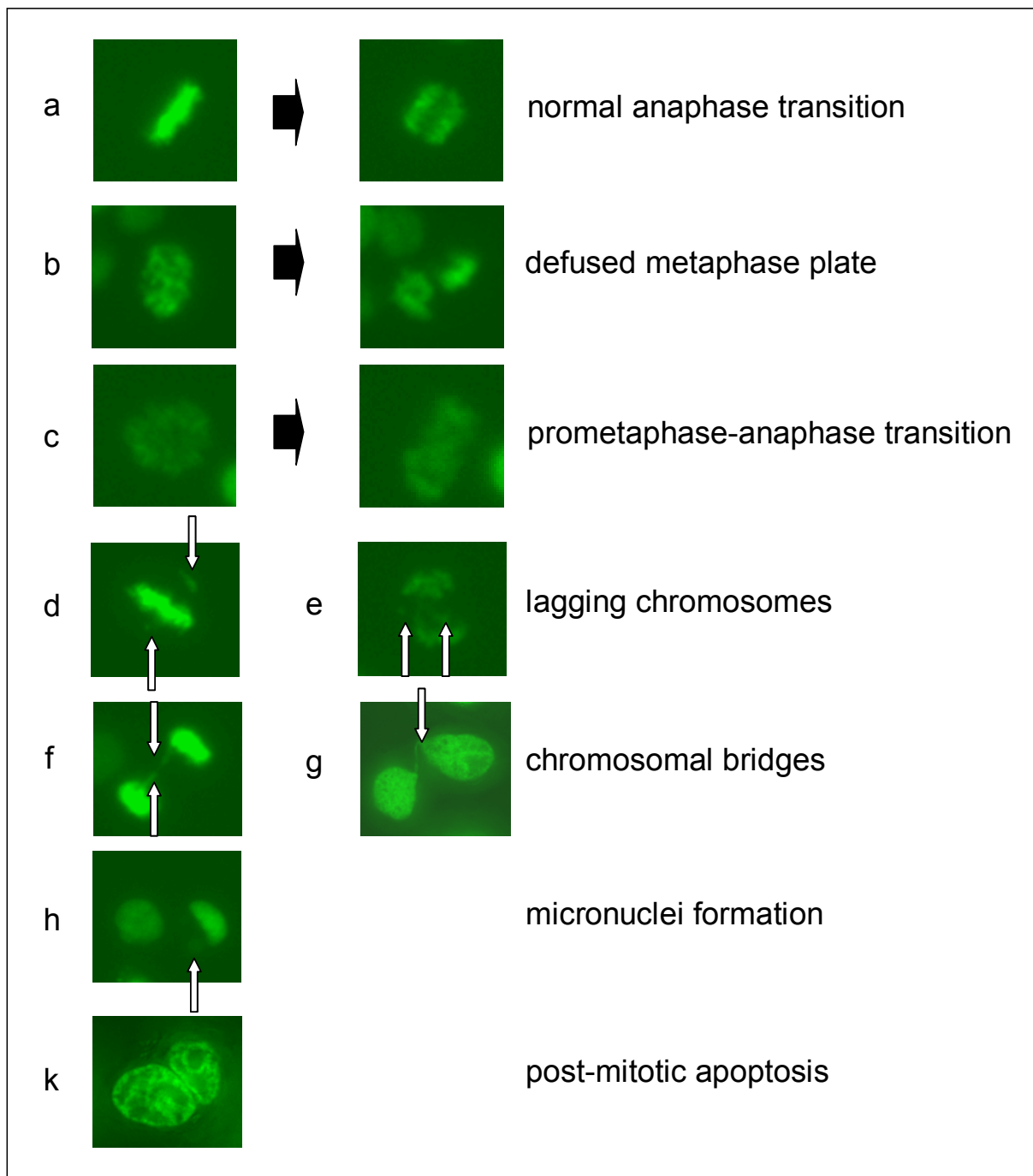


Figure 17 c-MYC activation leads to mitotic abnormalities, chromosomal perturbations, genomic instability and induction of post-mitotic apoptosis

(a) Example of normal meta-anaphase transition and formation of a proper metaphase plate. **(b)** Meta-anaphase transition with defused metaphase plate. **(c)** Prometa-anaphase transition. Metaphase plate does not form. Lagging chromosomes in **(d)** meta- or in **(e)** anaphase. Formation of chromosomal bridges throughout **(f)** anaphase and **(g)** telophase. **(h)** Micronucleus formation. **(k)** Synchronous apoptosis of two daughter cells following of mitotic division (post-mitotic apoptosis).

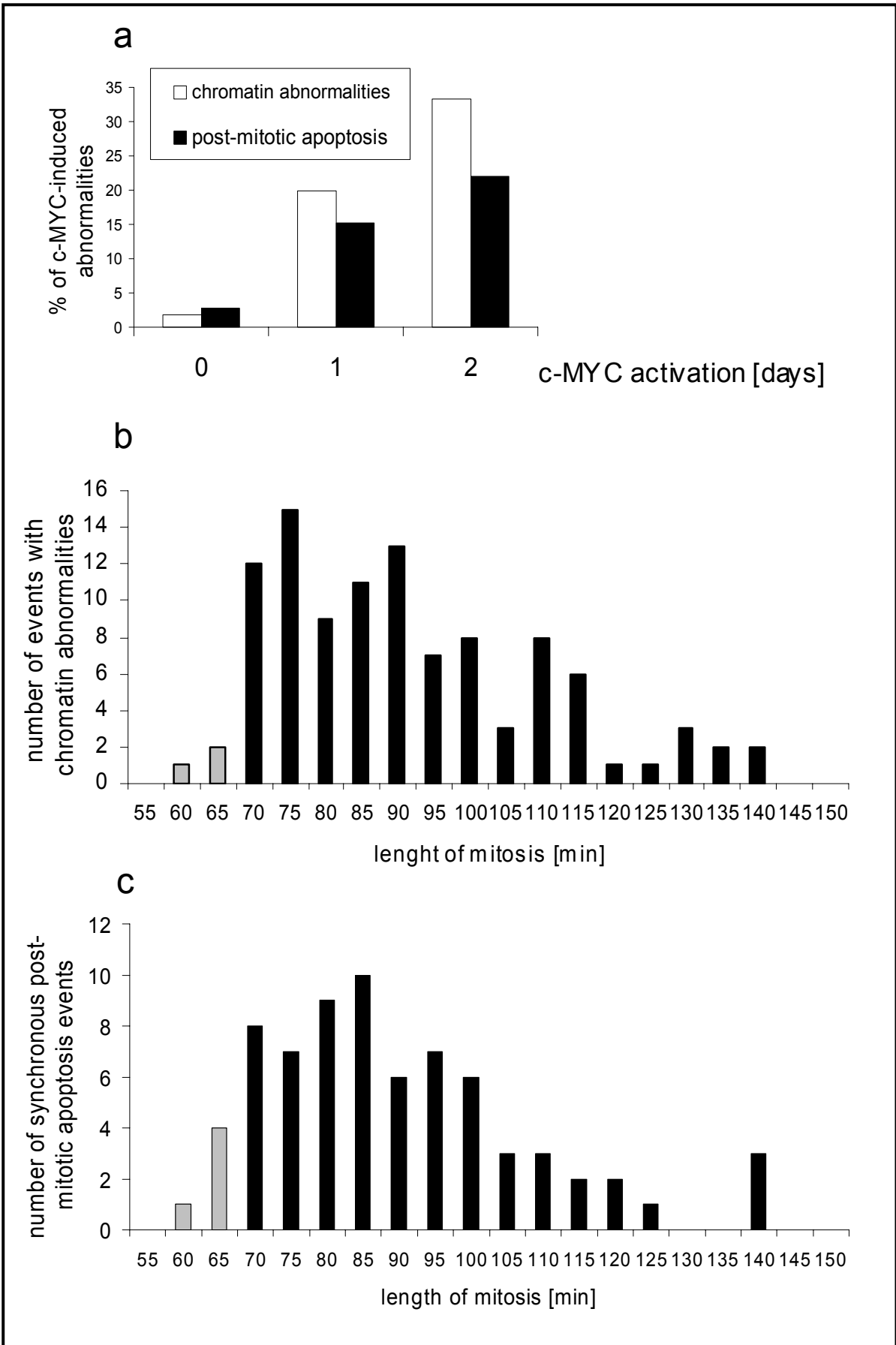


Figure 18 c-MYC-induced chromatin abnormalities and post-mitotic apoptosis which are associated with extended mitosis

(a) DLD-tTA-MYC cells were recorded for 18 hours after activation of c-MYC for 24 and 48 hours. The graph represents the percentage of mitotic events resulting in post-mitotic apoptosis. For the 24 and 48 hour time-point 150 and 222 mitotic events were analyzed, respectively. Distribution of mitotic length of cells displaying (b) chromatin abnormalities or (c) post-mitotic apoptosis after c-MYC activation in DLD-tTA-MYC cells. Grey bars represent cells which showed a mitosis duration also found in cells without c-MYC activation, black bars represent cells with extended mitotic durations.

5.4 Synchronous apoptosis in cells with delayed mitosis

The time-lapse recording allowed to distinguish different forms of c-MYC-induced apoptosis and characterize them as random single cell apoptosis and post-mitotic apoptosis, which represents approximately 30% and 70% of whole apoptosis fraction respectively (Figure 19b). Further analysis of the fraction of cells undergoing post-mitotic apoptosis revealed a number of interesting details. First of all, this fraction increased with time after c-MYC activation and reached ~15 and ~22 % of the population of dividing cells observed in the time-laps movies by the day 1 and 2 of c-MYC activation respectively (Figure 18a and 19a).

Interestingly, the time-point of apoptosis initiation was identical in the two daughter cells and in average has approximately four hours between the end of the anaphase and beginning of chromatin cleavage and condensation accepted as the beginning of late apoptotic processes. This synchronicity suggested that an initiating event took place before cell division, which primed the cells for apoptosis. Additional results suggest that this event could be the induction of DNA damage by c-MYC during S-phase in the parental cell (data not shown). This form of post-mitotic apoptosis was blocked by addition of a caspase 3 inhibitor (data not shown). As DLD-1 cells express mutant p53, this c-MYC-induced post-mitotic apoptosis is p53-independent. DLD-1 cells with RNA-interference mediated down-regulation of BubR1, but not cells with reduced levels of MAD2, showed a decrease of post-mitotic apoptosis after activation of c-MYC by ~20% (Figure 19c). Therefore, BubR1 may be involved in the induction of this form of apoptosis.

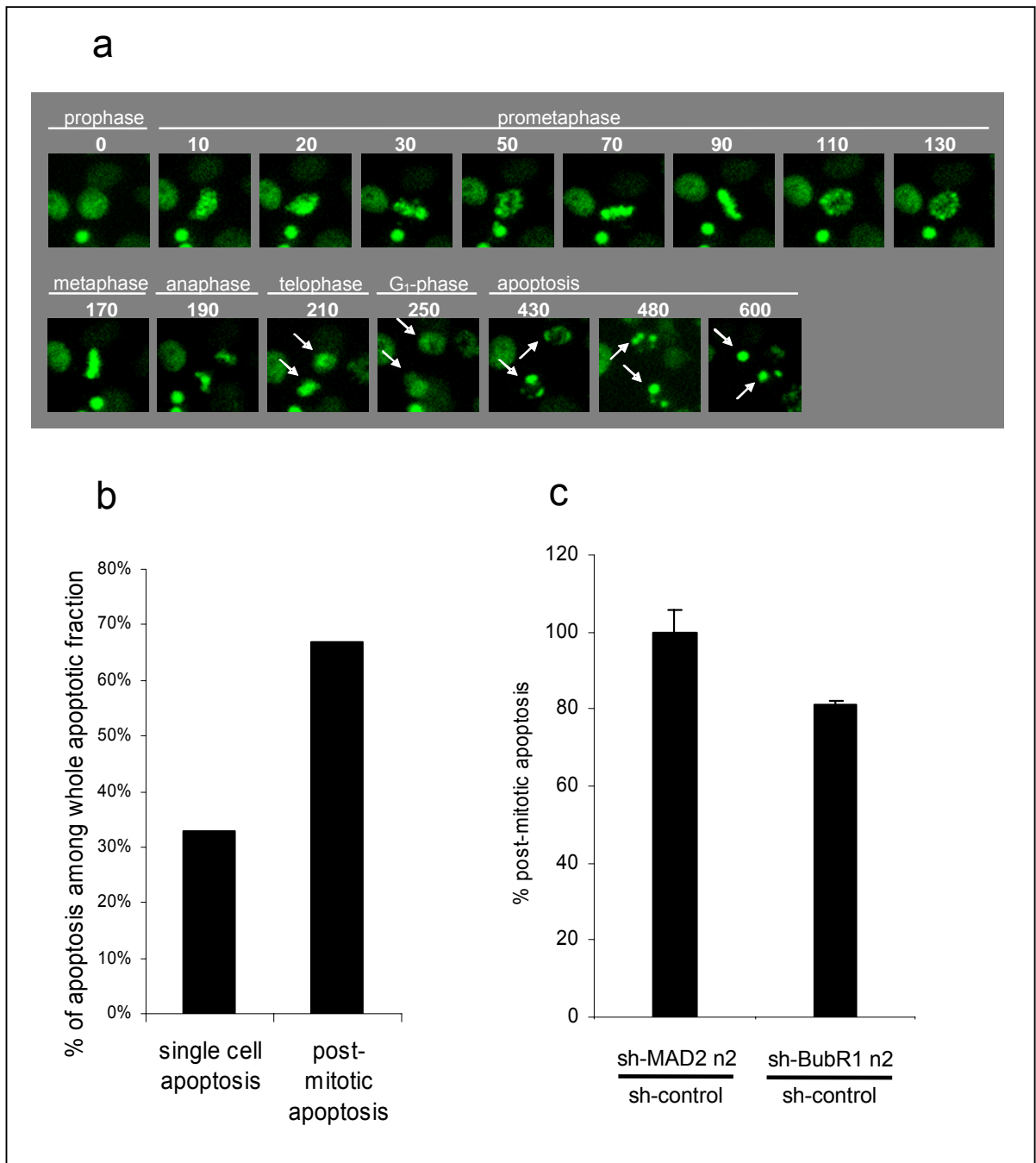


Figure 19 c-MYC-induced mitotic delay is followed by synchronous apoptosis

(a) Representative example of a time-lapse sequence showing a post-mitotic apoptosis after activation of c-MYC in H2B-YFP expressing DLD-tTA-MYC cells. Time-points (minutes) are indicated above the frames. (b) The types of apoptosis events were observed: single cells undergoing apoptosis and synchronous apoptosis of two daughter cells, post-mitotic apoptosis. Observation based on evaluation of 100 apoptotic events acquired by time-lapse microscopy from DLD-1-tTA-MYC cells after 36 hours of c-MYC activation. (c) Influence of RNA interference mediated down-regulation of MAD2 or BubR1 proteins on the frequency of mitotic events resulting in post-mitotic apoptosis after activation of c-MYC in DLD-tTA-MYC cells. For each genotype at least 200 mitotic events were evaluated. The frequency of mitosis resulting in synchronous apoptosis in cells expressing control sh-RNAs was set to 100%. The average of two independent experiments is depicted.

5.5 c-MYC induces CIN in MIN cell lines

DLD-1 cells are mismatch repair deficient and therefore display MIN. As most MIN cell lines, DLD-1 cells are diploid and have an intact SAC (Cahill et al., 1998). To determine extent of c-MYC-induced chromosomal instability micronuclei formation was quantified. Micronuclei represent acentric fragments or whole chromosomes not properly integrated into one of the two daughter nuclei during mitosis. After c-MYC activation a gradual increase in the frequency of cells with micronuclei was observed (Figure 20b). After eight days the frequency of cells with micronuclei had increased from 4% to more than 10% ($p < 0.001$). The induction of CIN after activation of ectopic c-MYC was confirmed by interphase-FISH analysis of chromosome 8 and 17 (Figure 20c). After eight days of c-MYC activation, the percentage of cells with aberrant number of signals had increased from 1.4% (chromosome 8) and 1.8% (chromosome 17) to 3.9% and 4.5%, respectively ($p < 0.001$). Therefore, the increase of numerical aberrations detected for chromosome 8 and 17 paralleled the increase in micronucleus formation. The frequency of micronuclei and the degree of CIN as detected by interphase FISH without c-MYC activation was in line with previously described basal levels of aneuploidy in DLD-1 cells (Lengauer et al., 1997).

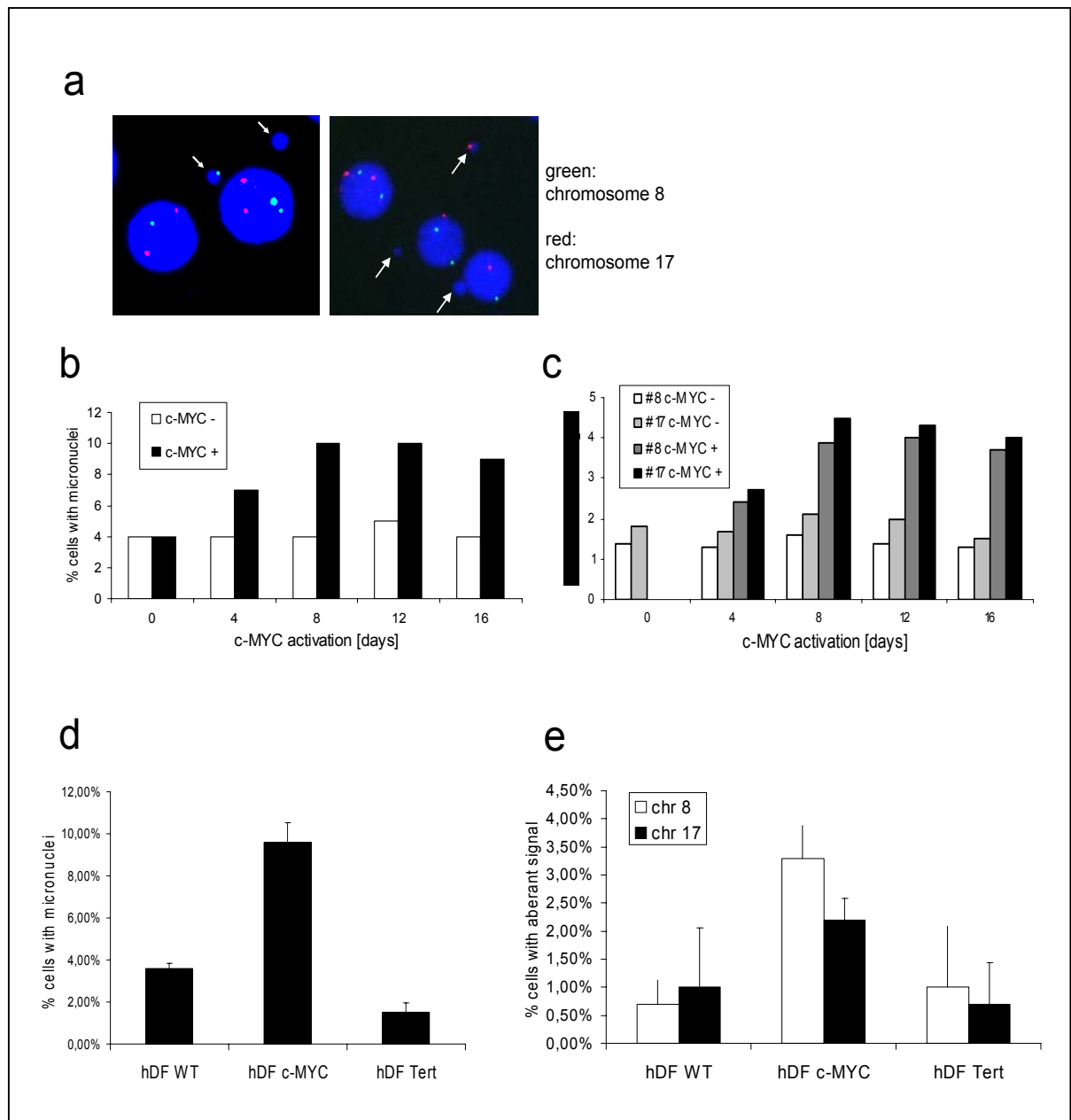


Figure 20 Analysis of c-MYC-induced CIN

(a) Examples of micronucleus formation (white arrows) 8 days after activation of c-MYC in DLD-tTA-MYC cells. Some micronuclei contain centromeric signals for chromosome 8 (green) and 17 (red). **(b)** The frequencies of micronucleus formation were determined microscopically at the indicated time points after activation of c-MYC in DLD-1-tTA-MYC cells. For each time point at least 600 nuclei were analyzed and differences in micronuclei percentages between -/+ c-MYC cells were highly significant for each time point as determined by the Chi-square test ($p < 0.005$). **(c)** Summary of results obtained by FISH analysis. At least 600 nuclei were analyzed at each time point and the difference in the percentage of cells with aberrant signals was highly significant after eight days of c-MYC activation ($p < 0.001$). (experiments were performed by Dr. Nils Hartmann, MPI of Biochemistry) **(d)** Determination of micronucleus frequencies. For each cell type ~1000 cells were evaluated. **(e)** FISH analysis of chromosome 8 and 17 using the centromeric probes shown in (c). ~600 nuclei of each cell line were analysed. (experiments were performed by Dr. Nils Hartmann, MPI of Biochemistry)

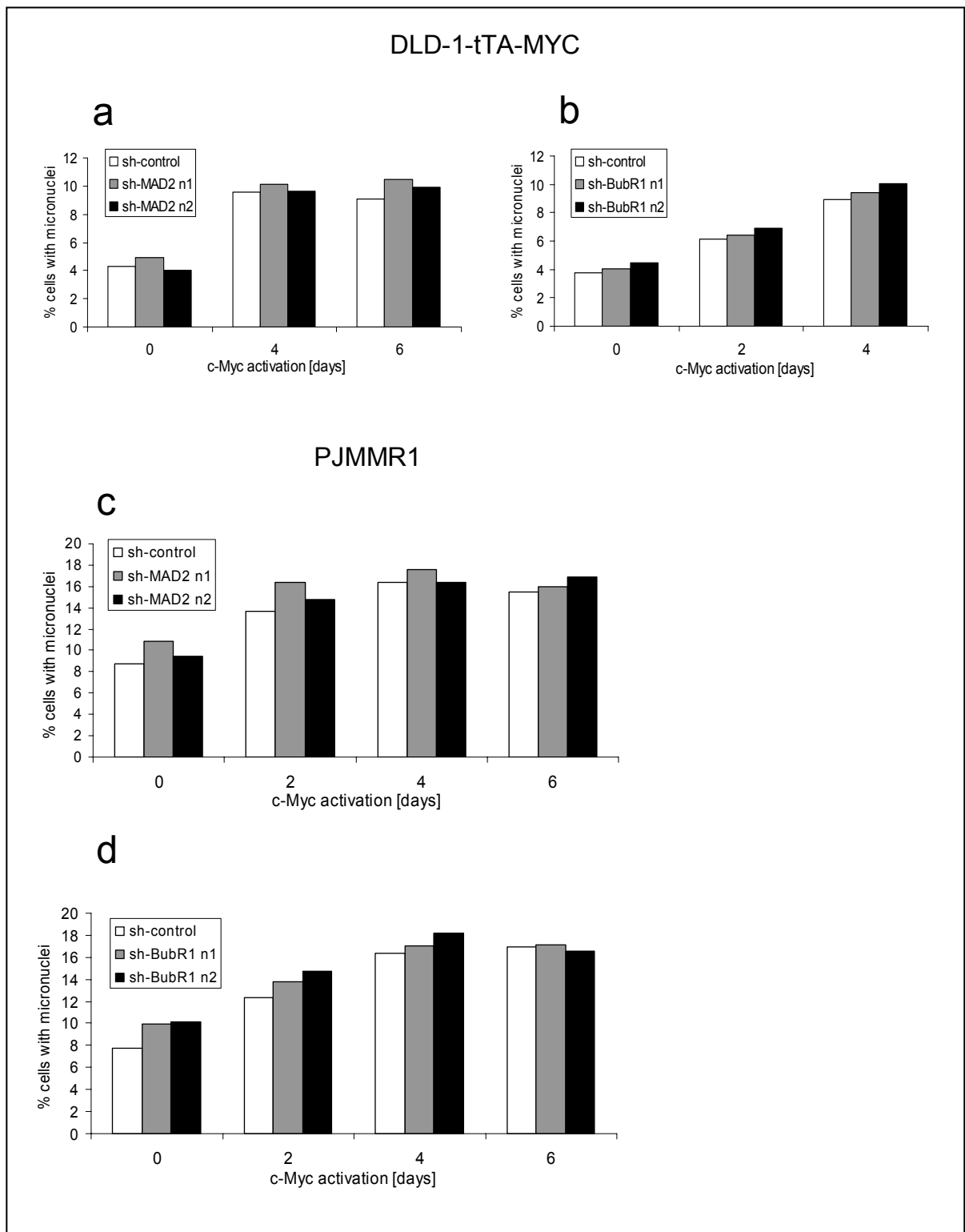


Figure 21 c-MYC-induced micronuclei formation in DLD-1-tTA-MYC and PJMMR1 cells is not influenced by the levels of MAD2 and BubR1 expression

Analysis of c-MYC-induced formation of micronuclei in DLD-tTA-MYC cells in the presence of RNA interference down-regulating MAD2 (**a**) or BubR1 (**b**) expression. Samples were fixed at the indicated time points. Each bar represents at least 1000 cells derived from several independent fields. Analysis of c-MYC-induced micronucleus formation in PJMMR1 cells in the presence of RNA interference down-regulating MAD2 (**c**) or BubR1 (**d**) expression. Each bar represents at least 1000 cells derived from several independent fields.

An increase in the frequency of micronuclei and numerical chromosome aberrations was also observed after activation of c-MYC in the MCF-7 derived aneuploid breast cancer cell line PJMMR1 (Figure 21, c and d; data not shown) and in primary human diploid fibroblasts stably expressing ectopic c-MYC (Figure 20, d and e).

5.6 Analysis of putative mediators of c-MYC-induced CIN

Alterations in protein expression of both MAD2 and BubR1 and some other components of spindle checkpoint machinery were previously linked to chromosomal instability (Dobles et al., 2000; Shin et al., 2003). Stable expression of shRNA was used to determine whether the down-regulation of MAD2 or BubR1 by RNA interference would not only affect progression through mitosis, but also leads to a decreased number of micronuclei as a measure of CIN. However, the frequency of micronuclei observed after c-MYC activation in DLD-1-tTA-MYC and PJMMR1 cells was not significantly altered in cells with MAD2 or BubR1 down-regulation (Figure 20).

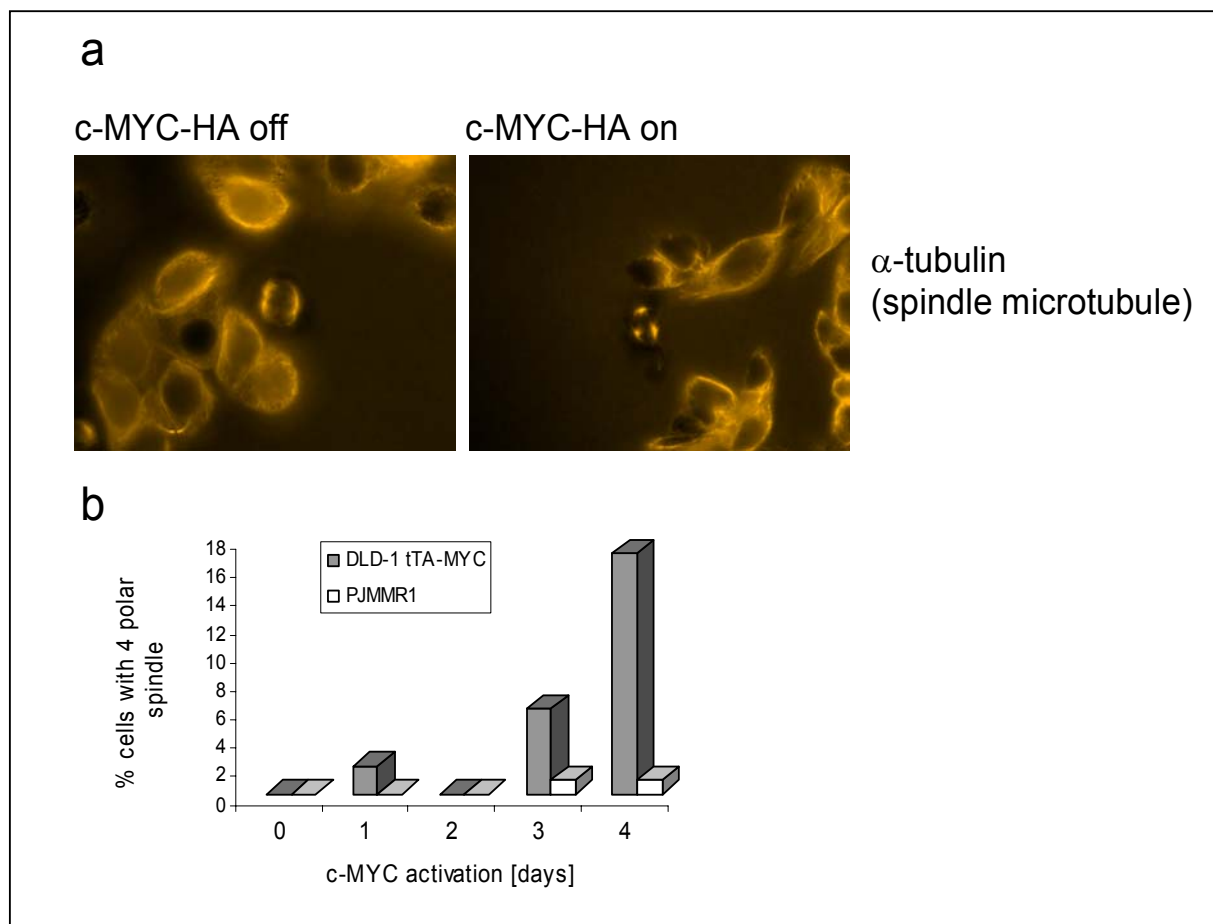


Figure 22 Evaluation of microtubule spindle numbers after activation of c-MYC in DLD-1-tTA-MYC and PJMMR1 cells

(a) Determination of microtubule spindle number upon activation of c-MYC in DLD-1-tTA-MYC and PJMMR1 cells. Cells were cultured on cover slips in the presence or absence of DOX to control c-MYC expression. Then they were fixed and stained with antibody to γ -tubulin to visualize microtubule spindles (yellow) by immunofluorescence. (b) The percentage of spindles with 4 poles was evaluated in a population of mitotic cells after c-MYC activation.

Furthermore, the rate of c-MYC-induced increase of aberrant microtubule spindles lagged behind the formation of micronuclei (Figure 22). Therefore, the increased rate of aneuploidy observed after activation of c-MYC was presumably not due to induction of aberrant spindle formation or deregulation of MAD2 or BubR1 expression.

5.7 Construction of episomal vectors for RNA interference

Recently, comprehensive libraries of microRNAs which were designed to facilitate the RNA interference mediated down-regulation of all human or mouse genes have been described (Silva et al., 2005). These microRNAs are publicly available and are provided in the pSHAG-MAGIC 2c (pSM2c) retroviral vector, which provides constitutive expression driven by a long terminal repeat (LTR). pRTS-1 was chosen as a basis expression vector with a number of convenient features bearing in one plasmid, including following: bi-directional CMV-based promoter (P_{tet}^{bi-1}) expressing fluorescent tracing protein (RFG/GFP) and transcript of interest in DOX-dependent manner; bicestronic expression cassette under control of chicken beta actin promoter encodes for highly DOX-sensitive reverse tetracycline controlled transactivator rtTA2^S-M2 and a Tet repressor-KRAB fusion protein (tTS^{KRAB}); selection marker (Hygromycin/Puromycin); oriP and EBNA-1 expressing cassette to maintain the plasmid episomality.

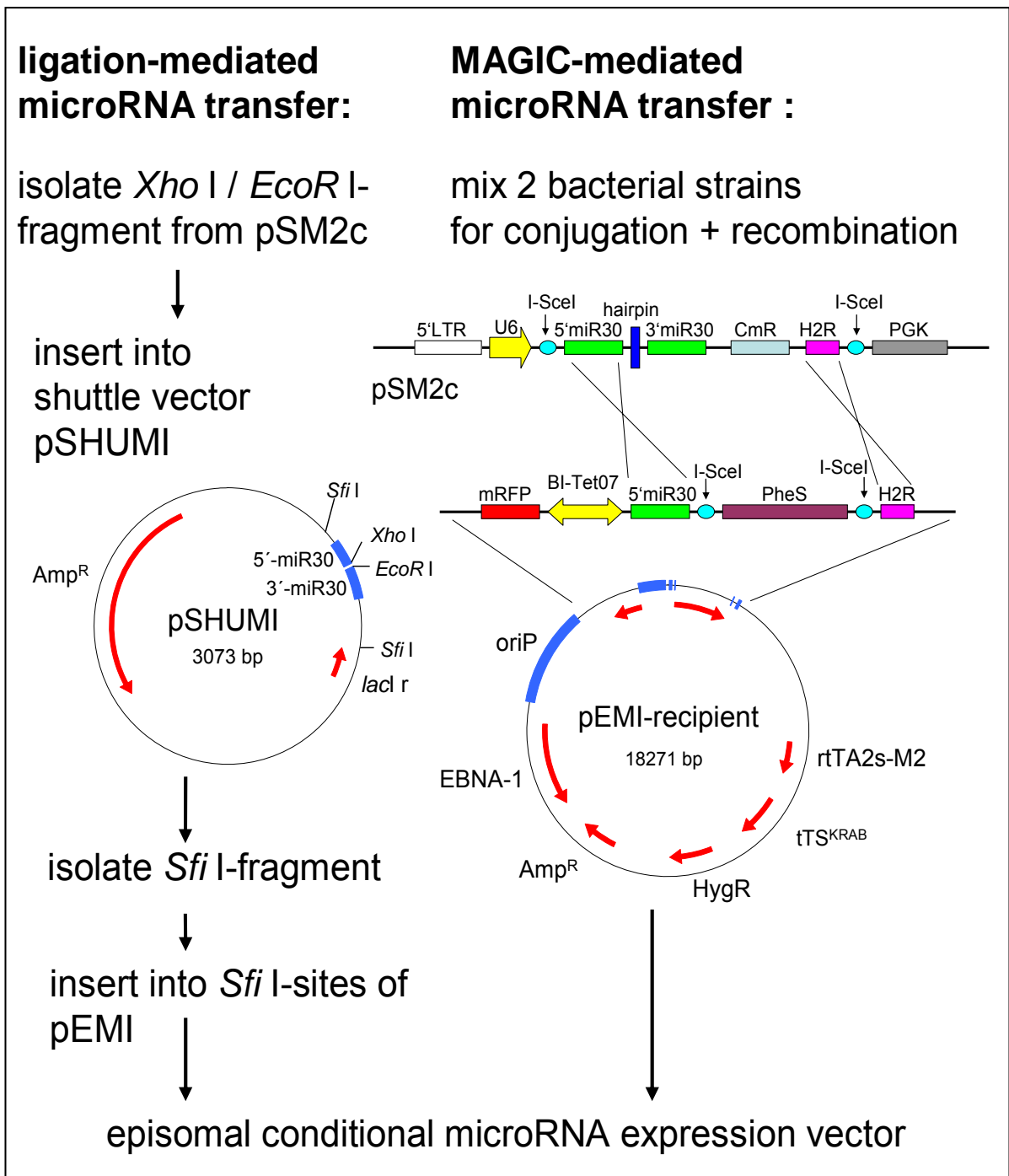


Figure 23 Generation of episomal vectors for conditional expression of microRNAs

Flow chart showing the steps necessary to generate pEMI-vectors harboring microRNA cassettes. Abbreviations: Amp^R: ampicillin resistance; Cm^R: chloramphenicol resistance; EBNA-1: EBV nuclear antigen required for Ori P function; EBV: Epstein-Bar virus; H2R: homology 2 region; Hyg^R: hygromycin B; LTR: long terminal repeats; MAGIC: mating-assisted genetically integrated cloning; miR-30: precursor microRNA; mRFP: monomeric red fluorescent protein; OriP: EBV origin of replication, pEMI: plasmid for episomal microRNA expression; pheS: phenylalanine synthase relaxed-specificity allele Gly294; P_{PGK}: PGK-promoter; pSHUMI: plasmid for shuttling of microRNAs, pSM2c: pSHAG-MAGIC 2c retroviral vector for microRNA expression; P_{tet-bi-1}: bidirectional tet-responsive promoter; rtTA2^S-M2: reverse tetracycline controlled transactivator; tT^{SKRAB}: tetracycline repressed silencer.

Several microRNA cassettes have been taken from the library or were newly designed to transfer to the pRTS-1 vector. Since pRTS is a relatively large vector (~18 kbp) the intermediate pUC19-based shuttle vector pSHUMI (plasmid for shuttling microRNAs) is necessary for the transfer procedure (Figure 23). For a faster transfer of microRNAs, pRTS vector was adapted to the ligation-free MAGIC technique (mating-assisted genetically integrated cloning)(Baek et al., 2005). The resulting pEMI (plasmid for episomal microRNA expression; Figure 23) harbors a *pheS* Gly294 allele encoding a tRNA synthase for phenylalanine with relaxed specificity, which incorporates toxic chloro-phenylalanine and thereby facilitates selection against non-recombinant clones. Bacteria containing the pEMI-recipient vector were conjugated with bacteria containing a pSM2c vector encoding a p53-specific microRNA. 79 of 80 (98.7%) of the resulting bacterial colonies harbored pEMI vectors containing the p53-microRNA as determined by colony PCR (data not shown). Successful recombination was also confirmed by restriction and sequence analysis (data not shown).

5.8 Functional evaluation of pEMI vectors

The human osteosarcoma cell line U2OS was transfected with pEMI vectors encoding either MAD2-, p53-specific or non-silencing microRNAs, which do not recognize any human mRNA. Selection for cells containing the pEMI vectors with hygromycin B was completed within 7 days. The resulting pools of resistant cells were analyzed for RT-PCR analysis to determine the expression of the ectopic microRNA after addition of doxycycline (DOX) (Figure 24). In the absence of DOX no MAD2-specific microRNA was detected after 30 PCR cycles. However, 24 hours after addition of DOX the microRNA was expressed. By 48 hours the expression increased further as determined by quantitative PCR (data not shown). As no microRNA expression was detected in the absence of DOX, these results show that the pEMI vectors mediate an extremely stringent control over microRNA expression. In line with this observation the cell pools were consistently devoid of mRFP (monomeric red fluorescent protein) expression in the absence of DOX as determined by live cell fluorescence microscopy (Figure 24b).

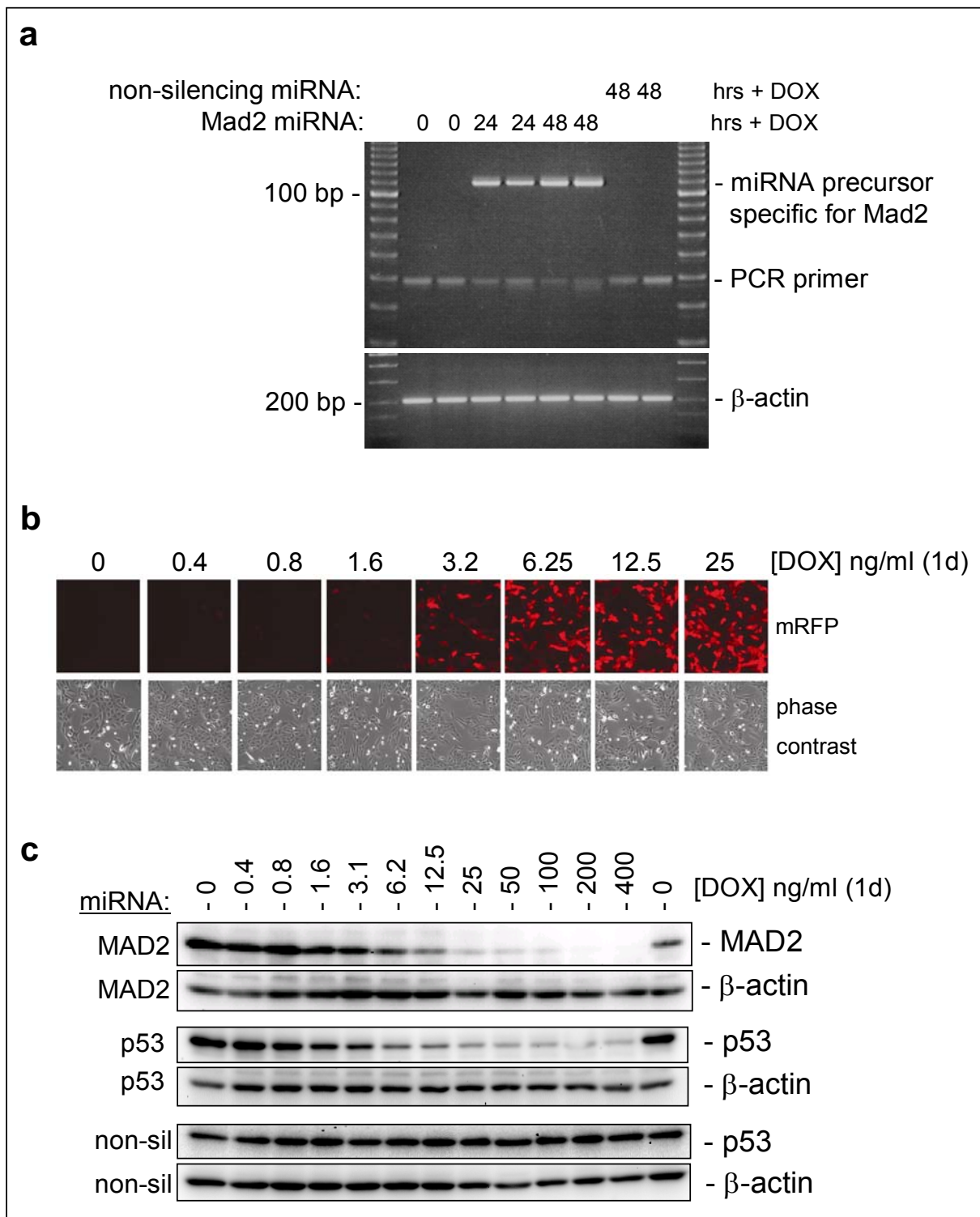


Figure 24 Conditional microRNA expression mediated by pEMI

(a) RT-PCR analysis of microRNA expression. U2OS cells stably transfected with pEMI encoding a Mad2-specific or non-silencing microRNA (miRNA) were treated with 200 ng/ml DOX for 24 or 48 hours. The experiment was performed in duplicates. After 30 cycles of PCR DNA fragments were separated either on 15% poly-acryl-amid gels (for detection of the Mad2-specific miRNA precursor) or 2% agarose gel (for β -actin). DNA-markers in outer lanes: 10 bp ladder (upper panel) and 100 bp ladder (lower panel). (b) Detection of monomeric red fluorescent protein (mRFP) expression 24 hours after addition of the indicated doxycycline (DOX) concentrations to U2OS cells transfected with pEMI

vectors encoding p53-specific miRNAs. Exposure times: 500 ms for mRFP, 50 ms for phase contrast. **(c)** Doxycycline (DOX) dose-reponse of p53 conditional knock-down: U2OS cell pools stably transfected with pEMI-p53miRNA plasmid were treated with the indicated DOX concentrations for 24 hours (upper panel). Control cells are also shown (middle panel). pEMI-MAD2miRNA-mediated down-regulation of MAD2 expression (lower panel). (Experiments with p53-specific microRNA were performed by Peter Jung, MPI for Biochemistry).

Within 24 hours after addition of DOX approximately half of the cells were positive for mRFP at 3.2 ng/ml DOX and virtually all cells were positive at 25 ng/ml (Figure 24b). Efficiency of protein down-regulation depends on number of factors including stability and turnover of the targeted mRNA/protein.

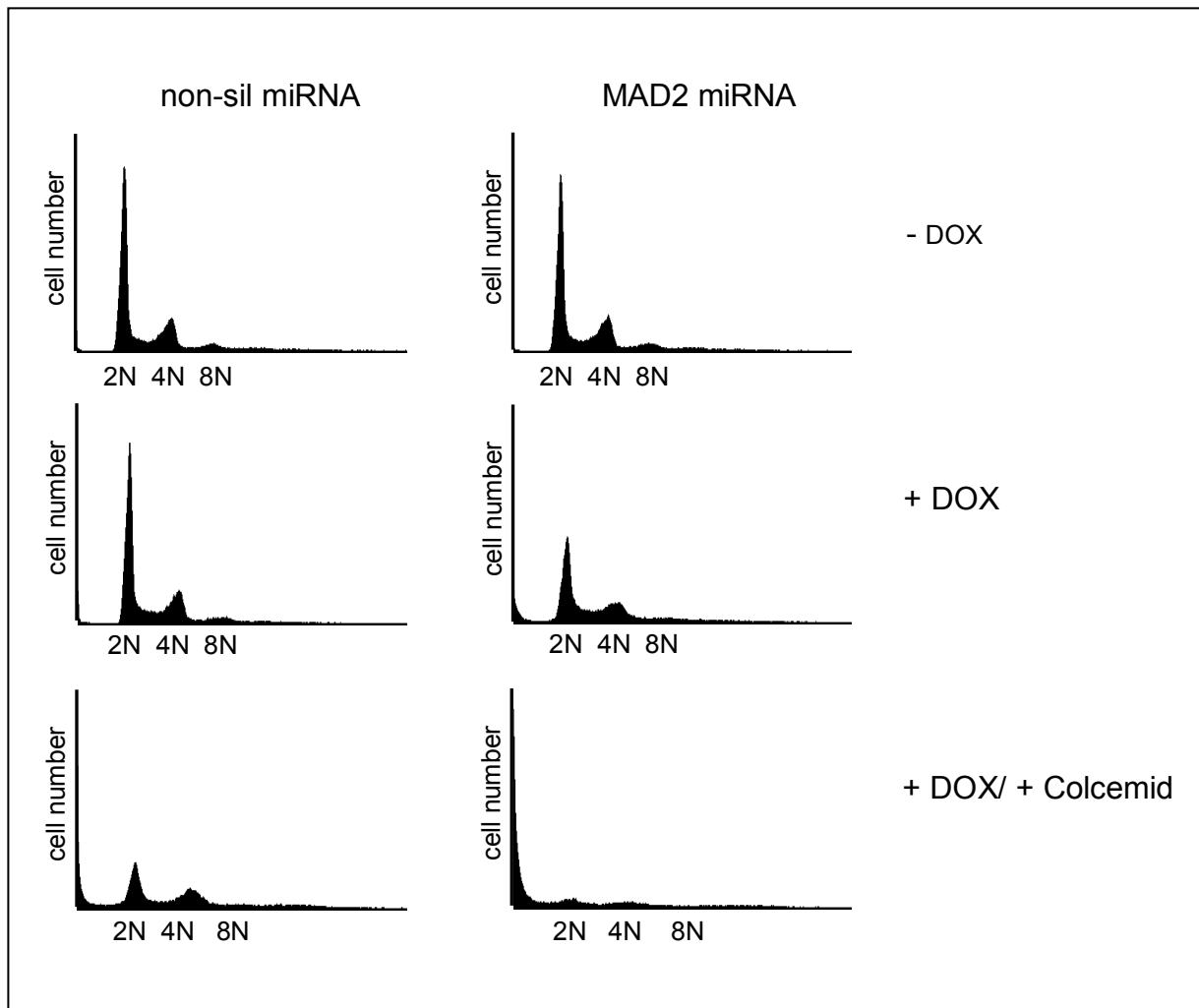


Figure 25 MAD2 knockdown sensitizes to spindle poison.

Fluorescence activated cell sorting (FACS) analysis of U2OS cells stably transfected with pEMI-MAD2miRNA or pEMI non-silencing-miRNA plasmids. Cells were cultured in 100 ng/ml DOX for 4 days and colcemid (25 µg/ml) was added 24 hours before harvesting

The pEMI microRNA expressing system markedly down-regulated the level of p53 protein already at concentrations of DOX between 0.8-1.6 ng/ml (Figure 24c). The most pronounced effects were observed in the range of 6.2-50 ng/ml with both MAD2 and p53 proteins. Induction of a non-silencing microRNA did not affect the levels of p53 protein.

As an example for the inactivation of an essential gene by the system introduced here we conditionally down-regulated the expression of the MAD2 protein, which was shown to result in mitotic failure and extensive cell death when permanently inactivated (Hernando et al., 2004; Kops et al., 2004). After introduction of the pEMI-plasmid encoding a MAD-specific microRNA we observed no effect on the viability and cell cycle distribution. Only when MAD2 was down-regulated by addition of DOX an increased fraction of apoptotic cells was observed. Treatment with colcemid, a drug depolymerizing spindle microtubules and thereby inactivating spindle formation during metaphase, led to increased apoptosis. In the presence of MAD2 knockdown this phenotype was again more pronounced. These results show that the expression of microRNAs can be tightly controlled using pEMI vectors, which are therefore useful for studying essential genes. Another example shows that p53 microRNA mediated knockdown prevents any significant increase in p53 and p21 protein level after DNA damage and p53 inhibited arrest in the G1-phase, both caused by etoposide (Jung et al., 2007 PNAS paper).

To rule out activation of the interferon system by the pEMI vector-driven microRNA expression, we analysed the expression of the *IFIT1* (interferon-induced protein with tetratricopeptide repeats 1) gene by quantitative PCR (qPCR). Others have shown that expression of *IFIT1* mRNA is rapidly induced upon interferon (IFN) treatment (Kusari and Sen, 1986). Besides interferon, double stranded RNA (dsRNA) and viral infection have been shown to increase the expression of *IFIT1* (Guo et al., 2000). pEMI-driven expression of a non-silencing microRNA for 2 and 4 days did not provoke an increased *IFIT1* expression (Figure 26). Also expression of a p53-specific microRNA did not lead to any increase in *IFIT1* expression, whereas transfection of U2OS cells with a synthetic double stranded RNA (poly I:C) led to a ~40-fold increase in *IFIT1* mRNA expression within 18 h after transfection. Incubation of U2OS cells in media containing poly I:C also increased the level of *IFIT1* up to ~7-fold (data not shown) indicating this cell line is in principle very sensitive towards the presence of dsRNA.

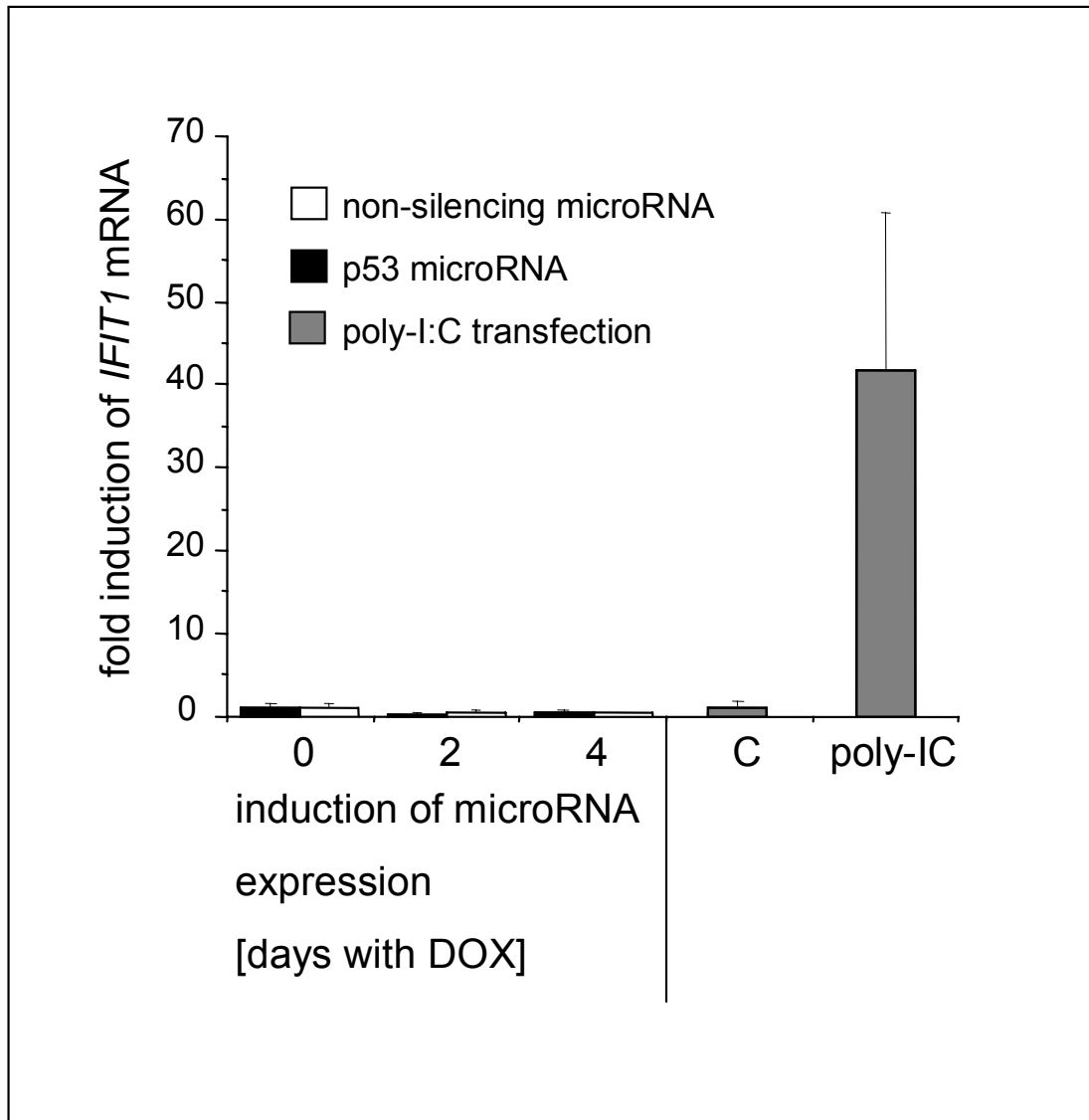


Figure 26 pEMI-driven microRNA expression does not elicit a dsRNA response

qPCR analysis of *IFIT1* (interferon-induced protein with tetratricopeptide repeats 1) expression after induction of microRNAs or treatment with poly I:C. U2OS pools were treated with 100 ng/ml DOX for the indicated time periods to induce non-silencing or a p53-specific microRNA driven by pEMI vector. As a positive control for *IFIT1* gene induction, U2OS cells were transfected with poly I:C dsRNA (IC) or subjected to a mock transfection (C) for 18 h. Shown are the relative expression levels of *IFIT1* normalized to β -actin expression. *IFIT1* expression levels in untreated or MOCK transfected cells were set to 1. All experiments were performed in triplicates. Error bars indicate standard deviations. (Analyses was performed by Peter Jung, MPI of Biochemistry).

Furthermore, proliferation assays showed no significant anti-proliferative effect of pEMI-driven microRNA over-expression and cells were viable for several weeks when expressing microRNAs not targeting essential genes, whereas treatment with poly I:C

led to an apoptotic response 2 days post transfection presumably by activating the dsRNA response (data not shown). Taken together, expression of ectopic microRNA by pEMI vectors does not lead to a dsRNA response or other toxic side effects.

6. Discussion

6.1 c-MYC-induced genomic instability

The induction of genomic instability by c-MYC activation has been repeatedly described in the literature (Felsher and Bishop, 1999; Louis et al., 2005; Mai et al., 1996a; Mai et al., 1996b; Vafa et al., 2002; Yin et al., 2001)). A number of observations suggested a pivotal role of c-MYC activation to drive cell cycle by exaggeration of intrinsic processes. Activation of cyclins and repression of CDK inhibitors together with ability to escape p53/p21 checkpoint machinery give an advantage for c-MYC overexpressing cells to maintain unrestricted proliferation. Oncogenic c-MYC expression in this context may cause DNA damage by different means. In the presence of oncogenically generated damaged DNA, c-MYC may drive cells through cell cycle by overriding p53/p21 dependent arrest (Hermeking and Eick, 1994; Seoane et al., 2002), which may result in genomic destabilization. Such model describes a case of temporary activated c-MYC after first hours-days of activation (Bartek and Lukas, 2001b). On the later time periods of days-weeks, genomic instability initiated by c-MYC overexpression leads to clonal selection of cells with intact checkpoint pathways or acquiring genetic alteration allowing c-MYC independent proliferation (Karlsson et al., 2003), and has a similarity with so called effect of tumor relapsation after inactivation of conditional c-MYC expression (Arvanitis and Felsher, 2006; Pelengaris et al., 2002a). Additionally, c-MYC overactivation can directly lead to chromosomal structure alterations through gene amplification and telomere remodeling.

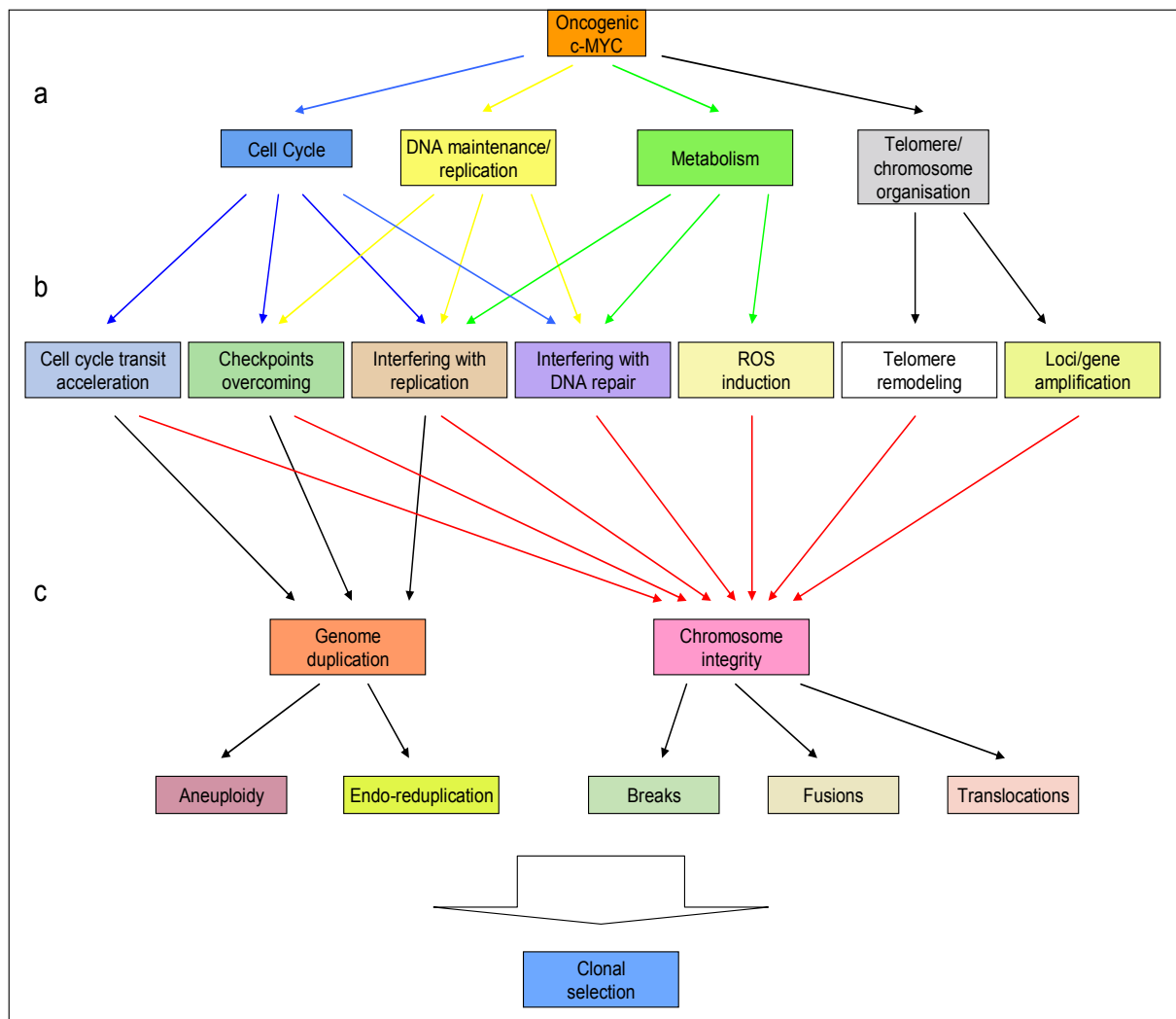


Figure 27 Exaggeration of cellular pathways and mechanisms by c-MYC overactivation cause genomic instability.

(a) Common cellular pathways and mechanisms affected by c-MYC. **(b)** Principal cellular processes initiated by c-MYC overactivation. **(c)** c-MYC caused genomic destabilization at two distinct levels leading either to changes of chromosome number such as aneuploidy and endo-reduplication or defects in chromosomal integrity including chromosomal breaks, fusions or translocations. Genomic instability furthermore could give an advantage for tumor initiation or progression.

In the studies presented here the activation of c-MYC expression results in comparable features and signs of unstable chromatin behavior. Conditional c-MYC activation in DLD-1 and MCF-7 cells leads to chromosomal instability measured by centromere probes hybridization or micronuclei counting. Furthermore, an increase of DNA damage as detected by γ -H2AX/53BP1 staining was observed (Menssen et al., 2007). By time lapse imaging of living cells abnormal transition and chromosome behavior throughout prometa-, meta- and anaphases was observed, which was

accompanied by distortion of the metaphase plate. c-MYC activation leads to elevation of mitotic events with disorganized metaphase plate structure. On chromatin level, c-MYC causes appearance of lagging chromosomes and chromatin bridges throughout anaphase and in following interphase. In some cases chromatin bridges led to fusion of two daughter cells and appearance of tetraploid cells. Breaks of bridges and improper separation of lagging chromosomes in anaphase generated daughter cells with unequally distributed genetic material due to loss or gains of chromosomes. Such c-MYC-dependent induction of chromatin abnormalities might potentially be explained by passaging of damaged DNA through G₂ checkpoint into mitosis (Syljuasen et al., 2006). c-MYC overexpression induces DNA damage and by abrogating the G₁/S checkpoint may push cells with partially repaired or unrepaired DNA into the G₂ phase (Bartek and Lukas, 2001b; Sheen and Dickson, 2002). In several cellular models c-MYC overexpression was shown to attenuate G₂ arrest (Sheen et al., 2003) and in the absence of active p53 pathway even efficiently overcome it (Yin et al., 2001; Yin et al., 1999). In some cellular systems c-MYC leads to attenuation of G₂ phase. In some cases extension exist even until beginning of prophase-like stage. Additionally we observed appearance of γ -H2AX foci on mitotic chromosomes, associated with c-MYC induction (data not shown). This might suggest that activated c-MYC allow G₂ arrested cells with damaged DNA to proceed into mitosis or the following S-phase, initiating endo-reduplication (Figure 28). Furthermore, in earlier stages of mitosis damaged, incompletely or improperly unrepaired DNA may become packaged into the chromosomes, which lead to formation of breaks and chromatin bridges in the following mitosis. All chromosomes have to be rearranged throughout mitosis to give an equal separation of genetic material into two daughter cells. However, those damaged chromosomes could cause attenuation and abnormal mitotic progression observed in time-lapse video that finally could leads to aneuploidy (Mikhailov et al., 2002). Furthermore, cells with severe DNA damage or chromosomal abnormalities may be eliminated from the population via apoptosis (Figure 28) (Gasser and Raulet, 2006).

How oncogenic c-MYC overexpression directly leads to DNA damage is not clear (Mai and Mushinski, 2003; Wade and Wahl, 2006). One potential explanation is the generation of ROS by c-MYC (Vafa et al., 2002) which causes DNA damage. Recently it was shown that c-MYC can induce double-stranded breaks, independently on ROS induction (Ray et al., 2006). Other potential effects of c-MYC activation might be the distortion of replication processes (Angus et al., 2002; Blagosklonny and

Pardee, 2002; Matsumura et al., 2003; Spruck et al., 1999; Walter et al., 1998), leading to improper replication followed by DNA breaks (Lengronne and Schwob, 2002).

6.2 c-MYC-induced mitotic delay

Results of this study show that c-MYC induces the expression of both BubR1 and MAD2 on the level of RNA and protein. These proteins inhibit CDC20-APC/C and progression into anaphase until all kinetochores are properly attached to microtubule spindles of opposite poles (Kops et al., 2005). In accordance with the literature, upregulation of these proteins mediated by c-MYC leads to extension of mitosis length at specifically stage – prometaphase, where both proteins have their main function (Hernando et al., 2004; Li et al., 1999). Modulation of gene expression using stable expression of shRNA constructs against either BubR1 or MAD2 blocked efficient upregulation of proteins by c-MYC induction and as following, decreased average length of mitosis. Interestingly, MAD2 protein downregulation in the presence of activated c-MYC has only partial effect on mitosis length, where BubR1 knockdown almost completely reversed this phenotype. Downregulation of BubR1, which is a transducer of “wait anaphase signal” through MAD2 and forms an inhibitory complex of CDC20 together with MAD2, may therefore more efficiently influence signal transduction than downregulation of final signalling effector MAD2 (Figure 3).

The potential biological purpose of the activation of BubR1 and MAD2 by c-MYC is an increased sensitivity of the spindle checkpoint machinery to recognize abnormal chromosomal organization and with following extension of prometaphase to give a time for chromosome reorganization, to ensure proper propagation of genome during cell division (Hernando et al., 2004). Probably due to the same reason to propagate intact genome c-MYC activates multiple genes involved in DNA repair when quiescent cells re-enter cell cycle (Menssen and Hermeking, 2002; Patel et al., 2004).

This observation gives rise to the questions whether the induction of BubR1 and MAD2 spindle checkpoint genes by c-MYC can directly lead to lengthening of mitosis or depends on DNA damage passing through G₂ checkpoint into mitosis. From one side chromosomes which contain DNA damage lesions could directly activate spindle checkpoint and extend mitosis (Menssen et al., 2007). Results of this study show that population of cells with chromatin abnormalities in mitosis associated with extended mitotic length, but the average mitotic length in this population only by

10 minutes more in comparison to population of cells without visible alterations (data not shown). Therefore, the c-MYC-induced DNA damage would only partially explain the mitotic delay. Furthermore, it would be interesting to prove whether after active ATM signalling in the cells with DNA damage overcomes G₂ arrest might influence on spindle checkpoint and if it does, how it modulate the activity. ATM signalling already was shown to influence mitotic progression in several ways: through downregulation of centrosome function (Sibon et al., 2000), Plk1 activity (Smits et al., 2000) and cyclin A degradation (Su and Jaklevic, 2001).

6.3 BubR1/MAD2-dependent mitotic delay does not influence c-MYC-induced genomic instability

Another question which arises is how the level of BubR1/MAD2 proteins might influence c-MYC-induced chromosomal instability. Ectopic expression of MAD2 in MEFs leads to multiple chromosomal abnormalities like broken chromosomes, anaphase bridges, and whole-chromosome gains and losses (Hernando et al., 2004; Sotillo et al., 2007). This is in accordance with the previous observation that MAD2 overexpression causes a hyperactive spindle checkpoint, which could result in the mitotic defects and chromosomal instability (Hernando et al., 2004). MAD2 overexpression in *in vivo* model leads to a wide range of tumors in more than 50% of the mice and was shown to accelerate lymphomagenesis in the E μ -myc mice (Sotillo et al., 2007). Recently, it has been shown that deregulation of the transcription factor E2F activates expression of *MAD2* and delays mitotic progression (Hernando et al., 2004). c-MYC presumably activates *MAD2* expression independent of E2F as we observed induction of *MAD2* by c-MYC in cells with knock-down of DP-1. However, E2F and c-MYC may act synergistically to activate *MAD2* expression (Sears et al., 1997). Hernando *et al.* proposed that the induction of *MAD2* itself is the cause for CIN (Hernando et al., 2004). The analysis of c-MYC-induced genomic instability in DLD-1-tTA-MYC and PJMMR1 cells did not reveal a requirement of *MAD2* induction for c-MYC-induced CIN. Moreover, experimental down-regulation of BubR1, which has a similar function as MAD2, also had no influence on c-MYC-induced CIN. In the experiments described here, partial down-regulation of BubR1 and MAD2 by stable shRNA expression prevents efficient c-MYC-dependent induction of these genes and leads to a minor increase of basal genomic instability level observed as elevation in micronuclei formation. Also no significant difference in abnormal chromatin formation

within mitotic progression was observed in time-lapse recordings when *BubR1* or *MAD2* knockdown and control populations were compared. These observations show that the induced expression of *BubR1* and *MAD2* mitotic checkpoint genes does not significantly participate in formation of chromosomal instability induced by *c-MYC*, but potentially plays a role in sensitizing the mitotic checkpoint. Aneuploidy caused by inactivation of *BubR1* or *MAD2* mitotic checkpoint genes has been implicated in tumorigenesis and suggests that these genes may function as tumor suppressors (van Deursen, 2007; Weaver et al., 2007). The reduction of both *BubR1* and *Mad2* proteins expression in mouse models results in chromosome missegregation. *BubR1^{H/H}* (hypomorphic *BubR1* mutation caused of *BubR1* protein reduction up to 10% of normal level) mice exhibit increased susceptibility to tumours induced by carcinogenesis (Dai et al., 2004). *BubR1^{+/-}ApcMin/+* compound mutant mice develop colorectal cancer at a 10x higher rate than *ApcMin/+* mice (Rao et al., 2005). As APC negatively regulates *c-MYC* (He et al., Science) these tumors are presumably caused, at least in part, by deregulation of *c-MYC*. Cells from these mice showed premature separation of sister chromatids and enhanced genomic instability. In addition, germ line mutations in *BubR1* have been linked to the rare cancer predisposition syndrome mosaic variegated aneuploidy (MVA) (Hanks et al., 2004; Matsuura et al., 2006). *MAD2^{+/-}* mice develop lung tumors at high rates after long latencies (Dobles et al., 2000). Furthermore, the current literature supports a function of *MAD2* as a tumor suppressor as inactivating mutations have been identified in the *MAD2* gene in bladder, breast and gastric cancer (Baek et al., 2005; Hernando et al., 2001; Percy et al., 2000).

Current cellular models (DLD-1-tTA-MYC and PJMMR1 cells) involved in this study in principle do not exclude a link between *MAD2* overexpression and chromosomal instability. One of the features of these systems is the rapid induction of *c-MYC* expression, both from CMV promoter, and the occurrence of pronounced *c-MYC*-induced phenotypes, including a rapid increase in cells with micronuclei representing CIN. The percentage of these cells in population rises up within first 4 days of *c-MYC* induction and reached a plateau of 10-20% where it is balanced by an increasing rate of apoptosis. Further ectopic expression of *c-MYC* leads to a strong degree of instability, which is accompanied by massive apoptosis in these cells. Potentially, chromosomal instability induced by *MAD2* (or/and *BubR1*) overexpression occurs in these *c-MYC*-inducible systems but is masked by *c-MYC*-induced apoptosis.

In this case would be interesting to modulate apoptosis rate by pan-caspase inhibitors which efficiently repress c-MYC-dependent cell death.

6.4 c-MYC-induced apoptosis

DLD-1-tTA-MYC cells, as others cells ectopically expressing c-MYC, show induction of apoptosis after induction of c-MYC. This apoptosis increases gradually. Two kinds of apoptosis were distinguished in time-lapse video of DLD-1-tTA-MYC cells after c-MYC activation. The first type of apoptosis represents spontaneous death of single cells and was not connected to mitotic progression. The second type, post-mitotic apoptosis, represents the populations of cells synchronously dying after mitosis with chromatin condensation observed as late apoptotic events in both daughter progeny. The ratio between these two kinds of apoptosis was approximately 1:3 with the a maximum in the post-mitotic fraction 2 days after c-MYC induction. As DLD-1 cells express a mutant p53 allele, post-mitotic apoptosis is p53-independent. The average time interval between the end of telophase and beginning of apoptotic chromatin condensation was around 4 hours after 2 days of c-MYC activation and drops down to 1-2 hours with a later time points (data not shown) probably due to increase of c-MYC-induced genomic instability formation as main reason for this. This average interval does not depend on the level of BubR1 or MAD2 protein expression. Itself, induction of post-mitotic apoptosis directly depend on c-MYC activation and reach 15 and 22 percent (23 out of 150 cells after 1 day and 49 out of 222 cells after 2 days of c-MYC induction, respectively) of mitotic cells after 1 and 2 days of induction respectively (Figure 14, a) and has tendency for further elevation. Unfortunately the 16x objective resolution applied for common time-lapse video acquisition did not allowed to observe smaller chromatin aberrations, which easily detectable with objectives with 40-60x magnification. Nevertheless, in cell populations undergoing post-mitotic apoptosis 35-40 percent (9 out of 23 and 17 out of 49 cells) contain detectible chromosomal aberrations in mitosis. As was described for chromosomal aberrations, the average length of mitosis of the cells undergoing post-mitotic apoptosis was 12 minutes more comparing to average mitotic cells without any aberrations or apoptosis. Almost whole population of cells with post-mitotic apoptosis has extended mitosis although some of the cells have completely normal mitotic progression. Interestingly, in time-lapse movie revealed BubR1 dependent formation of post-mitotic apoptosis in the population of mitotic cells after c-MYC activation.

BubR1 expression was controlled by shRNA mediated downregulation which prevents efficient BubR1 mRNA induction by c-MYC (Figure 7, b). After 48 hours of c-MYC expression I observed 4-5 % decrease of post-mitotic apoptosis in population of cells representing BubR1 downregulation in comparison to control (Figure 18, c). BubR1 dependent apoptosis was described in literature (Shin et al., 2003). No significant difference was observed in the presence of MAD2 knockdown. In addition, DLD-1-tTA-MYC cells undergoing massive apoptosis upon c-MYC activation in the presence of microtubule inhibitor nocodazol. All these observations show that post-mitotic apoptosis become induced before mitosis by c-MYC and could be modulated in mitosis, where induction of BubR1 spindle checkpoint serves tumor suppressive, proapoptotic function (Figure 28).

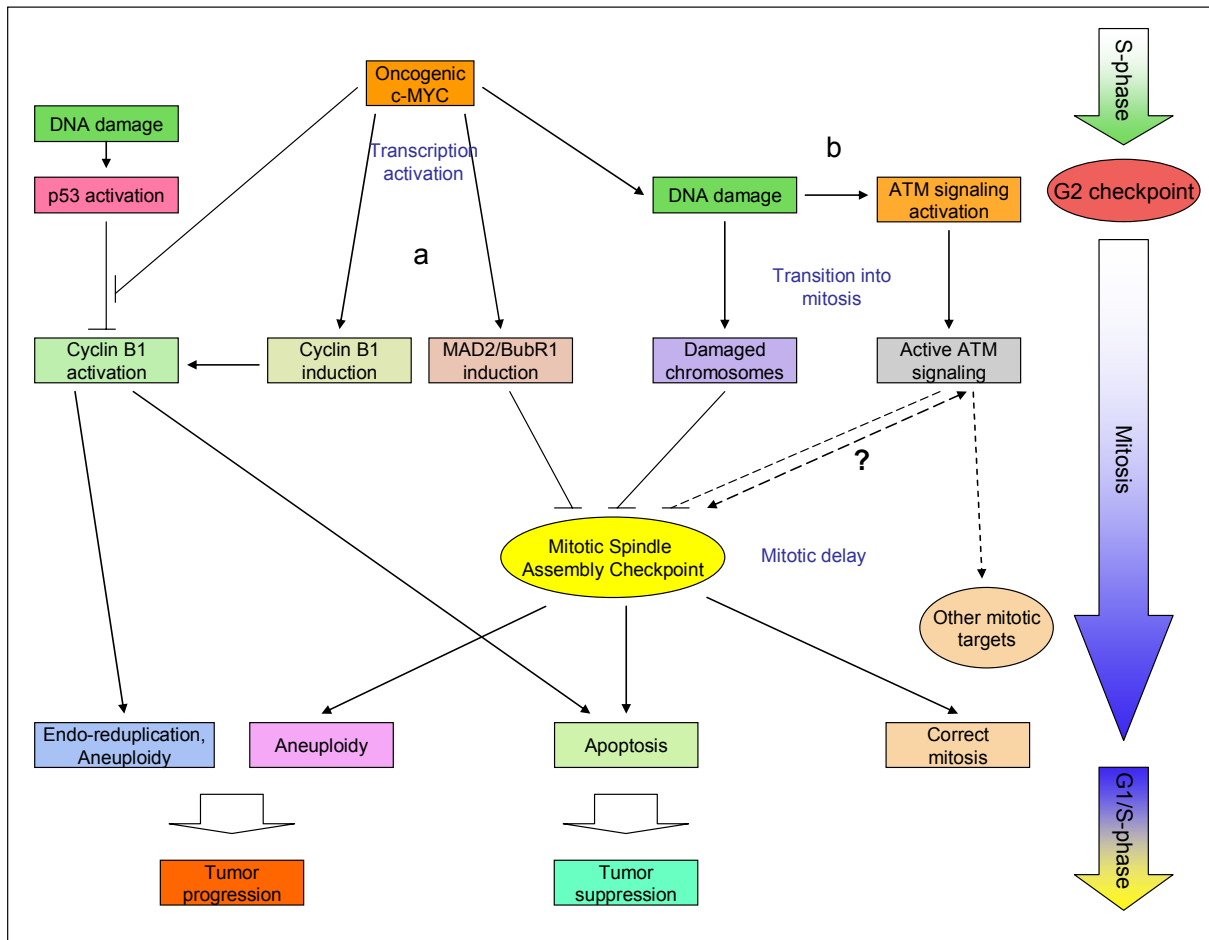


Figure 28 c-MYC activation alters progression through mitosis

(a) c-MYC can directly activate genes involved in spindle checkpoint machinery or mitotic progression, depending on cell type and conditions leading to genome destabilization or apoptosis induction. (b) Indirect influence of c-MYC overactivation on mitotic progression might function through the modulation of spindle checkpoint machinery by generated DNA damage or active ATM signaling transmitted into mitosis.

6.5. All-in-one conditional microRNA expressing system

A decade ago after discovery of RNA interference (RNAi) this mechanism has been implicated in a wide spectrum of genetic analysis and screens (Hannon, 2002; Meister and Tuschl, 2004; Paddison and Hannon, 2002; Paddison et al., 2004; Silva et al., 2004). The activation of the interference machinery involves the formation of ribo-protein complexes guiding site-directed cleavage of the mRNA of interest by the anti-sense ribo-sequence (Figure 4). The artificial delivery or vector-based expression of RNA templates in the cells allows effective and gentle manipulation of interference machinery. Despite simplicity and efficiency, the delivery of ssRNA or dsRNA itself by means of transfection approach is always limited by the efficacy of transfection and viability of introduced RNAs (Fewell and Schmitt, 2006). An alternative strategy is the expression of targeting shRNAs or miRNAs in cells achieved by vector-based expression. Such approaches allows its conditional regulation and co-expression of tracking proteins or selection markers. Furthermore, conditional regulation has a clear advantage of gentle physiological regulation in comparison to stable expression. However, the conditional systems published so far bear the necessary regulators on the separate plasmids, thereby complicating the generation of stable cell lines. Therefore our goal was to integrate all necessary components into the single plasmid to simplify procedures of cloning, delivery and integration of genetic elements allowing conditional regulation of miRNAs expression (Epanchintsev et al., 2006).

For conditional regulation a bi-directional promoter bearing a tet-operon, which is based on minimal CMV-promoter region and tightly controlled by highly DOX-sensitive reverse tetracycline trans-activator rtTA2^S-M2 and tet repressor-KRAB fusion proteins (tTS^{KRAB}) (Bornkamm et al., 2005). The system precisely responds to DOX level allowing expression of both a fluorescent protein and microRNA allele based on minimized version of mir30 transcript. In principle, the mir30 locus can be substituted by any other microRNA transcript, which broadens the flexibility of applications such as RNAi or translational inhibition (Figure 4). Additional features of the vector allow bacterial propagation and maintenance plasmid episomality in the target cells (Li and Elledge, 2005). The Mir30 expression allele was constructed with possibility of either conventionally cloning of miRNA target sequences through the shuttle vector or magic recombination transfer strategy of miRNA cassettes from the microRNA library (Silva et al., 2005).

The functionality of the all-in-one pEMI system was established using two distinct miRNA sequences targeted p53 tumor suppressor and MAD2, spindle checkpoint genes. Both systems show a fast response to the various DOX concentrations and represents tight off-state control. The depth of target protein knockdown gradually corresponds to the elevation of DOX concentration, has an effective down regulation at approximately 5 ng/ml of DOX and in case of MAD2 leads to almost complete protein depletion with already 100 ng/ml of DOX. The system also allows efficient knockdown restoration upon DOX withdrawal. The stability of pEMI integration was confirmed in different cell lines. U2OS and H1299 cell lines are susceptible to fast acquisition after transfection and selection procedures. Relatively long maintenance of the plasmid in the pool of cells last up to 4 weeks and allows preparation of conventionally long knockdown experiments. As well, the miRNA transcription from pEMI does not induce interferon pathway, confirming physiological compatibility of expression.

The controlled activation of the knockdown may be useful in certain therapeutic regimes and prevent the potential toxicity or immunogenicity which has been discussed for therapeutic applications of ectopic RNA interference. As mentioned above the pEMI vector is compatible with recently generated microRNA libraries and will therefore presumably become a widely used tool for conditional RNA interference.

7. Summary

c-MYC is one of the major human oncogenes, however, the mechanisms involved in tumor initiation and development by c-MYC are not completely understood. One important function of c-MYC is the stimulation of G₁/S-transition. However, the effects of c-MYC on G₂/M progression and mitosis have not been characterized so far. The goal of the present study was to investigate the influence of c-MYC activation on the mitosis. Therefore, time-lapse microscopy of living cells was used to analyse mitotic progression after c-MYC activation. This analysis revealed a c-MYC-dependent extension of mitosis in prometaphase. This finding together with microarray analysis of c-MYC-regulated genes directed the attention of this work towards the spindle checkpoint genes. Two of them, MAD2 and BubR1, were characterized as direct c-MYC target genes. Experimentally inactivation of MAD2 and BubR1 expression by RNA interference revealed that the c-MYC-induced lengthening of prometaphase is dependent on the induction of MAD2 and BubR1 by c-MYC.

Unexpectedly, further analysis did not reveal any influence of the c-MYC-induced expression of MAD2 and BubR1 on c-MYC-induced chromosomal instability. These results therefore question the previously described mechanism by which the transcription factor E2F induces chromosomal instability. Furthermore, a synchronous postmitotic form of c-MYC-induced apoptosis was characterized. A minor contribution of the induction of BubR1 expression for type of apoptosis was detected.

Taken together these results show that deregulated expression of c-MYC, as it occurs in the majority of cancers, has drastic effects on the progression through mitosis: it delays mitosis in a MAD2- and BubR1-dependent manner. Furthermore, the effects of c-MYC on mitosis presumably provoke a cellular response which is manifested in post-mitotic apoptosis.

Recently, libraries of retroviral expression constructs encoding microRNAs which target most of the human and mouse genes became available. To allow the transfer of these microRNA cassettes into a new inducible, episomal expression system by homologous recombination, a new vector was generated and characterized. This system will allow the rapid functional and biochemical characterization of essential gene products by conditional RNA interference.

8. ABBREVIATIONS

AML	Acute lymphocytic leukemia
APC	Adenomatous polyposis coli
APC/C	Anaphase Promoting Complex or Cyclosome
APS	Ammonium peroxodisulfate
ATM	Ataxia telangiectasia mutated
ATR	ATM and Rad3-related
BAX	BCL2-associated X protein
BCL-XL	B-cell leukemia-x long
Bcl2	B-cell leukemia 2
BIM	Bcl-2 interacting protein
BRCA	Breast cancer susceptibility gene 1/2
Bub	Budding uninhibited by benzimidazoles homolog
BubR1	Budding uninhibited by benzimidazoles 1 homolog beta; MAD3/BUB1-related protein kinase
c MYC	v-MYC avian myelocytomatosis viral oncogene homologue
c-src	Rous sarcoma viral oncogene homolog
CAD	Carbamoyl-phosphate synthetase 2
CCD	Charge-coupled device (camera)
CDC	Cell division cycle
CDK	Cyclin-dependent kinase
cDNA	Complementary DNA
Cdt1	Chromatin licensing and DNA replication factor 1
CENP	Centromere protein
Chk	Checkpoint kinase
ChIP	Chromatin immunoprecipitation
CIN	Chromosome instability
CMV	Cytomegalovirus (promoter)
CUL1	Cullin 1
Cy3	Cyanine 3
dMYC	Drosophila homolog of v-MYC
DAPI	2-(4-Amidinophenyl)-6-indolecarbamidine dihydrochloride
DHFR	Dihydrofolate reductase
DLCL	Diffuse large cell lymphoma
DMEM	Dulbecco's modified eagle medium
DMSO	Dimethylsulfoxide
dNTP	Deoxynucleotide triphosphate
DP1	Deleted in polyposis 1
DSB	Double strand breaks
dsRNA	Double stranded RNA
DTT	Dithiothreitol
E-box	Enhancer box
E2F1	E2F transcription factor 1
EBNA	Epstein-Barr virus nuclear antigen
<i>E. coli</i>	<i>Escherichia coli</i>
EDTA	Ethylenediamine-tetraacetic acid
EGTA	Ethylene glycol-0,0'-bis (2-aminoethylether)-N,N,N',N'-tetraacetic acid
FBS	Foetal bovine serum
G418	Geneticin®

GFP	Green fluorescent protein
HA	Hemagglutinin
H2AX	H2A histone family, member X
HBSS	Hanks' balanced salt solution
HNPCC	Hereditary nonpolyposis colon cancer
HPV	Human papillomavirus
HygB	Hygromycin B
ID2	Inhibitor of DNA binding 2
IF	Immunofluorescence
Ig	Immunoglobulin
IPTG	Isopropyl b-D-1-thiogalactopyranoside
IRES	Internal ribosome entry site
IFIT1	Interferon-induced protein with tetratricopeptide repeats 1
LMYC	Lung carcinoma-derived v-myc myelocytomatosis viral oncogene homologue
LB	Luria-Bertani
MAD	Mitotic arrest deficient-like
MCM2	Minichromosome maintenance deficient
Mdm2	Mouse double minute 2
MIN	Microsatellite instability
MIZ1	MYC-interacting zinc finger protein 1
miRNA	Micro RNA
MLH	MutL homolog
MM	Malignant melanoma
MMR	Mismatch repair
Mos	v-mos Moloney murine sarcoma viral oncogene homolog
MSH	MutS homologue
NBL	Neuroblastoma
NMYC	Neuroblastoma-derived v-myc myelocytomatosis viral oncogene homologue
NP40	Nonidet-P40
PCL	Primary plasma cell leukemia
p107	Retinoblastoma-like 1
PBS	Phosphate buffered saline
PCR	Polymerase chain reaction
pRB	Retinoblastoma protein
RAS	Rat sarcoma viral oncogene homologue
RNAi	RNA interference
ROS	Reactive oxygen species
RSV	Rous sarcoma virus
S-MYC	MYC-like oncogene
SAC	Spindle assembly checkpoint
SAGE	Serial analysis of gene expression
siRNA	Small interfering RNA
shRNA	Small interfering RNA
SCC	Squamous cell carcinoma
SCLC	Small cell lung carcinoma
SDS	Sodium dodecyl sulfate
tTA	Tetracycline-controlled transactivator
w/v	Weight per volume

9. References

- Aagaard, L., and Rossi, J.J. (2007). RNAi therapeutics: Principles, prospects and challenges. *Adv Drug Deliv Rev*.
- Abba, M.C., Laguens, R.M., Dulout, F.N., and Golijow, C.D. (2004). The c-myc activation in cervical carcinomas and HPV 16 infections. *Mutat Res* 557, 151-158.
- Alitalo, K., and Schwab, M. (1986). Oncogene amplification in tumor cells. *Adv Cancer Res* 47, 235-281.
- Andreassen, P.R., and Margolis, R.L. (1994). Microtubule dependency of p34cdc2 inactivation and mitotic exit in mammalian cells. *J Cell Biol* 127, 789-802.
- Angus, S.P., Wheeler, L.J., Ranmal, S.A., Zhang, X., Markey, M.P., Mathews, C.K., and Knudsen, E.S. (2002). Retinoblastoma tumor suppressor targets dNTP metabolism to regulate DNA replication. *J Biol Chem* 277, 44376-44384.
- Arvanitis, C., and Felsher, D.W. (2006). Conditional transgenic models define how MYC initiates and maintains tumorigenesis. *Semin Cancer Biol* 16, 313-317.
- Avet-Loiseau, H., Gerson, F., Magrangeas, F., Minvielle, S., Harousseau, J.L., and Bataille, R. (2001). Rearrangements of the c-myc oncogene are present in 15% of primary human multiple myeloma tumors. *Blood* 98, 3082-3086.
- Babu, J.R., Jeganathan, K.B., Baker, D.J., Wu, X., Kang-Decker, N., and van Deursen, J.M. (2003). Rae1 is an essential mitotic checkpoint regulator that cooperates with Bub3 to prevent chromosome missegregation. *J Cell Biol* 160, 341-353.
- Baek, K.H., Shin, H.J., Jeong, S.J., Park, J.W., McKeon, F., Lee, C.W., and Kim, C.M. (2005). Caspases-dependent cleavage of mitotic checkpoint proteins in response to microtubule inhibitor. *Oncol Res* 15, 161-168.
- Baker, D.J., Jeganathan, K.B., Cameron, J.D., Thompson, M., Juneja, S., Kopecka, A., Kumar, R., Jenkins, R.B., de Groen, P.C., Roche, P., *et al.* (2004). BubR1 insufficiency causes early onset of aging-associated phenotypes and infertility in mice. *Nat Genet* 36, 744-749.
- Baker, D.J., Jeganathan, K.B., Malureanu, L., Perez-Terzic, C., Terzic, A., and van Deursen, J.M. (2006). Early aging-associated phenotypes in Bub3/Rae1 haploinsufficient mice. *J Cell Biol* 172, 529-540.
- Baker, V.V., Borst, M.P., Dixon, D., Hatch, K.D., Shingleton, H.M., and Miller, D. (1990). c-myc amplification in ovarian cancer. *Gynecol Oncol* 38, 340-342.
- Bartek, J., and Lukas, J. (2001a). Mammalian G1- and S-phase checkpoints in response to DNA damage. *Curr Opin Cell Biol* 13, 738-747.

- Bartek, J., and Lukas, J. (2001b). Pathways governing G1/S transition and their response to DNA damage. *FEBS Lett* 490, 117-122.
- Bates, S., Ryan, K.M., Phillips, A.C., and Vousden, K.H. (1998). Cell cycle arrest and DNA endoreduplication following p21Waf1/Cip1 expression. *Oncogene* 17, 1691-1703.
- Baudino, T.A., McKay, C., Pendeville-Samain, H., Nilsson, J.A., Maclean, K.H., White, E.L., Davis, A.C., Ihle, J.N., and Cleveland, J.L. (2002). c-Myc is essential for vasculogenesis and angiogenesis during development and tumor progression. *Genes Dev* 16, 2530-2543.
- Bello-Fernandez, C., Packham, G., and Cleveland, J.L. (1993). The ornithine decarboxylase gene is a transcriptional target of c-Myc. *Proc Natl Acad Sci U S A* 90, 7804-7808.
- Bernards, R., Brummelkamp, T.R., and Beijersbergen, R.L. (2006). shRNA libraries and their use in cancer genetics. *Nat Methods* 3, 701-706.
- Berns, E.M., Klijn, J.G., van Putten, W.L., van Staveren, I.L., Portengen, H., and Foekens, J.A. (1992). c-myc amplification is a better prognostic factor than HER2/neu amplification in primary breast cancer. *Cancer Res* 52, 1107-1113.
- Berns, K., Hijmans, E.M., and Bernards, R. (1997). Repression of c-Myc responsive genes in cycling cells causes G1 arrest through reduction of cyclin E/CDK2 kinase activity. *Oncogene* 15, 1347-1356.
- Bitzer, M., Stahl, M., Arjumand, J., Rees, M., Klump, B., Heep, H., Gabbert, H.E., and Sarbia, M. (2003). C-myc gene amplification in different stages of oesophageal squamous cell carcinoma: prognostic value in relation to treatment modality. *Anticancer Res* 23, 1489-1493.
- Blagosklonny, M.V., and Pardee, A.B. (2002). The restriction point of the cell cycle. *Cell Cycle* 1, 103-110.
- Bornkamm, G.W., Berens, C., Kuklik-Roos, C., Bechet, J.M., Laux, G., Bachl, J., Korndoerfer, M., Schlee, M., Holzel, M., Malamoussi, A., *et al.* (2005). Stringent doxycycline-dependent control of gene activities using an episomal one-vector system. *Nucleic Acids Res* 33, e137.
- Boveri (1914). *Zur Frage der Entstehung maligner Tumoren*. Jena: Gustav Fischer Verlag.
- Boxer, L.M., and Dang, C.V. (2001). Translocations involving c-myc and c-myc function. *Oncogene* 20, 5595-5610.
- Brodeur, G.M. (1994). Molecular pathology of human neuroblastomas. *Semin Diagn Pathol* 11, 118-125.
- Brodeur, G.M. (1995). Molecular basis for heterogeneity in human neuroblastomas. *Eur J Cancer* 31A, 505-510.

Brummelkamp, T.R., Bernards, R., and Agami, R. (2002). Stable suppression of tumorigenicity by virus-mediated RNA interference. *Cancer Cell* 2, 243-247.

Burmeister, T., Schwartz, S., Horst, H.A., Rieder, H., Gokbuget, N., Hoelzer, D., and Thiel, E. (2005). Molecular heterogeneity of sporadic adult Burkitt-type leukemia/lymphoma as revealed by PCR and cytogenetics: correlation with morphology, immunology and clinical features. *Leukemia* 19, 1391-1398.

Cahill, D.P., da Costa, L.T., Carson-Walter, E.B., Kinzler, K.W., Vogelstein, B., and Lengauer, C. (1999). Characterization of MAD2B and other mitotic spindle checkpoint genes. *Genomics* 58, 181-187.

Cahill, D.P., Lengauer, C., Yu, J., Riggins, G.J., Willson, J.K., Markowitz, S.D., Kinzler, K.W., and Vogelstein, B. (1998). Mutations of mitotic checkpoint genes in human cancers. *Nature* 392, 300-303.

Campbell, M.S., Chan, G.K., and Yen, T.J. (2001). Mitotic checkpoint proteins HsMAD1 and HsMAD2 are associated with nuclear pore complexes in interphase. *J Cell Sci* 114, 953-963.

Carr, A.M. (2000). Cell cycle. Piecing together the p53 puzzle. *Science* 287, 1765-1766.

Chernova, O.B., Chernov, M.V., Ishizaka, Y., Agarwal, M.L., and Stark, G.R. (1998). MYC abrogates p53-mediated cell cycle arrest in N-(phosphonacetyl)-L-aspartate-treated cells, permitting CAD gene amplification. *Mol Cell Biol* 18, 536-545.

Chiang, Y.C., Teng, S.C., Su, Y.N., Hsieh, F.J., and Wu, K.J. (2003). c-Myc directly regulates the transcription of the NBS1 gene involved in DNA double-strand break repair. *J Biol Chem* 278, 19286-19291.

Chuang, T.C., Moshir, S., Garini, Y., Chuang, A.Y., Young, I.T., Vermolen, B., van den Doel, R., Mougey, V., Perrin, M., Braun, M., *et al.* (2004). The three-dimensional organization of telomeres in the nucleus of mammalian cells. *BMC Biol* 2, 12.

Dai, W., Wang, Q., Liu, T., Swamy, M., Fang, Y., Xie, S., Mahmood, R., Yang, Y.M., Xu, M., and Rao, C.V. (2004). Slippage of mitotic arrest and enhanced tumor development in mice with BubR1 haploinsufficiency. *Cancer Res* 64, 440-445.

Daksis, J.I., Lu, R.Y., Facchini, L.M., Marhin, W.W., and Penn, L.J. (1994). Myc induces cyclin D1 expression in the absence of de novo protein synthesis and links mitogen-stimulated signal transduction to the cell cycle. *Oncogene* 9, 3635-3645.

Dalla-Favera, R., Bregni, M., Erikson, J., Patterson, D., Gallo, R.C., and Croce, C.M. (1982). Human c-myc onc gene is located on the region of chromosome 8 that is translocated in Burkitt lymphoma cells. *Proc Natl Acad Sci U S A* 79, 7824-7827.

Dang, C.V. (1999). c-Myc target genes involved in cell growth, apoptosis, and metabolism. *Mol Cell Biol* 19, 1-11.

Deb-Basu, D., Karlsson, A., Li, Q., Dang, C.V., and Felsher, D.W. (2006). MYC can enforce cell cycle transit from G1 to S and G2 to S, but not mitotic cellular division, independent of p27-mediated inhibition of cyclin E/CDK2. *Cell Cycle* 5, 1348-1355.

Denko, N.C., Giaccia, A.J., Stringer, J.R., and Stambrook, P.J. (1994). The human Ha-ras oncogene induces genomic instability in murine fibroblasts within one cell cycle. *Proc Natl Acad Sci U S A* 91, 5124-5128.

Dickins, R.A., Hemann, M.T., Zilfou, J.T., Simpson, D.R., Ibarra, I., Hannon, G.J., and Lowe, S.W. (2005). Probing tumor phenotypes using stable and regulated synthetic microRNA precursors. *Nat Genet* 37, 1289-1295.

Dobles, M., Liberal, V., Scott, M.L., Benezra, R., and Sorger, P.K. (2000). Chromosome missegregation and apoptosis in mice lacking the mitotic checkpoint protein Mad2. *Cell* 101, 635-645.

Duensing, S., and Munger, K. (2002). The human papillomavirus type 16 E6 and E7 oncoproteins independently induce numerical and structural chromosome instability. *Cancer Res* 62, 7075-7082.

Eagle, L.R., Yin, X., Brothman, A.R., Williams, B.J., Atkin, N.B., and Prochownik, E.V. (1995). Mutation of the MXI1 gene in prostate cancer. *Nat Genet* 9, 249-255.

Egle, A., Harris, A.W., Bouillet, P., and Cory, S. (2004). Bim is a suppressor of Myc-induced mouse B cell leukemia. *Proc Natl Acad Sci U S A* 101, 6164-6169.

Eilers, M., Picard, D., Yamamoto, K.R., and Bishop, J.M. (1989). Chimaeras of myc oncoprotein and steroid receptors cause hormone-dependent transformation of cells. *Nature* 340, 66-68.

Eischen, C.M., Woo, D., Roussel, M.F., and Cleveland, J.L. (2001). Apoptosis triggered by Myc-induced suppression of Bcl-X(L) or Bcl-2 is bypassed during lymphomagenesis. *Mol Cell Biol* 21, 5063-5070.

Eisenman, R.N. (2001). Deconstructing myc. *Genes Dev* 15, 2023-2030.

Epanchintsev, A., Jung, P., Menssen, A., and Hermeking, H. (2006). Inducible microRNA expression by an all-in-one episomal vector system. *Nucleic Acids Res* 34, e119.

Falck, J., Mailand, N., Syljuasen, R.G., Bartek, J., and Lukas, J. (2001). The ATM-Chk2-Cdc25A checkpoint pathway guards against radioresistant DNA synthesis. *Nature* 410, 842-847.

Fang, Y., Liu, T., Wang, X., Yang, Y.M., Deng, H., Kunicki, J., Traganos, F., Darzynkiewicz, Z., Lu, L., and Dai, W. (2006). BubR1 is involved in regulation of DNA damage responses. *Oncogene* 25, 3598-3605.

Felsher, D.W., and Bishop, J.M. (1999). Transient excess of MYC activity can elicit genomic instability and tumorigenesis. *Proc Natl Acad Sci U S A* 96, 3940-3944.

- Felsher, D.W., Zetterberg, A., Zhu, J., Tlsty, T., and Bishop, J.M. (2000). Overexpression of MYC causes p53-dependent G2 arrest of normal fibroblasts. *Proc Natl Acad Sci U S A* *97*, 10544-10548.
- Fernandez, P.C., Frank, S.R., Wang, L., Schroeder, M., Liu, S., Greene, J., Cocito, A., and Amati, B. (2003). Genomic targets of the human c-Myc protein. *Genes Dev* *17*, 1115-1129.
- Fewell, G.D., and Schmitt, K. (2006). Vector-based RNAi approaches for stable, inducible and genome-wide screens. *Drug Discov Today* *11*, 975-982.
- Filipowicz, W., Jaskiewicz, L., Kolb, F.A., and Pillai, R.S. (2005). Post-transcriptional gene silencing by siRNAs and miRNAs. *Curr Opin Struct Biol* *15*, 331-341.
- Frank, S.R., Schroeder, M., Fernandez, P., Taubert, S., and Amati, B. (2001). Binding of c-Myc to chromatin mediates mitogen-induced acetylation of histone H4 and gene activation. *Genes Dev* *15*, 2069-2082.
- Frost, M., Newell, J., Lones, M.A., Tripp, S.R., Cairo, M.S., and Perkins, S.L. (2004). Comparative immunohistochemical analysis of pediatric Burkitt lymphoma and diffuse large B-cell lymphoma. *Am J Clin Pathol* *121*, 384-392.
- Fukasawa, K., and Vande Woude, G.F. (1997). Synergy between the Mos/mitogen-activated protein kinase pathway and loss of p53 function in transformation and chromosome instability. *Mol Cell Biol* *17*, 506-518.
- Galaktionov, K., Chen, X., and Beach, D. (1996). Cdc25 cell-cycle phosphatase as a target of c-myc. *Nature* *382*, 511-517.
- Gamberi, G., Benassi, M.S., Bohling, T., Ragazzini, P., Molendini, L., Sollazzo, M.R., Pompetti, F., Merli, M., Magagnoli, G., Balladelli, A., *et al.* (1998). C-myc and c-fos in human osteosarcoma: prognostic value of mRNA and protein expression. *Oncology* *55*, 556-563.
- Gasser, S., and Raulet, D. (2006). The DNA damage response, immunity and cancer. *Semin Cancer Biol* *16*, 344-347.
- Gomez-Roman, N., Grandori, C., Eisenman, R.N., and White, R.J. (2003). Direct activation of RNA polymerase III transcription by c-Myc. *Nature* *421*, 290-294.
- Grandori, C., Wu, K.J., Fernandez, P., Ngouenet, C., Grim, J., Clurman, B.E., Moser, M.J., Oshima, J., Russell, D.W., Swisshelm, K., *et al.* (2003). Werner syndrome protein limits MYC-induced cellular senescence. *Genes Dev* *17*, 1569-1574.
- Gugger, M., Burckhardt, E., Kappeler, A., Hirsiger, H., Laissue, J.A., and Mazzucchelli, L. (2002). Quantitative expansion of structural genomic alterations in the spectrum of neuroendocrine lung carcinomas. *J Pathol* *196*, 408-415.
- Guo, J., Peters, K.L., and Sen, G.C. (2000). Induction of the human protein P56 by interferon, double-stranded RNA, or virus infection. *Virology* *267*, 209-219.

Haggerty, T.J., Zeller, K.I., Osthus, R.C., Wonsey, D.R., and Dang, C.V. (2003). A strategy for identifying transcription factor binding sites reveals two classes of genomic c-Myc target sites. *Proc Natl Acad Sci U S A* 100, 5313-5318.

Hahn, W.C., Counter, C.M., Lundberg, A.S., Beijersbergen, R.L., Brooks, M.W., and Weinberg, R.A. (1999). Creation of human tumour cells with defined genetic elements. *Nature* 400, 464-468.

Hanks, S., Coleman, K., Reid, S., Plaja, A., Firth, H., Fitzpatrick, D., Kidd, A., Mehes, K., Nash, R., Robin, N., *et al.* (2004). Constitutional aneuploidy and cancer predisposition caused by biallelic mutations in BUB1B. *Nat Genet* 36, 1159-1161.

Hannon, G.J. (2002). RNA interference. *Nature* 418, 244-251.

Hanseemann, v. (1890). Ueber asymmetrische Zellteilung in Epithelkrebsen und deren biologische Bedeutung. *Virchows Arch Patholog Anat* 119, 299-326.

Harrison, C.J. (2000). The genetics of childhood acute lymphoblastic leukaemia. *Baillieres Best Pract Res Clin Haematol* 13, 427-439.

He, T.C., Sparks, A.B., Rago, C., Hermeking, H., Zawel, L., da Costa, L.T., Morin, P.J., Vogelstein, B., and Kinzler, K.W. (1998). Identification of c-MYC as a target of the APC pathway. *Science* 281, 1509-1512.

Hermeking, H., and Eick, D. (1994). Mediation of c-Myc-induced apoptosis by p53. *Science* 265, 2091-2093.

Hermeking, H., Rago, C., Schuhmacher, M., Li, Q., Barrett, J.F., Obaya, A.J., O'Connell, B.C., Mateyak, M.K., Tam, W., Kohlhuber, F., *et al.* (2000). Identification of CDK4 as a target of c-MYC. *Proc Natl Acad Sci U S A* 97, 2229-2234.

Hernando, E., Nahle, Z., Juan, G., Diaz-Rodriguez, E., Alaminos, M., Hemann, M., Michel, L., Mittal, V., Gerald, W., Benezra, R., *et al.* (2004). Rb inactivation promotes genomic instability by uncoupling cell cycle progression from mitotic control. *Nature* 430, 797-802.

Hernando, E., Orlow, I., Liberal, V., Nohales, G., Benezra, R., and Cordon-Cardo, C. (2001). Molecular analyses of the mitotic checkpoint components hsMAD2, hBUB1 and hBUB3 in human cancer. *Int J Cancer* 95, 223-227.

Herold, S., Wanzel, M., Beuger, V., Frohme, C., Beul, D., Hillukkala, T., Syvaioja, J., Saluz, H.P., Haenel, F., and Eilers, M. (2002). Negative regulation of the mammalian UV response by Myc through association with Miz-1. *Mol Cell* 10, 509-521.

Hoang, A.T., Lutterbach, B., Lewis, B.C., Yano, T., Chou, T.Y., Barrett, J.F., Raffeld, M., Hann, S.R., and Dang, C.V. (1995). A link between increased transforming activity of lymphoma-derived MYC mutant alleles, their defective regulation by p107, and altered phosphorylation of the c-Myc transactivation domain. *Mol Cell Biol* 15, 4031-4042.

- Hua, X.H., Yan, H., and Newport, J. (1997). A role for Cdk2 kinase in negatively regulating DNA replication during S phase of the cell cycle. *J Cell Biol* 137, 183-192.
- louk, T., Kerscher, O., Scott, R.J., Basrai, M.A., and Wozniak, R.W. (2002). The yeast nuclear pore complex functionally interacts with components of the spindle assembly checkpoint. *J Cell Biol* 159, 807-819.
- Iritani, B.M., and Eisenman, R.N. (1999). c-Myc enhances protein synthesis and cell size during B lymphocyte development. *Proc Natl Acad Sci U S A* 96, 13180-13185.
- Iwanaga, Y., Chi, Y.H., Miyazato, A., Sheleg, S., Haller, K., Peloponese, J.M., Jr., Li, Y., Ward, J.M., Benezra, R., and Jeang, K.T. (2007). Heterozygous deletion of mitotic arrest-deficient protein 1 (MAD1) increases the incidence of tumors in mice. *Cancer Res* 67, 160-166.
- Johnston, L.A., Prober, D.A., Edgar, B.A., Eisenman, R.N., and Gallant, P. (1999). *Drosophila* myc regulates cellular growth during development. *Cell* 98, 779-790.
- Kalitsis, P., Fowler, K.J., Griffiths, B., Earle, E., Chow, C.W., Jamsen, K., and Choo, K.H. (2005). Increased chromosome instability but not cancer predisposition in haploinsufficient Bub3 mice. *Genes Chromosomes Cancer* 44, 29-36.
- Karlsson, A., Deb-Basu, D., Cherry, A., Turner, S., Ford, J., and Felsher, D.W. (2003). Defective double-strand DNA break repair and chromosomal translocations by MYC overexpression. *Proc Natl Acad Sci U S A* 100, 9974-9979.
- Karn, J., Watson, J.V., Lowe, A.D., Green, S.M., and Vedeckis, W. (1989). Regulation of cell cycle duration by c-myc levels. *Oncogene* 4, 773-787.
- Kastan, M.B., and Bartek, J. (2004). Cell-cycle checkpoints and cancer. *Nature* 432, 316-323.
- Khan, S.H., and Wahl, G.M. (1998). p53 and pRb prevent rereplication in response to microtubule inhibitors by mediating a reversible G1 arrest. *Cancer Res* 58, 396-401.
- Kienitz, A., Vogel, C., Morales, I., Muller, R., and Bastians, H. (2005). Partial downregulation of MAD1 causes spindle checkpoint inactivation and aneuploidy, but does not confer resistance towards taxol. *Oncogene* 24, 4301-4310.
- Kim, D.H., and Rossi, J.J. (2007). Strategies for silencing human disease using RNA interference. *Nat Rev Genet* 8, 173-184.
- Kim, M., Murphy, K., Liu, F., Parker, S.E., Dowling, M.L., Baff, W., and Kao, G.D. (2005). Caspase-mediated specific cleavage of BubR1 is a determinant of mitotic progression. *Mol Cell Biol* 25, 9232-9248.
- Kim, R., Trubetskoy, A., Suzuki, T., Jenkins, N.A., Copeland, N.G., and Lenz, J. (2003). Genome-based identification of cancer genes by proviral tagging in mouse retrovirus-induced T-cell lymphomas. *J Virol* 77, 2056-2062.

- Koch, H.B., Zhang, R., Verdoodt, B., Bailey, A., Zhang, C.D., Yates, J.R., 3rd, Menssen, A., and Hermeking, H. (2007). Large-scale identification of c-MYC-associated proteins using a combined TAP/MudPIT approach. *Cell Cycle* 6, 205-217.
- Kops, G.J., Foltz, D.R., and Cleveland, D.W. (2004). Lethality to human cancer cells through massive chromosome loss by inhibition of the mitotic checkpoint. *Proc Natl Acad Sci U S A* 101, 8699-8704.
- Kops, G.J., Weaver, B.A., and Cleveland, D.W. (2005). On the road to cancer: aneuploidy and the mitotic checkpoint. *Nat Rev Cancer* 5, 773-785.
- Kung, A.L., Sherwood, S.W., and Schimke, R.T. (1990). Cell line-specific differences in the control of cell cycle progression in the absence of mitosis. *Proc Natl Acad Sci U S A* 87, 9553-9557.
- Kusari, J., and Sen, G.C. (1986). Regulation of synthesis and turnover of an interferon-inducible mRNA. *Mol Cell Biol* 6, 2062-2067.
- Kuschak, T.I., Taylor, C., McMillan-Ward, E., Israels, S., Henderson, D.W., Mushinski, J.F., Wright, J.A., and Mai, S. (1999). The ribonucleotide reductase R2 gene is a non-transcribed target of c-Myc-induced genomic instability. *Gene* 238, 351-365.
- Labib, K., and Diffley, J.F. (2001). Is the MCM2-7 complex the eukaryotic DNA replication fork helicase? *Curr Opin Genet Dev* 11, 64-70.
- Lambert, P.F., Kashanchi, F., Radonovich, M.F., Shiekhhattar, R., and Brady, J.N. (1998). Phosphorylation of p53 serine 15 increases interaction with CBP. *J Biol Chem* 273, 33048-33053.
- Lanni, J.S., and Jacks, T. (1998). Characterization of the p53-dependent postmitotic checkpoint following spindle disruption. *Mol Cell Biol* 18, 1055-1064.
- Lasorella, A., Nosedà, M., Beyna, M., Yokota, Y., and Iavarone, A. (2000). Id2 is a retinoblastoma protein target and mediates signalling by Myc oncoproteins. *Nature* 407, 592-598.
- Lengauer, C. (2005). Aneuploidy and genetic instability in cancer. *Semin Cancer Biol* 15, 1.
- Lengauer, C., Kinzler, K.W., and Vogelstein, B. (1997). Genetic instability in colorectal cancers. *Nature* 386, 623-627.
- Lengronne, A., and Schwob, E. (2002). The yeast CDK inhibitor Sic1 prevents genomic instability by promoting replication origin licensing in late G(1). *Mol Cell* 9, 1067-1078.
- Leone, G., DeGregori, J., Sears, R., Jakoi, L., and Nevins, J.R. (1997). Myc and Ras collaborate in inducing accumulation of active cyclin E/Cdk2 and E2F. *Nature* 387, 422-426.

- Li, C.X., Parker, A., Menocal, E., Xiang, S., Borodyansky, L., and Fruehauf, J.H. (2006). Delivery of RNA interference. *Cell Cycle* 5, 2103-2109.
- Li, M.Z., and Elledge, S.J. (2005). MAGIC, an in vivo genetic method for the rapid construction of recombinant DNA molecules. *Nat Genet* 37, 311-319.
- Li, Q., and Dang, C.V. (1999). c-Myc overexpression uncouples DNA replication from mitosis. *Mol Cell Biol* 19, 5339-5351.
- Li, W., Lan, Z., Wu, H., Wu, S., Meadows, J., Chen, J., Zhu, V., and Dai, W. (1999). BUBR1 phosphorylation is regulated during mitotic checkpoint activation. *Cell Growth Differ* 10, 769-775.
- Loeb, L.A. (2001). A mutator phenotype in cancer. *Cancer Res* 61, 3230-3239.
- Louis, S.F., Vermolen, B.J., Garini, Y., Young, I.T., Guffei, A., Lichtensztein, Z., Kuttler, F., Chuang, T.C., Moshir, S., Mougey, V., *et al.* (2005). c-Myc induces chromosomal rearrangements through telomere and chromosome remodeling in the interphase nucleus. *Proc Natl Acad Sci U S A* 102, 9613-9618.
- Lui, W.O., Tanenbaum, D.M., and Larsson, C. (2001). High level amplification of 1p32-33 and 2p22-24 in small cell lung carcinomas. *Int J Oncol* 19, 451-457.
- Lutz, W., Leon, J., and Eilers, M. (2002). Contributions of Myc to tumorigenesis. *Biochim Biophys Acta* 1602, 61-71.
- Mai, S. (1994). Overexpression of c-myc precedes amplification of the gene encoding dihydrofolate reductase. *Gene* 148, 253-260.
- Mai, S., Fluri, M., Siwarski, D., and Huppi, K. (1996a). Genomic instability in MycER-activated Rat1A-MycER cells. *Chromosome Res* 4, 365-371.
- Mai, S., and Garini, Y. (2005). Oncogenic remodeling of the three-dimensional organization of the interphase nucleus: c-Myc induces telomeric aggregates whose formation precedes chromosomal rearrangements. *Cell Cycle* 4, 1327-1331.
- Mai, S., Hanley-Hyde, J., and Fluri, M. (1996b). c-Myc overexpression associated DHFR gene amplification in hamster, rat, mouse and human cell lines. *Oncogene* 12, 277-288.
- Mai, S., and Mushinski, J.F. (2003). c-Myc-induced genomic instability. *J Environ Pathol Toxicol Oncol* 22, 179-199.
- Mailand, N., Falck, J., Lukas, C., Syljuasen, R.G., Welcker, M., Bartek, J., and Lukas, J. (2000). Rapid destruction of human Cdc25A in response to DNA damage. *Science* 288, 1425-1429.
- Martin, S.E., and Caplen, N.J. (2007). Applications of RNA Interference in Mammalian Systems. *Annu Rev Genomics Hum Genet*.

- Marx, J. (2002). Debate surges over the origins of genomic defects in cancer. *Science* 297, 544-546.
- Mateyak, M.K., Obaya, A.J., Adachi, S., and Sedivy, J.M. (1997). Phenotypes of c-Myc-deficient rat fibroblasts isolated by targeted homologous recombination. *Cell Growth Differ* 8, 1039-1048.
- Matsumura, I., Tanaka, H., and Kanakura, Y. (2003). E2F1 and c-Myc in cell growth and death. *Cell Cycle* 2, 333-338.
- Matsuura, S., Matsumoto, Y., Morishima, K., Izumi, H., Matsumoto, H., Ito, E., Tsutsui, K., Kobayashi, J., Tauchi, H., Kajiwara, Y., *et al.* (2006). Monoallelic BUB1B mutations and defective mitotic-spindle checkpoint in seven families with premature chromatid separation (PCS) syndrome. *Am J Med Genet A* 140, 358-367.
- Meister, G., and Tuschl, T. (2004). Mechanisms of gene silencing by double-stranded RNA. *Nature* 431, 343-349.
- Menssen, A., and Hermeking, H. (2002). Characterization of the c-MYC-regulated transcriptome by SAGE: identification and analysis of c-MYC target genes. *Proc Natl Acad Sci U S A* 99, 6274-6279.
- Meyer, N., Kim, S.S., and Penn, L.Z. (2006). The Oscar-worthy role of Myc in apoptosis. *Semin Cancer Biol* 16, 275-287.
- Michel, L., Diaz-Rodriguez, E., Narayan, G., Hernando, E., Murty, V.V., and Benezra, R. (2004). Complete loss of the tumor suppressor MAD2 causes premature cyclin B degradation and mitotic failure in human somatic cells. *Proc Natl Acad Sci U S A* 101, 4459-4464.
- Michel, L.S., Liberal, V., Chatterjee, A., Kirchwegger, R., Pasche, B., Gerald, W., Dobles, M., Sorger, P.K., Murty, V.V., and Benezra, R. (2001). MAD2 haplo-insufficiency causes premature anaphase and chromosome instability in mammalian cells. *Nature* 409, 355-359.
- Mikhailov, A., Cole, R.W., and Rieder, C.L. (2002). DNA damage during mitosis in human cells delays the metaphase/anaphase transition via the spindle-assembly checkpoint. *Curr Biol* 12, 1797-1806.
- Miranda Peralta, E.I., Valles Ayoub, Y., Hernandez Mendoza, L., Rangel Ramirez, L.M., Castrejon Rojas, A., Collazo-Jaloma, J., Gutierrez Romero, M., Gonzalez Constance, R., and Gariglio Vidal, P. (1991). [MYC protein and proteins antigenically related with MYC in acute lymphoblastic leukemia]. *Rev Invest Clin* 43, 139-145.
- Mitchell, K.O., Ricci, M.S., Miyashita, T., Dicker, D.T., Jin, Z., Reed, J.C., and El-Deiry, W.S. (2000). Bax is a transcriptional target and mediator of c-myc-induced apoptosis. *Cancer Res* 60, 6318-6325.
- Muller, D., Bouchard, C., Rudolph, B., Steiner, P., Stuckmann, I., Saffrich, R., Ansorge, W., Huttner, W., and Eilers, M. (1997). Cdk2-dependent phosphorylation of

- p27 facilitates its Myc-induced release from cyclin E/cdk2 complexes. *Oncogene* 15, 2561-2576.
- Munger, K., and Howley, P.M. (2002). Human papillomavirus immortalization and transformation functions. *Virus Res* 89, 213-228.
- Musacchio, A., and Hardwick, K.G. (2002). The spindle checkpoint: structural insights into dynamic signalling. *Nat Rev Mol Cell Biol* 3, 731-741.
- Myung, K., Smith, S., and Kolodner, R.D. (2004). Mitotic checkpoint function in the formation of gross chromosomal rearrangements in *Saccharomyces cerevisiae*. *Proc Natl Acad Sci U S A* 101, 15980-15985.
- Nanus, D.M., Lynch, S.A., Rao, P.H., Anderson, S.M., Jhanwar, S.C., and Albino, A.P. (1991). Transformation of human kidney proximal tubule cells by a src-containing retrovirus. *Oncogene* 6, 2105-2111.
- Nesbit, C.E., Tersak, J.M., and Prochownik, E.V. (1999). MYC oncogenes and human neoplastic disease. *Oncogene* 18, 3004-3016.
- Nichols, W.W., Levan, A., Heneen, W.K., and Peluse, M. (1965). Synergism of the Schmidt-Ruppin strain of the Rous sarcoma virus and cytidine triphosphate in the induction of chromosome breaks in human cultured leukocytes. *Hereditas* 54, 213-236.
- Niculescu, A.B., 3rd, Chen, X., Smeets, M., Hengst, L., Prives, C., and Reed, S.I. (1998). Effects of p21(Cip1/Waf1) at both the G1/S and the G2/M cell cycle transitions: pRb is a critical determinant in blocking DNA replication and in preventing endoreduplication. *Mol Cell Biol* 18, 629-643.
- Nilsson, J.A., and Cleveland, J.L. (2003). Myc pathways provoking cell suicide and cancer. *Oncogene* 22, 9007-9021.
- Nupponen, N.N., Kakkola, L., Koivisto, P., and Visakorpi, T. (1998). Genetic alterations in hormone-refractory recurrent prostate carcinomas. *Am J Pathol* 153, 141-148.
- O'Connell, B.C., Cheung, A.F., Simkevich, C.P., Tam, W., Ren, X., Mateyak, M.K., and Sedivy, J.M. (2003). A large scale genetic analysis of c-Myc-regulated gene expression patterns. *J Biol Chem* 278, 12563-12573.
- O'Hagan, R.C., Ohh, M., David, G., de Alboran, I.M., Alt, F.W., Kaelin, W.G., Jr., and DePinho, R.A. (2000). Myc-enhanced expression of Cul1 promotes ubiquitin-dependent proteolysis and cell cycle progression. *Genes Dev* 14, 2185-2191.
- Oster, S.K., Ho, C.S., Soucie, E.L., and Penn, L.Z. (2002). The myc oncogene: Marvelously Complex. *Adv Cancer Res* 84, 81-154.
- Paddison, P.J., and Hannon, G.J. (2002). RNA interference: the new somatic cell genetics? *Cancer Cell* 2, 17-23.

- Paddison, P.J., Silva, J.M., Conklin, D.S., Schlabach, M., Li, M., Aruleba, S., Balija, V., O'Shaughnessy, A., Gnoj, L., Scobie, K., *et al.* (2004). A resource for large-scale RNA-interference-based screens in mammals. *Nature* 428, 427-431.
- Patel, J.H., Loboda, A.P., Showe, M.K., Showe, L.C., and McMahon, S.B. (2004). Analysis of genomic targets reveals complex functions of MYC. *Nat Rev Cancer* 4, 562-568.
- Pelengaris, S., Khan, M., and Evan, G. (2002a). c-MYC: more than just a matter of life and death. *Nat Rev Cancer* 2, 764-776.
- Pelengaris, S., Khan, M., and Evan, G.I. (2002b). Suppression of Myc-induced apoptosis in beta cells exposes multiple oncogenic properties of Myc and triggers carcinogenic progression. *Cell* 109, 321-334.
- Percy, M.J., Myrie, K.A., Neeley, C.K., Azim, J.N., Ethier, S.P., and Petty, E.M. (2000). Expression and mutational analyses of the human MAD2L1 gene in breast cancer cells. *Genes Chromosomes Cancer* 29, 356-362.
- Pompetti, F., Rizzo, P., Simon, R.M., Freidlin, B., Mew, D.J., Pass, H.I., Picci, P., Levine, A.S., and Carbone, M. (1996). Oncogene alterations in primary, recurrent, and metastatic human bone tumors. *J Cell Biochem* 63, 37-50.
- Popescu, N.C., and Zimonjic, D.B. (2002). Chromosome-mediated alterations of the MYC gene in human cancer. *J Cell Mol Med* 6, 151-159.
- Pourquier, P., and Pommier, Y. (2001). Topoisomerase I-mediated DNA damage. *Adv Cancer Res* 80, 189-216.
- Prendergast, G.C. (1999). Mechanisms of apoptosis by c-Myc. *Oncogene* 18, 2967-2987.
- Prochownik, E.V., Eagle Grove, L., Deubler, D., Zhu, X.L., Stephenson, R.A., Rohr, L.R., Yin, X., and Brothman, A.R. (1998). Commonly occurring loss and mutation of the MXI1 gene in prostate cancer. *Genes Chromosomes Cancer* 22, 295-304.
- Rajagopalan, H., and Lengauer, C. (2004). Aneuploidy and cancer. *Nature* 432, 338-341.
- Rajagopalan, H., Nowak, M.A., Vogelstein, B., and Lengauer, C. (2003). The significance of unstable chromosomes in colorectal cancer. *Nat Rev Cancer* 3, 695-701.
- Rao, C.V., Yang, Y.M., Swamy, M.V., Liu, T., Fang, Y., Mahmood, R., Jhanwar-Uniyal, M., and Dai, W. (2005). Colonic tumorigenesis in BubR1^{+/+}-ApcMin^{+/+} compound mutant mice is linked to premature separation of sister chromatids and enhanced genomic instability. *Proc Natl Acad Sci U S A* 102, 4365-4370.
- Ray, S., Atkuri, K.R., Deb-Basu, D., Adler, A.S., Chang, H.Y., Herzenberg, L.A., and Felsher, D.W. (2006). MYC can induce DNA breaks in vivo and in vitro independent of reactive oxygen species. *Cancer Res* 66, 6598-6605.

- Root, D.E., Hacohen, N., Hahn, W.C., Lander, E.S., and Sabatini, D.M. (2006). Genome-scale loss-of-function screening with a lentiviral RNAi library. *Nat Methods* 3, 715-719.
- Rotman, G., and Shiloh, Y. (1999). ATM: a mediator of multiple responses to genotoxic stress. *Oncogene* 18, 6135-6144.
- Rubinfeld, B., Robbins, P., El-Gamil, M., Albert, I., Porfiri, E., and Polakis, P. (1997). Stabilization of beta-catenin by genetic defects in melanoma cell lines. *Science* 275, 1790-1792.
- Santoni-Rugiu, E., Falck, J., Mailand, N., Bartek, J., and Lukas, J. (2000). Involvement of Myc activity in a G(1)/S-promoting mechanism parallel to the pRb/E2F pathway. *Mol Cell Biol* 20, 3497-3509.
- Schar, P. (2001). Spontaneous DNA damage, genome instability, and cancer--when DNA replication escapes control. *Cell* 104, 329-332.
- Schuhmacher, M., Staeger, M.S., Pajic, A., Polack, A., Weidle, U.H., Bornkamm, G.W., Eick, D., and Kohlhuber, F. (1999). Control of cell growth by c-Myc in the absence of cell division. *Curr Biol* 9, 1255-1258.
- Sears, R., Ohtani, K., and Nevins, J.R. (1997). Identification of positively and negatively acting elements regulating expression of the E2F2 gene in response to cell growth signals. *Mol Cell Biol* 17, 5227-5235.
- Seoane, J., Le, H.V., and Massague, J. (2002). Myc suppression of the p21(Cip1) Cdk inhibitor influences the outcome of the p53 response to DNA damage. *Nature* 419, 729-734.
- Sheen, J.H., and Dickson, R.B. (2002). Overexpression of c-Myc alters G(1)/S arrest following ionizing radiation. *Mol Cell Biol* 22, 1819-1833.
- Sheen, J.H., Woo, J.K., and Dickson, R.B. (2003). c-Myc alters the DNA damage-induced G2/M arrest in human mammary epithelial cells. *Br J Cancer* 89, 1479-1485.
- Sherr, C.J., and Roberts, J.M. (1999). CDK inhibitors: positive and negative regulators of G1-phase progression. *Genes Dev* 13, 1501-1512.
- Shim, H., Dolde, C., Lewis, B.C., Wu, C.S., Dang, G., Jungmann, R.A., Dalla-Favera, R., and Dang, C.V. (1997). c-Myc transactivation of LDH-A: implications for tumor metabolism and growth. *Proc Natl Acad Sci U S A* 94, 6658-6663.
- Shin, H.J., Baek, K.H., Jeon, A.H., Park, M.T., Lee, S.J., Kang, C.M., Lee, H.S., Yoo, S.H., Chung, D.H., Sung, Y.C., *et al.* (2003). Dual roles of human BubR1, a mitotic checkpoint kinase, in the monitoring of chromosomal instability. *Cancer Cell* 4, 483-497.

- Sibon, O.C., Kelkar, A., Lemstra, W., and Theurkauf, W.E. (2000). DNA-replication/DNA-damage-dependent centrosome inactivation in *Drosophila* embryos. *Nat Cell Biol* 2, 90-95.
- Silva, J., Chang, K., Hannon, G.J., and Rivas, F.V. (2004). RNA-interference-based functional genomics in mammalian cells: reverse genetics coming of age. *Oncogene* 23, 8401-8409.
- Silva, J.M., Li, M.Z., Chang, K., Ge, W., Golding, M.C., Rickles, R.J., Siolas, D., Hu, G., Paddison, P.J., Schlabach, M.R., *et al.* (2005). Second-generation shRNA libraries covering the mouse and human genomes. *Nat Genet* 37, 1281-1288.
- Smits, V.A., Klompaker, R., Arnaud, L., Rijksen, G., Nigg, E.A., and Medema, R.H. (2000). Polo-like kinase-1 is a target of the DNA damage checkpoint. *Nat Cell Biol* 2, 672-676.
- Sotillo, R., Hernando, E., Diaz-Rodriguez, E., Teruya-Feldstein, J., Cordon-Cardo, C., Lowe, S.W., and Benezra, R. (2007). Mad2 overexpression promotes aneuploidy and tumorigenesis in mice. *Cancer Cell* 11, 9-23.
- Soucie, E.L., Annis, M.G., Sedivy, J., Filmus, J., Leber, B., Andrews, D.W., and Penn, L.Z. (2001). Myc potentiates apoptosis by stimulating Bax activity at the mitochondria. *Mol Cell Biol* 21, 4725-4736.
- Spruck, C.H., Won, K.A., and Reed, S.I. (1999). Deregulated cyclin E induces chromosome instability. *Nature* 401, 297-300.
- Stewart, Z.A., Leach, S.D., and Pietsenpol, J.A. (1999). p21(Waf1/Cip1) inhibition of cyclin E/Cdk2 activity prevents endoreduplication after mitotic spindle disruption. *Mol Cell Biol* 19, 205-215.
- Su, T.T., and Jaklevic, B. (2001). DNA damage leads to a Cyclin A-dependent delay in metaphase-anaphase transition in the *Drosophila* gastrula. *Curr Biol* 11, 8-17.
- Sugimoto, I., Murakami, H., Tonami, Y., Moriyama, A., and Nakanishi, M. (2004). DNA replication checkpoint control mediated by the spindle checkpoint protein Mad2p in fission yeast. *J Biol Chem* 279, 47372-47378.
- Syljuasen, R.G., Jensen, S., Bartek, J., and Lukas, J. (2006). Adaptation to the ionizing radiation-induced G2 checkpoint occurs in human cells and depends on checkpoint kinase 1 and Polo-like kinase 1 kinases. *Cancer Res* 66, 10253-10257.
- Tanaka, H., Matsumura, I., Ezoe, S., Satoh, Y., Sakamaki, T., Albanese, C., Machii, T., Pestell, R.G., and Kanakura, Y. (2002). E2F1 and c-Myc potentiate apoptosis through inhibition of NF-kappaB activity that facilitates MnSOD-mediated ROS elimination. *Mol Cell* 9, 1017-1029.
- Treszl, A., Adany, R., Rakosy, Z., Kardos, L., Begany, A., Gilde, K., and Balazs, M. (2004). Extra copies of c-myc are more pronounced in nodular melanomas than in superficial spreading melanomas as revealed by fluorescence in situ hybridisation. *Cytometry B Clin Cytom* 60, 37-46.

Trumpp, A., Refaeli, Y., Oskarsson, T., Gasser, S., Murphy, M., Martin, G.R., and Bishop, J.M. (2001). c-Myc regulates mammalian body size by controlling cell number but not cell size. *Nature* 414, 768-773.

Tsichlis, P.N. (1987). Oncogenesis by Moloney murine leukemia virus. *Anticancer Res* 7, 171-180.

Unger, T., Juven-Gershon, T., Moallem, E., Berger, M., Vogt Sionov, R., Lozano, G., Oren, M., and Haupt, Y. (1999). Critical role for Ser20 of human p53 in the negative regulation of p53 by Mdm2. *Embo J* 18, 1805-1814.

Vafa, O., Wade, M., Kern, S., Beeche, M., Pandita, T.K., Hampton, G.M., and Wahl, G.M. (2002). c-Myc can induce DNA damage, increase reactive oxygen species, and mitigate p53 function: a mechanism for oncogene-induced genetic instability. *Mol Cell* 9, 1031-1044.

van Deursen, J.M. (2007). Rb loss causes cancer by driving mitosis mad. *Cancer Cell* 11, 1-3.

Vennstrom, B., Sheiness, D., Zabielski, J., and Bishop, J.M. (1982). Isolation and characterization of c-myc, a cellular homolog of the oncogene (v-myc) of avian myelocytomatosis virus strain 29. *J Virol* 42, 773-779.

Vita, M., and Henriksson, M. (2006). The Myc oncoprotein as a therapeutic target for human cancer. *Semin Cancer Biol* 16, 318-330.

Vogelstein, B., Lane, D., and Levine, A.J. (2000). Surfing the p53 network. *Nature* 408, 307-310.

Wade, M., and Wahl, G.M. (2006). c-Myc, genome instability, and tumorigenesis: the devil is in the details. *Curr Top Microbiol Immunol* 302, 169-203.

Wadhwa, R., Kaul, S.C., Miyagishi, M., and Taira, K. (2004). Vectors for RNA interference. *Curr Opin Mol Ther* 6, 367-372.

Wagner, A.J., Meyers, C., Laimins, L.A., and Hay, N. (1993). c-Myc induces the expression and activity of ornithine decarboxylase. *Cell Growth Differ* 4, 879-883.

Wahl, G.M., and Carr, A.M. (2001). The evolution of diverse biological responses to DNA damage: insights from yeast and p53. *Nat Cell Biol* 3, E277-286.

Walter, J., Sun, L., and Newport, J. (1998). Regulated chromosomal DNA replication in the absence of a nucleus. *Mol Cell* 1, 519-529.

Wang, Q., Liu, T., Fang, Y., Xie, S., Huang, X., Mahmood, R., Ramaswamy, G., Sakamoto, K.M., Darzynkiewicz, Z., Xu, M., *et al.* (2004a). BUBR1 deficiency results in abnormal megakaryopoiesis. *Blood* 103, 1278-1285.

Wang, Z., Cummins, J.M., Shen, D., Cahill, D.P., Jallepalli, P.V., Wang, T.L., Parsons, D.W., Traverso, G., Awad, M., Silliman, N., *et al.* (2004b). Three classes of genes

- mutated in colorectal cancers with chromosomal instability. *Cancer Res* 64, 2998-3001.
- Watson, J.D., Oster, S.K., Shago, M., Khosravi, F., and Penn, L.Z. (2002). Identifying genes regulated in a Myc-dependent manner. *J Biol Chem* 277, 36921-36930.
- Weaver, B.A., Silk, A.D., Montagna, C., Verdier-Pinard, P., and Cleveland, D.W. (2007). Aneuploidy acts both oncogenically and as a tumor suppressor. *Cancer Cell* 11, 25-36.
- Wei, K., Kucherlapati, R., and Edelman, W. (2002). Mouse models for human DNA mismatch-repair gene defects. *Trends Mol Med* 8, 346-353.
- White, A.E., Livanos, E.M., and Tlsty, T.D. (1994). Differential disruption of genomic integrity and cell cycle regulation in normal human fibroblasts by the HPV oncoproteins. *Genes Dev* 8, 666-677.
- Wiznerowicz, M., Szulc, J., and Trono, D. (2006). Tuning silence: conditional systems for RNA interference. *Nat Methods* 3, 682-688.
- Yang, W., Shen, J., Wu, M., Arsur, M., FitzGerald, M., Suldan, Z., Kim, D.W., Hofmann, C.S., Pianetti, S., Romieu-Mourez, R., *et al.* (2001). Repression of transcription of the p27(Kip1) cyclin-dependent kinase inhibitor gene by c-Myc. *Oncogene* 20, 1688-1702.
- Yin, X.Y., Grove, L., Datta, N.S., Katula, K., Long, M.W., and Prochownik, E.V. (2001). Inverse regulation of cyclin B1 by c-Myc and p53 and induction of tetraploidy by cyclin B1 overexpression. *Cancer Res* 61, 6487-6493.
- Yin, X.Y., Grove, L., Datta, N.S., Long, M.W., and Prochownik, E.V. (1999). C-myc overexpression and p53 loss cooperate to promote genomic instability. *Oncogene* 18, 1177-1184.
- Yoon, Y.M., Baek, K.H., Jeong, S.J., Shin, H.J., Ha, G.H., Jeon, A.H., Hwang, S.G., Chun, J.S., and Lee, C.W. (2004). WD repeat-containing mitotic checkpoint proteins act as transcriptional repressors during interphase. *FEBS Lett* 575, 23-29.
- Yu, J., Zhang, L., Hwang, P.M., Rago, C., Kinzler, K.W., and Vogelstein, B. (1999). Identification and classification of p53-regulated genes. *Proc Natl Acad Sci U S A* 96, 14517-14522.
- Zimonjic, D., Brooks, M.W., Popescu, N., Weinberg, R.A., and Hahn, W.C. (2001). Derivation of human tumor cells in vitro without widespread genomic instability. *Cancer Res* 61, 8838-8844.
- Zindy, F., Eischen, C.M., Randle, D.H., Kamijo, T., Cleveland, J.L., Sherr, C.J., and Roussel, M.F. (1998). Myc signaling via the ARF tumor suppressor regulates p53-dependent apoptosis and immortalization. *Genes Dev* 12, 2424-2433.
- zur Hausen, H. (1991). Human papillomaviruses in the pathogenesis of anogenital cancer. *Virology* 184, 9-13.

10. Acknowledgements

I am sincerely grateful to my supervisor PD Dr. Heiko Hermeking for the opportunity to do my PhD thesis in his laboratory, for the possibility to work on interesting projects, for accompanying them with his scientific interest and support, and for helpful discussions.

I would like to thank Dr. Dimitri Lodygin for the excellent scientific help and support, constructive and interesting discussions, and being a real guide in all scientific directions.

I want to thank Peter Jung for his constant optimism, exciting competition and help.

I would like to thank Henrike Körner for the different scientific point of view and constructive work together, ended up with “DMD” paper.

I would like to thank Dr. Pjeter Knyazev and Tatyana Knyazeva for constant scientific and life support.

I want to thank Dr. Peter Palm for the nice collaboration on sequencing of DMD gene and good sequencing advices. Also thank Dr. Wolfgang Klinkert for assistance with flow cytometry.

I am grateful to all my colleges for their daily help and communication with regard to research and beyond, especially to following people: once again, to Dima Lodygin, from the first days in Munich, through the Alps and until the last beergarten; to Anne Benzinger, Robin Steigerwald, Heike Koch, Henrike Körner, Ru Zhang, Peter Jung and James Scrivens, for the nice time spent together; to Mikhail Nosov, Valery Tarasov and Alexandr Konovalov, to be my “another” life in and around Munich.

11. CURRICULUM VITAE

Epanchintsev Alexey Yurevich

Date of birth | December 13, 1978
Nationality | Russian
Place of birth | Bratsk, Russia

EDUCATION & QUALIFICATIONS

1996 - 2001 | **Novosibirsk State University, Faculty of Natural Sciences, Department of Molecular Biology**
Graduate studies in Applied & Theoretical Biology

1995-1996 | **Specialized Educational Scientific Center of Novosibirsk State University**
Specialization in Biology and Chemistry

WORK EXPERIENCE

2002 - 2007 | **Max- Planck Institute of Biochemistry, Department of Molecular Oncology**
Graduate research training
PD Dr. Heiko Hermeking
82152, Martinsried 18a, Munich, Germany

1998 - 2001 | **Institute of Chemical Biology and Fundamental Medicine, Department of Nucleic Acids Biochemistry**
Undergraduate research training
Prof. Dr. Vladimir Vlasov, Dr. Marina Zenkova
630090, Lavrentiev Av. 8, Novosibirsk, Russia

1997-1998 | **Institute of Cytology and Genetics, Department of Cell Biology**
Research assistant
Dr. Alexandr Blinov
630090, Lavrentiev Av. 10, Novosibirsk, Russia